UNIVERSITEIT VAN PRETORIA
UNIVERSITY OF PRETORIA
YUNIBESITHI YA PRETORIA

ARTICULATED VEHICLE STABILITY CONTROL USING BRAKE-BASED TORQUE VECTORING

by

Jamie Catterick

15007538

Submitted in partial fulfillment of the requirements for the degree

Master of Engineering (Mechanical Engineering)

in the

Department of Mechanical and Aeronautical Engineering

Faculty of Engineering, Built Environment and Information Technology

UNIVERSITY OF PRETORIA

Sunday 1st August, 2021

To Robin James Catterick

My Father, my hero, my role model

You inspired me to become the engineer I am today and I will continue to make you proud in every aspect of my career and life.

ABSTRACT

ARTICULATED VEHICLE STABILITY CONTROL USING BRAKE-BASED TORQUE VECTORING

by

Jamie Catterick

Supervisor(s):	Dr TR Botha and Prof PS Els
Department:	Mechanical and Aeronautical Engineering
University:	University of Pretoria
Degree:	Master of Engineering (Mechanical Engineering)

Statistics show that unstable articulated vehicles pose a serious threat to the occupants driving them as well as the occupants of the vehicles around them. An articulated vehicle typically experiences three types of instability: snaking, jack-knifing and rollover. An articulated vehicle subjected to any of these instabilities can result in major accidents. It is also known that many individuals are unaware of how to properly tow or pack a loaded articulated vehicle. These individuals are, therefore, at a high risk of causing the vehicle system to become unstable. It can hence be confidently said that a method in which an articulated vehicle can stabilise itself is a worthy research question. The method that is implemented in this study is to create a control system, using Nonlinear Model Predictive Control (NMPC), that has the capability of stabilising an articulated vehicle by applying torque vectoring to the trailer. In order for this control system to be applied, a nonlinear articulated vehicle MSC ADAMS model was constructed. The NMPC controller works by using a nonlinear explicit model to predict the future states of the vehicle and then finding the optimal left and right braking forces of the trailer by minimising the cost function using least squares minimisation. The cost function includes the towing vehicle yaw rate, trailer yaw rate and hitch angle and is minimised by minimising the error between the desired vehicle states and the actual states. It was found that the NMPC is capable of not only preventing instability but also causes the vehicle system to behave as if the trailer is unloaded. This conclusion means that this type of control system can be used on all types of articulated vehicles and shall ensure the safety of not only the vehicle occupants but other road users as well.

Unfortunately, due to the impact of the 2020 COVID-19 pandemic, the experimental validation of the model had to be delayed significantly. It is for this reason that the experimental validation for the controller could not be done.

Acknowledgements

I would like to thank and acknowledge the following entities who made contributions to this study:

- The Vehicle Dynamics Group of the University of Pretoria for providing a constructive environment that allowed me to grow and develop throughout the course of this dissertation.
- The South African Transportation Conference for providing the funds needed for this research study.

I would like to thank and acknowledge the following people who all made significant contributions and helped me reach the completion of this study:

- Dr Theunis Botha, for your constant support, motivation and mentorship throughout the duration of this study.
- Prof Schalk Els for your guidance and support and for creating such a supportive and constructive environment that has allowed me to develop into the engineer I am today.
- Wian Botes and Andries Peenze for all of your assistance throughout my research. You taught me a great deal and I am forever grateful to you both.
- To my colleagues who have become close friends: Kimberly Alves, Kirsten Braun, Aiden Carvalho, Ricardo de Sousa, Benjamin de Wet, Lafras Fritz, Ryan Balshaw and Johann Bouwer, I cherish our friendship and the support you gave me throughout our journey together.
- To my colleagues Carl Bekker, Herman Hammersma, Cor-jacques Kat, Wietsche Penny and Glenn Guthrie, thank you for your technical assistance and guidance whenever needed.

Finally, I would like to express gratitude to the important people in my life:

- To Cameron Green, thank you for all the love and support you have constantly given me. You have kept me sane and motivated throughout this journey and I am forever grateful to you.
- To my parents Robin and Sharon Catterick, thank you for always believing in me and giving me the means to achieve all that I have.
- To my sister Tayla Catterick, Thank you for your love and support.

Table of Contents

Nomenclature

Abbreviations

Abbreviations	Description
ABS	Anti-lock Brake System
ACADO	Automatic Control and Dynamic Optimization
ADAMS	Automatic Dynamic Analysis of Mechanical Systems
CAD	Computer-aided Design
CAN	Controller Area Network
CG	Centre of Gravity
CTC	Car Trailer Combination
DLC	Double Lane Change
DOF	Degrees of Freedom
DYC	Direct Yaw Control
ESC	Electronic Stability Control
ESTM	Extended Single Track Model
FBD	Free Body Diagram
4S4	Four State Semi-active Suspension System
FWS	Forward Wheel Steering
GPS	Global Positioning System
IMU	Inertial Measurement Unit
ISO	International Organisation of Standardisation
LMIs	Linear Matric Inequalities
LQR	Linear Quadratic Regulator
MABX	MicroAutoBox
MPC	Model Predictive Control
NMPC	Nonlinear Model Predictive Control
PBS	Performance Based Standards
PID	Proportional Integral Derivative
RWS	Rear Wheel Steering
SISO	Single Input Single Ouput
SMC	Sliding Mode Control
SSF	Static Stability Factor

Abbreviations	Description
STM	Single Track Model
SUV	Sports Utility Vehicle
VSC	Variable Structure Control
VDG	Vehicle Dynamics Group

Roman Symbols

Symbol	Description	Units
A	Area	m^2
A	Stiffness Matrix	-
a	Acceleration or	m/s^2
	Distance	m
C	Cornering Stiffness or	N/rad
	Coefficient of Damping	Ns/rad
c	Distance	m
D	Diameter	m
d	Damping Factor	-
E	Disturbance Matrix	-
e	Distance or	m
	Error	-
F	Force	N
g	Gravitational Acceleration	m/s^2
h	Distance	m
I	Moment of Inertia	kgm^2
K	Spring Stiffness or	N/rad
	Gain	-
J_0	Cost Function	-
M	Moment	Nm
m	Mass	kg
P	Pressure	Pa
P	Terminal Weight Matrix	-

Symbol	Description	Units
Q	Stage Weight Matrix	-
R	Input Weight Matrix	-
s	Distance between suspension struts	m
T	Torque	Nm
t	Track width	m
U	Input Vector	-
u	Control input	-
V	Volume	m^3
v	Velocity	m/s
x	State Vector	-
Y	Lateral Hitch Force	N
z	Vertical displament	m

Greek Symbols

Symbol	Description	Units
α	Slip angle	deg
δ	Steering angle	deg
ε	Roll steering coefficient	-
θ	Hitch angle	deg
$\dot{\theta}$	Hitch rate	deg/s
$\ddot{\theta}$	Hitch angular acceleration	deg/s^2
μ	Road friction coefficient	-
ϕ	Roll angle	deg
$\dot{\phi}$	Roll rate	deg/s
$\ddot{\phi}$	Roll angular acceleration	deg/s^2
ψ	Yaw angle	deg
$\dot{\psi}$	Yaw rate	deg/s
$\ddot{\psi}$	Yaw angular acceleration	deg/s^2
ω	Natural frequency	rad/s

Subscripts

Symbol	Description
0	Initial state
1	Towing vehicle
2	Trailer
collinear	Collinear component
CG	About CG
f	Front
H	Hitch point
i	Inside
o	Outside
piston	Piston component
r	Rear
s	Sprung mass
strut	Strut component
t	Trailer
us	Unsprung Mass
x	In the x-direction
y	In the y-direction
z	In the z-direction

List of Figures

List of Tables

1. Introduction

1.1 Background

An articulated vehicle is described as a vehicle that can have a pivoting joint, which is either permanent or semi-permanent, connecting two or more parts of the vehicle [Azad, 2006]. A semi-permanent joint is a joint that can be disconnected and re-attached whereas a permanent joint means that once the articulation is made, it is fixed. Any vehicle that is towing a trailer or semi-trailer are referred to as an articulated vehicle. The stability of articulated vehicles is a growing concern in recent years due to the fact that transport is moving towards larger and longer trucks and trailer combinations for better efficiency which in turn leads to an increased number of possible safety risks [Grīslis, 2011]. There are three types of trailer instabilities: roll in the roll plane, jack-knifing and snaking in the yaw plane [Azad, 2006]. According to the state of Road Safety Report for January-March 2018, 3.6% of major crashes were due to jack-knifing [Road Traffic Management Corporation, 2018]. To further highlight the importance of instability in articulated vehicles, research was done involving some statistics on trailer accidents. It was found that in the last 20 years, over 400 fatalities have occurred every year in road accidents that involved trailers being towed by passenger vehicles [Koenigsberg, 2008]. In a 12 month survey that was completed in the UK, it was found that jack-knifing was the cause for 15% of accidents in Leicester and 7% in Warwickshire. Trailer swing or snaking was the cause for 9% in Leicester and 3% in Warwickshire. Poor braking and other handling faults made up the rest of the score but did not play a major role. The statistics clearly show that handling problems are one of the major hazards regarding articulated vehicles and that providing a method of stabilisation shall be highly worthwhile [Farr and Neilson, 2012]. This survey showed that jack-knifing occurs in over half of handling incidents. Snaking also occurs in a large part of accidents which suggests that preventative measures are needed. Majority of other handling accidents that are not due to jack-knifing or snaking occur due to the inability to negotiate corners, most likely due to excessive speed but also because of high loads leading to a higher centre of gravity [Farr and Neilson, 2012]. Farr and Neilson (2010) also show that other road users were ten times more at risk of suffering injuries or fatalities than the driver of the articulated vehicle [Farr and Neilson, 2012]. This highlights the safety concerns of these types of vehicles as far more people are being placed in harms way due to an articulated vehicle. In accidents where a serious injury or fatality occurred, an estimated half were due to other road users, a quarter to jack-knifing and an eighth to snaking [Farr and Neilson, 2012]. This study highlights just how safety critical the stability of an articulated vehicle is.

Majority of already existing research which concerns articulated vehicles only takes the yaw dynamics of an articulated vehicle into account due to the fact that snaking and jack-knifing occur in the yaw plane. Figure 1.1 represents the relationship between yaw and roll instability for commercial vehicles and hence highlights the importance of considering both types of instabilities [O'Neal Arant, 2013].

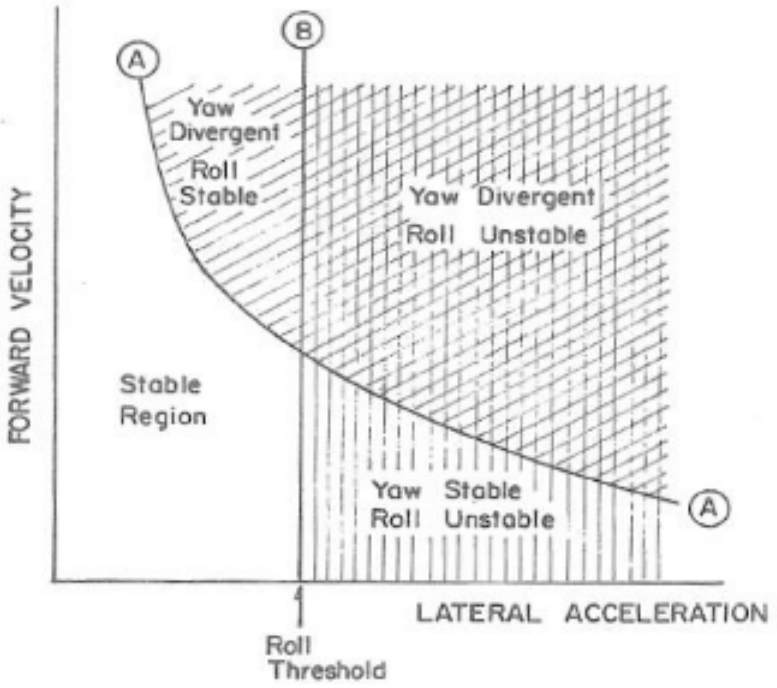

Figure 1.1. Yaw and roll stability regimes [O'Neal Arant, 2013]

From Figure 1.1, it can be seen that instability can be caused by either roll or yaw or by both simultaneously and is dependent on the forward velocity and lateral acceleration. Majority of the studies that have been conducted on the control of articulated vehicles, focus more on linear vehicle dynamics by using a linear controller model in the yaw plane and therefore do not take the roll dynamics into account. There is therefore a necessity to generate an articulated vehicle model that considers both the yaw and roll vehicle dynamics. The main goal or objective of this study is to use active control strategies to prevent instability in articulated vehicles as well as improve overall handling and reduce rollover.

1.2 Problem Statement

Articulated vehicles are prone to instabilities which can result in severe collisions. The problem is therefore to investigate the improvement of safety for articulated vehicles. Currently literature only focuses on the planar dynamics and neglecting the roll degree of freedom. Investigating the possibility of estimating the roll would add an additional aspect which could be looked at in terms of the constraints of the vehicle. This study shall aim to use active control strategies to improve the safety of articulated vehicles by preventing instability.

1.3 Overview of Report

This report begins with a literature review containing all the relevant research and literature. Chapter 3 describes the process used to construct and validate an MSC ADAMS model that is also set-up to have a co-simulation with SIMULINK. Chapter 4 describes the design of a simple gain controller as well as the more complex Nonlinear Model Predictive Controller(NMPC). Chapter 5 highlight's the controller evaluation in simulation by testing the performance and capability of the controller to reduce instability. Finally, Chapter 6 states the conclusion of the study and briefly describes what recommendations can be made for future work.

2. Literature Study

2.1 Introduction

Information about articulated vehicles concerning what they are, how they function and what they are used for is discussed. Literature is given on control systems to highlight how stability control has been implemented before and what methods are feasible for this study. The literature review also includes an extensive section focusing on the stability of trailers and what type of instabilities can occur. This is necessary to ensure that all significant types of instabilities and why they occur are fully understood.

2.2 Articulated Vehicles

An articulated vehicle is a vehicle that consists of two or more separate sections, a tractor and a trailer. These vehicles can carry heavy loads and take quite sharp turns [Prem, 2014]. There are different types of articulated vehicles, but the most general definition of an articulated vehicle is a vehicle towing a trailer. An articulated vehicle can include types of trucks, buses, trains and rail as well as certain heavy equipment and military vehicles. An articulated vehicle can also include a vehicle that has been developed according to the South African Performance Based Standards (PBS) [de Saxe et al., 2018]. The PBS concept involves heavy vehicle use that is strictly controlled by certain regulations. These standards are based on manoeuvrability and stability as well as the vehicles impact on infrastructure. Vehicle mass and structural dimensions are more relaxed. The performance of the vehicle is based on its efficiency for its given purpose. Using these regulations can ultimately result in vehicle designs that are unsafe or impose extreme loads on the infrastructure [de Saxe et al., 2018]. These vehicles can be articulated and it is for this reason that they play a role in this study. If the results of this thesis can successfully remove the threat of instability, these heavy vehicles have a greater chance of being successful. It is known that there are relatively few accidents involving articulated vehicles when looking at traffic statistics but it is believed that many of these accidents occur because the trailer begins oscillating, also known as snaking, about the hitch point. Accidents are more prone to happen when snaking occurs due to the fact that the driver usually does not react or reacts in an improper manner. The oscillation of the trailer can be caused by different disturbances that include: uneven roads, wind gust, driver steering input amongst others [Williams and Mohn, 2004]. There has been a lot of previous research into the different factors that affect trailer stability and all this work provided

very similar results. In order for an articulated vehicle to remain stable the car mass to trailer mass ratio should be maximised, the trailer moment of inertia should be minimised and the distance from the rear car axle to the hitch point should be minimised [Williams and Mohn, 2004]. High vehicle speed is also one of factors that affect or influence oscillatory instability [Williams and Mohn, 2004]. The trailer Centre of Gravity(CG) to hitch point distance has an optimal range, if its too far forward it adversely affects the static lateral stability and to far back affects oscillatory stability. The trailer CG longitudinal location therefore has an optimal range [Williams and Mohn, 2004]. The driver of the articulated vehicle is therefore responsible for ensuring that all these factors have been taken into consideration as well as ensuring the trailer has been equipped and loaded properly. Unfortunately, many drivers do not go to these lengths to ensure the stability of the vehicle and it is for this reason that trailer instability is a significant safety risk.

A schematic diagram of a Car-Trailer Combination(CTC) is depicted in Figure 2.1. This diagram can be used to highlight the difference between articulated vehicles and a single passenger car.

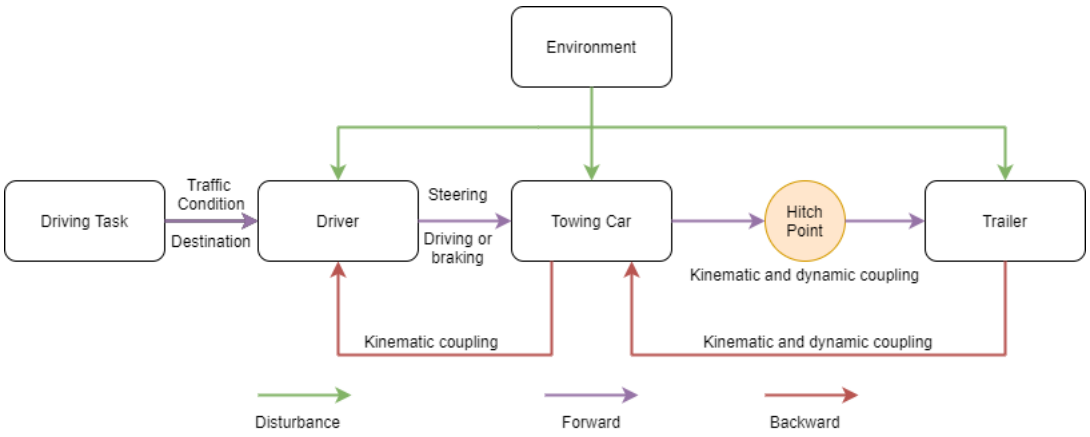

Figure 2.1. Schematic diagram of a CTC [Zhang, 2015]

The differences between an articulated vehicle and a single passenger vehicle, seen in Figure 2.1, include the fact that since there is a trailer connection, the dynamics, as well as the kinematics of the trailer and towing vehicle, are coupled. A CTC has a dynamic critical speed which is used to determine whether the system is stable or not. A single-vehicle does not have a critical speed, when referring to straight line driving, since, at very high velocities, the stability of the system remains intact [Zhang, 2015].

2.2.1 SUV and testing trailer

The articulated vehicle used is an SUV with a testing trailer. There are two possible loading conditions: unloaded and loaded. The unloaded condition is depicted in Figure 2.2 and the loaded condition can be seen in Figure 2.3.

Figure 2.2. SUV and testing trailer: Unloaded

Figure 2.3. SUV and testing trailer: Loaded

2.3 Stability of articulated vehicles

The instability of an articulated vehicle is the greatest concern for this study, and therefore, a thorough understanding of the types of instability experienced by articulated vehicles, is a necessity. When taking the stability of vehicles into account, there are three types of instability that could occur. Two of these occur in the yaw plane and exhibit both static and dynamic instability. These include jack-knifing and snaking. The third type of instability is rollover in which the system overturns. Rollover instability is also the most dangerous type of instability as the majority of fatalities caused are due to rollover. The next two sections shall give a more in-depth description of each type of instability an articulated vehicle can experience.

2.3.1 Yaw Stability

Every articulated vehicle has a pre-determined, very specific dynamic critical speed which is used to determine the dynamic stability boundary. The dynamic critical speed has quite a close relationship with the yaw damping ratio. If the dynamic critical speed is reached, the yaw damping ratio shall converge to zero and become negative as the articulated vehicle increases its speed beyond the critical speed. Ultimately the yaw rate of the system shall begin to increase, resulting in an unstable situation which could end in a traffic accident [Zhang, 2015]. Vehicles that are towing trailers can be subjected to two types of yaw instability: jack-knifing and snaking. Jack-knifing, depicted in Figure 2.4, is a periodic as well as catastrophic instability where the towing vehicle yaws in one direction continuously while the trailer only yaws very slightly. Snaking, depicted in Figure 2.5, on the other hand, is the complete opposite where the trailer yaws continuously and the towing vehicle yaws slightly. These two types of instabilities are commonly referred to as divergent instabilities [Kurtz and Anderson, 1977].

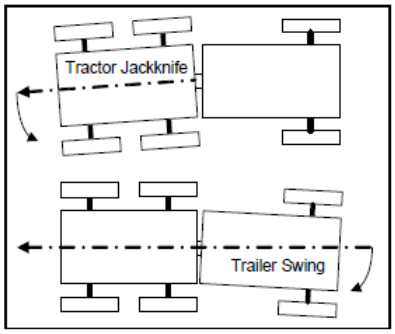

Figure 2.4. Jack-knifing [Azad, 2006]

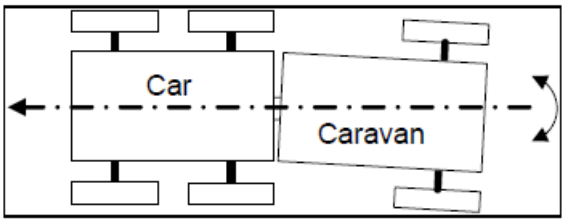

Figure 2.5. Snaking [Azad, 2006]

As mentioned previously stability can be static or dynamic and both types of stability shall be discussed here.

2.3.1.1 Static Stability

The static stability of an articulated vehicle is dependent on the parameters of the towing car. The mass of the trailer, as well as the horizontal position of the trailer CG, can affect the vertical load of the trailer. It can be shown that lessening the vertical load at the hitch can actually help improve the static stability. Static stability is ultimately indicated by the understeer gradient [Zhang, 2015]. A non-articulated vehicle can exhibit three possibilities of steer: neutral steer, understeer and oversteer. The three possibilities are described using a manoeuvre known as a constant radius turn. Neutral steer shall exhibit no change in steer angle as speed is varied. For a vehicle with understeer, the steering angle will have to increase with speed that is proportional to the understeer gradient multiplied by the lateral acceleration. The lateral acceleration at the CG shall cause the front tyres of the vehicle to slip sideways at a greater extent than that of the rear tyres, and therefore the front wheels must be steered to increase the angle. Oversteer is the opposite of understeer where the steering angle will decrease with speed, the slip on the rear wheels is greater than that at the front wheels, and therefore the steering angle needs to be reduced to maintain the radius [Gillespie, 1992]. The three types of steer are depicted in Figure 2.6 below.

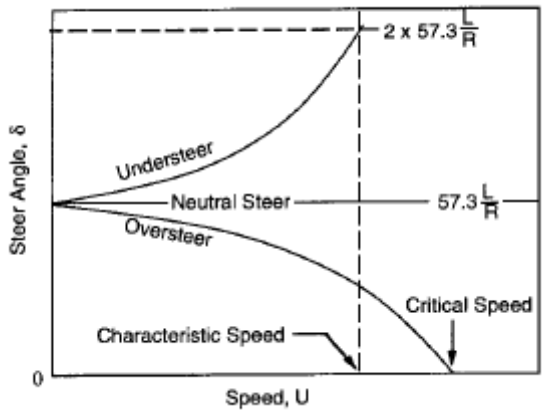

Figure 2.6. Change of steer angle with speed in a passenger vehicle [Gillespie, 1992]

From Figure 2.6 it can be seen that with neutral steer, the steering angle that needs to be maintained is simply the Ackerman angle while with understeer the angle continues to increase until the characteristic speed is reached. In the oversteer case, a critical speed exists, and if this speed is exceeded, the vehicle shall become unstable. It must be noted that this critical speed is with reference to steady-state cornering and not the critical speed associated with articulated vehicles.

The three steering cases can also be represented using the yaw velocity gain. The definition of yaw velocity is the rate of rotation in the heading angle. The relationship between yaw velocity gain and speed is portrayed in Figure 2.7.

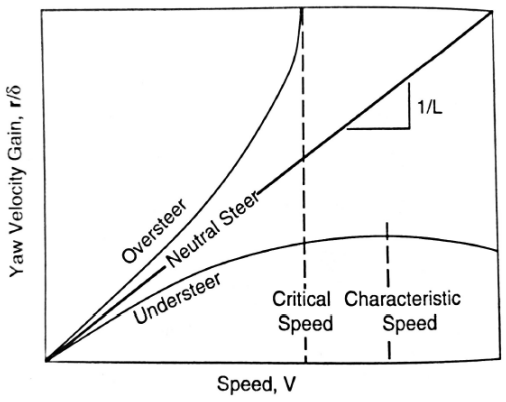

Figure 2.7. Yaw velocity gain as a function of speed in a passenger vehicle [Gillespie, 1992]

From Figure 2.7, it can be seen that for an oversteering behaviour the yaw gain velocity at the critical speed is infinite.

Unlike a passenger vehicle, an articulated vehicle has a more complex load distribution. It is not possible to clearly characterise the system with optimal steering characteristics. Therefore more focus is placed on the towing vehicle and its operating speeds. A towing vehicle should be designed to have more understeer in order to avoid situations that are undrivable at certain speeds and instability at high speeds [Zhang, 2015]. Figure 2.8 portrays a typical response of a tractor with a loaded trailer.

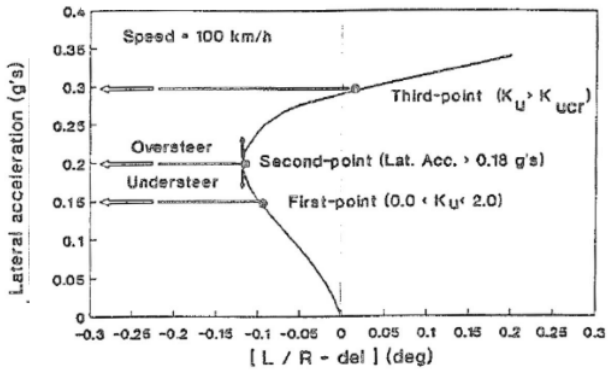

Figure 2.8. Constant radius understeer results of a tractor towing a trailer [O'Neal Arant, 2013, El-Gindy, 1995]

Figure 2.8 comes from the handling performance measure that is know as the 'three-point measure'. This figure is constructed using the front steering angle, x-axis, and the lateral acceleration, y-axis, of the articulated vehicle [El-Gindy, 1995]. The purpose of the three-point measure is to represent the handling of the system over a more complete range. The first point is used to place limits on the understeer coefficient. This is done to ensure that there is some controllability of articulated vehicles in the lower realms of lateral acceleration. The second point addresses where and when the vehicle will transition from understeer to oversteer. This lateral acceleration should not be less the 0.18 g's. This is to ensure that the behaviour of the vehicle remains somewhat constant. The third and final point looks at the understeer coefficient at a higher lateral acceleration. This coefficient must be greater than the critical understeer coefficient in order to prevent the driver from causing a loss in directional stability [El-Gindy, 1995]. From Figure 2.8, it can be seen that the articulated vehicle begins understeering but ultimately converts to oversteer. This shows that each unit of an articulated vehicle can either be understeering or oversteering. There are four stability combinations that can relate the behaviour of articulated vehicles. [O'Neal Arant, 2013]

- **Vehicle and trailer both understeer:** The articulation angle gain of the articulated vehicle shall tend to the ratio of understeer gradients as the speed increases. The vehicle is stable in this

situation.

- **Vehicle understeer and trailer oversteer:** The understeer gradient of the trailer is negative, the yaw gain of the trailer shall initially be positive but shall later become negative. This situation shall cause the trailer to swing out, and the vehicle is therefore unstable. The articulation gain should remain positive.
- **Vehicle oversteer and trailer understeer:** The speed shall increase until the critical speed is reached and the yaw gain shall approach infinity. This situation will result in a jackknife and is, therefore, an unstable situation.
- **Vehicle and trailer both oversteer:** This situation is dependent on, if the ratio of the understeer gradient is less than or greater than the ratio of the wheelbases as the yaw gain will approach either positive or negative infinity. This shall cause a swing or a jackknife and the vehicle is unstable.

2.3.1.2 Dynamic Stability

Hac et al (2008) proposed a linear single-track model of an articulated vehicle. This linear analytical model describes the yaw and lateral motions of a vehicle-trailer combination and was used to study the effects of parameter variations of the trailer on the dynamic stability of the system and limitations of different control strategies. This model was used as the basis for the reference model in this study and its complete derivation can be found in Section 4.2.2. In order to study the dynamic stability, a free system that is described without the steering input in Equation 2.1. [Hac et al., 2008]

$$\dot{\mathbf{x}} = \mathbf{A}\mathbf{x} \tag{2.1}$$

The yaw-plane equation of a single passenger vehicle is a 2nd order system, and it, therefore, has only one pair of conjugate roots and only a single yaw damping ratio. An articulated vehicle, on the other hand, is at least a 4th order system which means that there are two pairs of complex conjugate roots with a damping ratio for each pair. A stable system shall have a negative real part of the roots. The system shall become dynamically unstable when any pair of roots has a positive real part. If the system has a complex pair of poles in the form seen in Equation 2.2 then the yaw damping ratio can be calculated according to Equation 2.3, where a negative damping ratio is an indication of an unstable system.

$$s_{1,2} = -d \pm j\omega_d \tag{2.2}$$

where d is the damping factor and ω_d is the damped natural frequency.

$$\xi = \frac{-d}{\sqrt{d^2 + \omega_d^2}} \tag{2.3}$$

The damping ratio is a function of longitudinal speed; therefore, it is possible to find the dynamic critical speed by plotting the damping ratio against longitudinal speed.

2.3.2 Roll Stability

Rollover is extremely dangerous, not because it occurs often but rather due to the fact that most rollovers result in fatalities [Young et al., 2008]. This is why vehicle roll stability has been the main subject in research over the years. When assessing roll stability the most simplistic parameter is known as the Static Stability Factor (SSF) or rollover threshold [O'Neal Arant, 2013, Dahlberg, 2000, Dahlberg and Stensson, 2006a]. The SSF is defined as the ratio of the vehicle's wheelbase, denoted as T, to the CG height, denoted as h_{CG}, as seen in Equation 2.4.

$$SSF = \frac{T}{2h_{cg}} \tag{2.4}$$

Equation 2.4, however, does not take the vehicle's compliance's into account. This compliance shall reduce the effective wheelbase of the vehicle as the vehicle is rolling through a turn. Equation 2.5 takes the compliance into account where $\triangle y$ is the effective wheelbase. Figure 2.9 depicts the roll displacements as well as the roll reactions of a vehicle.

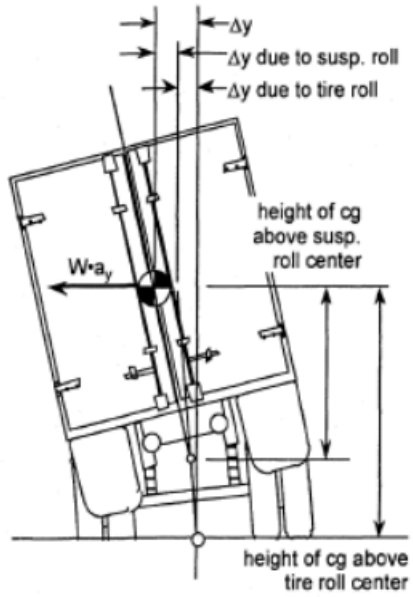

Figure 2.9. Roll Displacements and reactions [Wrinkler and Ervin, 1995]

$$SSF_{compliance} = \frac{\left(\frac{T}{2} - \triangle y\right)}{h_{cg}} \tag{2.5}$$

It can be stated that the higher the CG or, the narrower the effective track, the less stable the vehicle shall be. It can be seen that the CG height of a vehicle and trailer plays a big part in the rollover threshold. For most types of articulated vehicles, the CG height of the load usually tends to increase along the length of the vehicle [Fu and Cebon, 2002, International Standard of Organisation, 2002]. The lowest CG is typically at the steer axle with the highest CG height acting at the rear of the vehicle. The majority of the weight on the front axle is due to the engine and transmission, which causes the CG height at the front of the vehicle to be fairly low. The total CG height at the rear of the vehicle and front of the trailer is lowered due to the weight of the drive axles. The trailer axle or axles do not have as much of a significant mass as those of the towing vehicle as there are no power transmission components, it can, therefore, be said that the CG height of the rear of the trailer is closer to the CG height of load that the trailer is carrying. If it is assumed that the CG height of the load is constant along the length of the trailer, the CG height shall drift upward towards the rear end of the towing vehicle. This CG drift indicates that the part of the system that shall have the lowest rollover threshold shall be the rear of the trailer. The next lowest shall be the drive axles followed by the steer axle. In order to increase the roll stability, changes can be made to heighten the rear roll centres as well as to stiffen the suspension. These changes reduce the lateral deflection of the CG or $\triangle y$ term, which in

turn increases the roll stability. Unfortunately, even with these changes, most rollovers start at the rear of the vehicle and move forwards towards the steer axle [Macnabb et al., 2002].

Load transfer occurs when the vehicle relays vertical load from one wheel to the other by generating a moment that counters the overturning moment. By making the assumption that the vehicle is able to generate sufficient lateral forces that prevent sliding, the load transfer shall continue to build until the vertical load on the inner wheel is zero. This point is referred to as the vehicle's stability limit even though the vehicle shall not roll over until the CG location is moved outside the wheelbase or if the roll inertia is greater than that of the stabilising moment [O'Neal Arant, 2013]. The mechanics that govern the roll moment that is applied to an axle are shown in the model depicted in Figure 2.10.

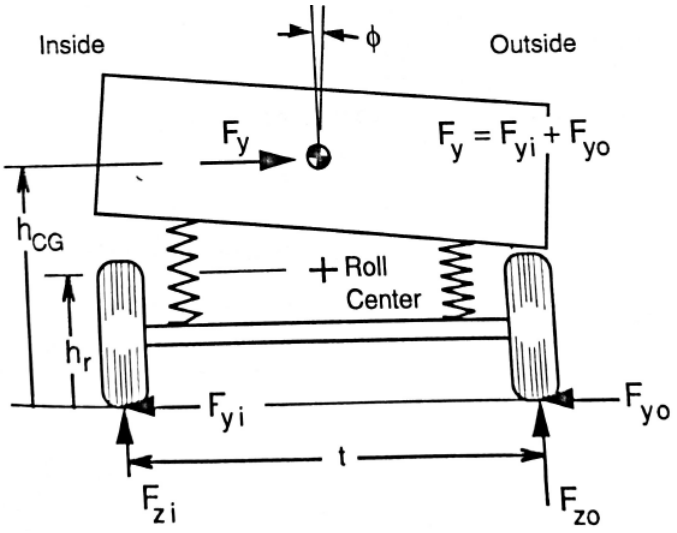

Figure 2.10. Force analysis of a simple vehicle in cornering [Gillespie, 1992]

Equation 2.6 describes the change in vertical force at the tyres and hence describes the lateral load transfer [Gillespie, 1992].

$$F_{zo} - F_{zi} = 2F_y\frac{h_r}{t} + 2K_\phi\frac{\phi}{t} = 2\triangle F_z \tag{2.6}$$

where F_{zo} is the load on the outside wheel in the turn, F_{zi} is the load on the inside wheel in the turn, F_y is the lateral force, h_r is the roll centre height, t is the track width, K_ϕ is the roll stiffness of the suspension and ϕ is the roll angle.

2.4 Active Stability Control Systems

The main goal for this study is to find a way to stabilise an articulated vehicle. There has been a lot of research done on different types of active controllers for articulated vehicles over the past years which shall be discussed in this section. Active stability control systems were introduced decades ago, and these systems were used to direct the vehicle to behaviour that is predictable, which ultimately prevented the vehicle from drifting or spinning out. This was achieved by controlling the vehicle yaw rate, which allowed the drivers to have better control of the vehicle. This is formally known as yaw moment control [Azad, 2006].

2.4.1 Types of Control Strategies

Yaw moment control can be implemented in many ways but there are three main control strategies that have been the focus for many years. These strategies include active steering control, active braking or torque-vectoring and adjusting the swing torque. Active steering is achieved by introducing an additional steer angle to the front or rear wheels of the towing vehicle or trailer or both [Azad, 2006]. Differential braking or torque-vectoring is performed by generating a yaw moment using either driving or braking force on both sides of the vehicle. Adjusting the swing torque is achieved using a variable geometry approach. The concept of the variable geometry approach is to control the lateral displacement of the hitch to improve stability. Shamim et al (2011) performed a comparative study analysing the performance of the three different types of controller strategies. In order to perform this comparison, three controllers were derived and their respective yaw plane models were developed and tailored for each type of control strategy [Shamim et al., 2011]. The active trailer braking introduced a control moment, the active steering case introduced a steering angle input to the trailer wheels and the adjustment of the swing torque was achieved using a variable geometry approach. Once all three models were developed, a Linear Quadratic Regulator (LQR) technique was used in the design of each controller to find each control gain matrix respectively. The aspects of the articulated vehicle that was used to generate the comparison includes: the lateral acceleration of the towing vehicle, the yaw rate of the towing vehicle, the yaw rate of the trailer and the hitch angle. The variable geometry approach showed the worst performance with the longest settling time and largest overshoots. The active trailer braking had smaller dynamic responses in all aspects except the hitch angle in comparison with the active steering control, but the active steering control had shorter settling times in all aspects. Overall, this paper showed that the active trailer braking has the best capability of rejecting external disturbance in order to maintain stable operating of the articulated vehicle at high speeds. Unlike

Shamim et al (2011), who investigated the yaw stability of articulated vehicles, Li et al (2016) also compared the same three control strategies in terms of their abilities to affect roll instability. It was found that active braking is conducive to improve roll stability during turning, active steering improves roll stability during turning and passing over obstacles and adjusting the swing torque improves roll stability by changing vehicle posture and CG [Li et al., 2016]. From this information, it was decided that an active braking or torque-vectoring based yaw moment controller shall be the focus for this study. This decision is also made because most new trailers have ABS brakes already installed. These brakes can be modified for active braking whereas an active steering controller on the trailer would need a new trailer design.

2.4.2 Types of Controllers

There are many different types of controllers but most literature focuses on four main types. These types of controllers include: Feedback Controllers, Sliding Mode controllers, Model Predictive Control (MPC) and Fuzzy Logic Controllers.

2.4.2.1 Feedback Controller

A feedback controller measures the output of a process and from that manipulates the input variable/variables as much as is required to drive the process variable to a desired outcome. The controller reacts to the set point changes as well as to random disturbances to the process variable caused by external forces. The process is repeated over and over until the process variable reaches the desired result [Vandoren, 2012].

Azad (2006) proposed a robust feedback controller for a torque vectoring system. The control input torque is transferred to the wheels of a certain axle; hence, the input power from the engine is adjustable and can be delivered to one or all the axles at specific ratios. A Lyapunov function, as well as a state feedback matrix of the controller, are found by solving Linear Matrix Inequalities (LMIs). The control is generated by applying an equal but opposite change in torque $\triangle T$ to the rear wheels. Thus the wheel on one side is braked while the wheel on the opposite side is accelerated. This torque provides the baseline for the control system using the torque vectoring device. The transferred torque $\triangle T$ is adjustable and is used to stabilise the vehicle when it encounters snaking. This torque is found using a full state feedback system as defined in Equation 2.7. [Azad, 2006]

$$\triangle T = \mathbf{KX} \tag{2.7}$$

Where **K** is the feedback matrix. **X** is the states that are described in Equation 2.8.

$$\mathbf{X} = [v, \dot{\psi}, \dot{\theta}, \theta, \omega_f, \omega_r]^T \tag{2.8}$$

where ω_f and ω_r are the front and rear wheel angular velocity of the towing vehicle.

The state feedback matrix is solved using LMIs and Azad (2006) used quadratic stabilisation of polytopic systems. Ultimately it was found that by using the resulting feedback matrix **K**, the baseline vehicle can be stabilised in a variety of driving conditions.

Zanchetta et al (2019) proposed a Torque Vectoring (TV) formulation that made used of the combined hitch angle and yaw rate of an articulated vehicle. This formulation used a direct yaw moment that is generated on the towing vehicle. The control system was based on a Single-Input Single-Output (SISO) feedback control structure where the yaw rate of the towing vehicle is altered when instability is detected using a hitch angle sensor. The controller includes the continuous feedback control of the vehicle yaw rate and the control of the measured hitch angle. The reference yaw moment is computed from a single control variable, which is the weighted combination of the yaw rate error as well as the hitch angle error. The hitch angle error is only used when it exceeds pre-determined thresholds. The design of the feedback controller includes Proportional Integral (PI) gains that are selected for appropriate yaw control and a gain scheduling scheme that is developed with the single-track model of the isolated vehicle to keep constant stability margins. The results show that a TV controller based only on yaw rate is insufficient and the proposed controller, which includes the hitch angle, provides safe trailer behaviour during the manoeuvres therefore justifying the hitch angle measurement [Zanchetta et al., 2019].

Milani et al (2019) proposed a type of feedback control known as a Linear Quadratic Regulator (LQR). This study was performed to investigate the potential of active steering control of a semi-trailer [Milani et al., 2019]. This study is described in the literature review to give more information on the LQR and if this type of control is a possibility for the authors current study. The LQR optimal state feedback control is used to regulate the rearward amplification ratio and roll at high speeds as well as minimise the tracking error at low speeds [Milani et al., 2019]. The basic theory behind a LQR is that the system is described by a set of linear differential equations. The cost that is to be minimised

is defined using a quadratic function. Milani et al (2019) introduced three different types of control algorithms. The first control strategy is to minimise the amount of high-speed transient off-tracking by providing a rearward amplification ratio of 1. Control strategy two focuses on minimising the rearward amplification ratio which reduces the roll motion but at the expense of large high-speed transient off-tracking values. Finally, the third control strategy adds an additional roll control input torque. This controller is able to keep the rearward amplification ratio low as well as limit the roll motions. The results of this study showed that dynamic behaviour of an articulated vehicle can be improved to an acceptable level with a simple linear feedback approach. It was also found that each controller had its merits in different situations [Milani et al., 2019].

2.4.2.2 Sliding Mode Controllers

Sliding Mode Control (SMC) contains an algorithm that is inherently robust to changes within its parameters, external disturbances, uncertainties and nonlinear models [Martinez and Cao, 2019]. SMC is based on variable structure systems that have been composed with independent structures of different properties as well as a switching logic between them [Ibraheem et al., 2000]. The control structure is switched when the system state trajectory has crossed a particular hypersurface in state space. When this surface is reached, there is a constraint to keep the state trajectory in place which in turns keeps a motion along its trajectory on that surface, and this is why it is known as the sliding mode. The main advantage of this particular technique is that the system dynamics during this sliding mode can be completely determined based on the choice of this hypersurface. The main disadvantage of this technique is that there is chattering due to a discontinuity that occurs due to control effort because switching is not instantaneous. This chattering can be reduced by using a higher order SMC. In the development of the controller, the norm of the uncertainty function, which includes non-linearities and parameter uncertainties was assumed to be known. The control law itself is separated into two different sections, linear feedback as well as a switching function. The first element of the control is there to compute the desirable dynamics of the system on the selected sliding surface; conventional control law is generally used. The second element is designed to maintain the system trajectory on the selected sliding surface [Azad, 2006].

Azad (2006) proposed a robust variable structure control system. In this control system, the applied braking torque at the rear wheels is adjusted to produce the required yaw moment that will, in turn, stabilise the vehicle. This particular control system is based on Variable Structure Control (VSC). This type of control was chosen by Azad (2006) as it works on the basis of sliding mode theory

[Azad, 2006, Edwards and Spurgeon, 1998]. The input model is modified to include the differential braking strategy. This controller proved to have more robustness as well as better performance in comparison to classical controllers.

Mokhiamar (2015) proposed a control design concept for an optimum distribution of longitudinal and lateral forces of the four tyres of the towing vehicle. This controller is based on sliding control law using planar equations of motion. A sliding control theory is used to derive control laws of total lateral force and yaw moment required for the controlled vehicle to follow the model response. Two controllers are described: the first being an integrated control type of direct yaw moment plus active rear wheel steering plus active front wheel steering (DYC+ RWS+ FWS) aiming at utilising overall tyre ability to maximise both stability limit and responsiveness of an articulated vehicle. In this system, tyre longitudinal force is calculated directly from direct yaw moment while tyre lateral force is calculated based on simple force sharing tyre load. The total lateral force is split between the front and rear tyres and the split ratio is directly proportional to the estimated vertical load. The second controller is the proposed optimum tyre force distribution which is used to determine how much force should be generated at each tyre to obtain the target lateral total force and yaw moment required to follow the model response as well as to meet with the drivers traction/braking command. The inputs are the driver's commands and the outputs are the longitudinal and lateral forces on all four vehicle tyres. The cost function is a weighted sum of the absolute normalised forces produced at the tyres. The two controllers were able to stabilise the articulated vehicle motion. However, the effect of the proposed optimum control is more obvious especially on the response of the trailer part. In a more severe situation, the combined control-type DYC+RWS+FWS failed to achieve a desirable response. On the other hand, the proposed optimum control successively achieves smooth and reasonable responses [Mokhiamar, 2015].

2.4.2.3 Model Predictive Control

Classical controllers require linear systems which means that they do not have the ability to handle constraints and nonlinearites [Blet et al., 2002]. Constraints limit the performance of a closed loop system and therefore must be implemented in an efficient way to ensure that performance is kept as a priority. An MPC makes a prediction of the future behaviour or states of a plantm, in this case an articulated vehicle. It makes these predictions by using an explicit model of the process. The reason behind selecting an MPC is due to the fact that an MPC can indeed handle constraints and nonlinearities [Blet et al., 2002]. A Nonlinear Model Predictive Controller (NMPC) can also use a nonlinear model

to make predictions. An MPC for an articulated vehicle is more complex due to the fact that it has more states than inputs, and these states are also coupled. Basically, the controller simulates the behaviour of the system over a series of time steps, for each point in time. A combined output and input cost function is minimised. The control demand at the initial time step is taken and applied to the real system. This process is repeated with each time step. MPC's that are implemented specifically for vehicle stability control have usually been used with a reference vehicle model that defines the desired behaviour of the dynamics of the vehicle [O'Neal Arant, 2013, Anwar, 2005, Falcone et al., 2008, Lee and Yoo, 2009]. Having this reference model is a great advantage as it estimates a stable trajectory for the vehicle to follow. The only downside is ensuring the mathematical or reference model is accurate enough.

O'Neal Arant (2013) proposes a new approach in solving this problem for implementing MPC. This approach does not use a reference model and therefore does not demand the same level of accuracy on parameter estimation. It can also be evaluated with a much larger time step without losing fidelity and it is therefore a more efficient solver [O'Neal Arant, 2013]. In the stability control research presented by O'Neal Arant (2013), the proposed cost function does not contain any information on the control outputs of the system. Usually, this would result in no control or extreme control, but since the outputs are bounded, the controller is activated to ensure the outputs remain within the bounds. This means that the controller remains dormant until a stability risk or a violation of the bounds is detected. It is at this point that the controller will activate and implement the minimum control action needed to stabilise the system. The MPC system placed onto the vehicle works by converting the control action into braking forces. The MPC control variables were moments placed at ground and were then passed onto a brake controller [O'Neal Arant, 2013]. This brake controller also managed the anti-lock brake system (ABS) with its main objective to prevent wheel lock. It was found that this MPC approach was able to predict future stability risk quite elegantly. Using the linear model forward in time to optimise the control approach allowed accurate estimations to be made. It was found that the most powerful feature of this MPC was its ability to anticipate probable instability and that a system controller worked better than a unit controller.

Nayl (2013) focused on the modelling, control and path planning problems for articulated vehicles. He took on a novel error dynamic modelling approach where the nonlinear kinematic model of the vehicle has been transformed into a linear switching model representation, which is also able to take under consideration the effect of slip angles. Along with the switching modelling, a switching MPC scheme was proposed. In the proposed control scheme, the varying slip angle and speed have been

considered as the switching signal for selecting the active controller. The MPC action is the rate of the articulation angle and is based on a finite horizon continue time minimisation of predicted tracking error with constraints on the control inputs and state variables. The formulation of the MPC is based on the current full state feedback, the active constraints on the system, the estimated slip angles, the measured velocity and the mode selector signal. This controller was indeed successful in increasing the stability of the articulated vehicle [Nayl, 2013].

Abroshan et al (2020) developed an MPC to prevent instability in an articulated vehicle equipped with differential braking. Abroshan et al (2020) investigated differential braking only on the towing vehicle and also investigated differential braking only on the trailer. This was done to study the two options comparatively. The MPC controller that was developed uses an affine tyre force model with the control actions limits based on tyre capacity. A planar bicycle model of an articulated vehicle that has 3DOF is defined as the MPC predictive model. This model also included a yaw moment that was used as the control output. For the towing vehicle, the braking is applied on the left or right tyre, on both axles, to produce the desired control moment defined by the controller. The same is done for the single axle trailer except the braking is applied only to the left and right tyres. The purpose or aim of this particular controller was to try and enforce the towing vehicle and trailer to follow a reference model or desired vehicle response. The tracking variables included the towing vehicle yaw rate and the hitch angle. Constraints were also placed on this controller which proves to show that being able to handle constraints is a favourable trait to have in a control system. These constraints are applied on the control moment by defining a maximum and minimum moment derived using the friction circle. The results that were found with this controller showed that it effectively prevents both instability modes, snaking and jack-knifing; however, differential braking has much more capacity when it is applied to the towing vehicle with these tracking variables [Abroshan et al., 2020].

2.4.2.4 Fuzzy Logic Control

Fuzzy logic control is based on whether an input is contained to a given membership function and specifically what rules apply to the function and what functions apply to the rules. An input parameter can be a member of one or more membership functions with one or more rules applying and one or more active output memberships. O'Neal Arant (2013) implemented a fuzzy controller that only takes the state of the vehicle into account and therefore does not make use of a reference model. It makes use of the fact that the trailer experiences events after the towing vehicle indicating a time lag between the two which provides the controller with enough time to predict a potential trailer stability

risk. The basis of the controller design is that the inputs are tested against the input membership functions, and then these functions are applied to the rules that hence define the control action that needs to be implemented. The result is a certain control action for each system input. There were three objectives that the controller ultimately had to meet. The first objective was the look into the future to predict possible future stability risks. The second objective was to somehow balance the needs of the vehicle in order to improve the overall performance of the system. The third and final objective was to smooth out the Electronic Stability Control (ESC) system. This is to ensure that the driver does not experience multiple harsh actions caused by the vehicle. The fuzzy logic controller is very easy to scale as it breaks the vehicle up into its units. This means it looks at the towing vehicle and trailer/trailers as individual units. This is due to the fact that the only change is to add additional states, rules and outputs. These outputs being in the form of brake demands. It was found that the fuzzy logic controller performed relatively well for different loads, road conditions and driving manoeuvres. The only downside is that the tuning of the controller is quite demanding since the set groupings, rule structure and bound selection had to satisfy competing needs for a variety of different stability risks [O'Neal Arant, 2013].

2.4.3 Controller Comparison

All the controller types described above were each successful in stabilising the articulated vehicles but some had a greater performance than others. It should also be noted that none of the controllers described here take the longitudinal deceleration into account. Taking the longitudinal deceleration into account would ultimately be beneficial since the stability of an articulated vehicle is closely related to a decrease in speed. Ultimately, from reviewing literature, the two most successful controllers were those that involved MPC as well as SMC. Miyahara et al (2019) developed a benchmark to compare yaw rate control methods by active steering. The yaw rate controllers that were investigated included: model predictive control, linear quadratic integral control and yaw moment observer-based control. The four evaluation indices included: slew rate of actuator input, emergency performance, robustness against disturbance and the stability performance of the sideslip angle [Miyahara et al., 2019]. All three controllers had their strengths but the MPC controller was the only controller that performed well taking all evaluation indices into account. Further review shows that an MPC performs the control quite elegantly and had the extra advantage of being able to predict the future states of the vehicle. MPC also has the added benefit of being able to introduce constraints as well as nonlinearities to the system. A nonlinear explicit model shall be used for this study. This is why it is imperative that the chosen controller be able to handle the nonlinearities. It is for this reason that an MPC, more specifically a

controller using Nonlinear Model Predictive Control (NMPC) was selected for this study. It is also worthy to mention that over the years, DYC was used mainly for braking the towing vehicle. However more trailers are moving to ABS braking systems thus one can now apply it to the towing trailer. It is therefore a worthy research question to investigate how braking the trailer can affect articulated vehicle stability.

2.5 Conclusion

This chapter highlighted the necessary literature needed to continue on with this study. This literature helped refined the types of instabilities an articulated vehicle is subjected to. The different aspects of control were introduced and a decision was made on what type of control shall be applied for this particular study. A NMPC model shall be used to predict lateral stability with added roll constraints to ensure roll stability. The controller shall make use of two models: a linear reference model to generate reference trajectories and a nonlinear explicit model that shall predict actual vehicle handling. This controller shall be used to implement braking on the trailer of the articulated vehicle.

3. Articulated Vehicle Model

3.1 Introduction

This chapter describes the articulated vehicle model and related model parameters. This chapter specifically outlines how the MSC ADAMS model for the Land Rover and testing trailer were combined to create the articulated vehicle model. It also places some focus on certain model parameters that need to be known for the development of the controller. Once the model was generated in ADAMS, a co-simulation is set up in MATLAB using SIMULINK. This co-simulation allows for simulations to be run on the ADAMS model and interface these results with MATLAB. The model is then validated through experimental testing by performing a double lane change as well as a constant radius turn. The tests were performed for both a soft and a hard suspension. The results of these tests allow the author to validate the simulation model by showing, that it is representative of a realistic situation.

3.2 MSC ADAMS Model Construction

The articulated vehicle model was built by combining two already existing validated models, that of the Land Rover or SUV and the testing trailer. The SUV ADAMS model was built years ago and is a fully validated nonlinear model with 16 degrees of unconstrained freedom of the vehicle. [Thoresson, 2007, Uys et al., 2006, Cronje, 2008] The body of the vehicle is represented by two rigid bodies that have been connected with a torsional spring in order to model the torsional stiffness of the vehicle chassis. The Land Rover can be interchanged between a soft and hard suspension due to the $4S_4$ suspension system. The test trailer model was built by previous masters student in 2018 [van der Merwe, 2018]. The trailer consists of a frame with two separate masses. These masses can be removed or moved to change the trailer characteristics. The test trailer model can be used as is, the only part of the Land Rover that needed to be updated was to build the tow-bar on the Land Rover. Once the geometry of the tow bar and hitch ball were constructed, the required constraints could be created. This constraint was created by placing a spherical joint between the hitch ball and the trailer body. The final model is portrayed in Figure 3.1 and has the ability for individual torques to be applied to the wheels as well to set steering angle path and vehicle speed. The co-simulation with SIMULINK is used to control the steering path as well as the suspension forces within the vehicle and the trailer. The displacements and velocities at the attachment points are read from the ADAMS model into SIMULINK which then calculates the required suspension forces that are then sent back to ADAMS. A static force analysis

was performed in order to update the current forces on the system and shall be discussed in the next section.

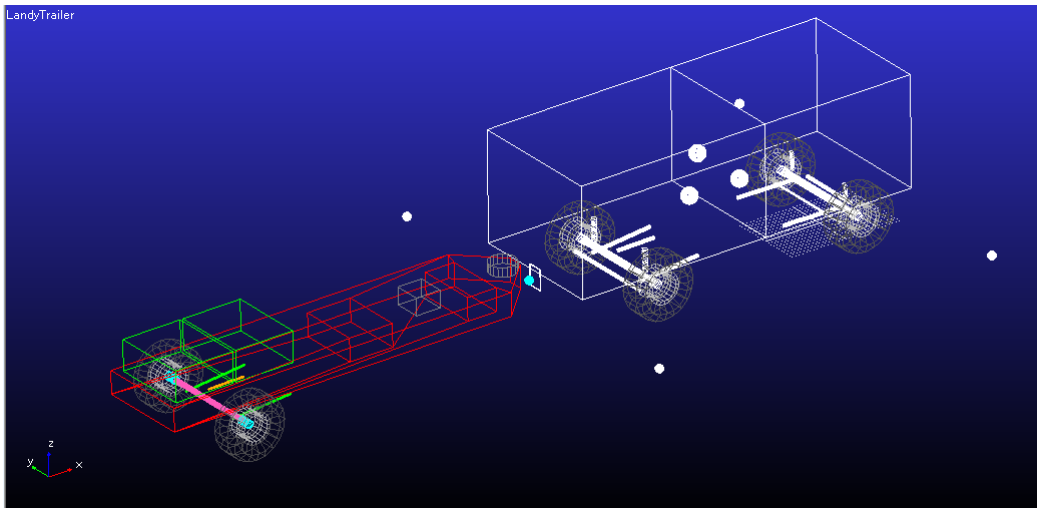

Figure 3.1. Final ADAMS model of the articulated vehicle

3.2.1 Tyre Models

Two types of tyre models can be used in the ADAMS model; these include a Pacejka tyre model and a FTire model. The Pacejka tyre model is a non-linear tyre model that models the contact patch as a single point load [Pacejka et al., 1989]. The FTire model is a non-linear physics based model of the Michelin LTX A/T2 235/85R16 SUV tyre. This model is a far more accurate representation of a realistic tyre due to the fact that it takes tyre parametrization data such as the footprint, hardness, vertical stiffness as well as lateral, longitudinal and torsional stiffness into account [Gipser, 2004]. A FTire model is able to handle intricate geometry and therefore can handle rough road profiles whereas a Pacejka tyre model is only accurate on smooth roads. A FTire model can also handle higher frequencies and more complex tread geometry. The reason that two tyre models are investigated is due to the fact that both models are valuable. They both are able to simulate the dynamics required for this study for with FTire being slightly more accurate. The Pacejka tyre model is used first for simulations due to the fact that it is far less computationally expensive than FTire. The simulation time is thus a lot shorter than FTire which meant that results were able to be analysed sooner. Once the initial results with Pacejka are deemed satisfactory the simulations are performed using FTire for the increased accuracy.

3.3 Static Force Analysis

A force analysis is performed to determine the static vertical forces at the tyres. These forces are required as an input to the simulation model and also form part of the SUV suspension spring model. To complete this force analysis, the articulated vehicle is separated into two rigid bodies and a sum of forces and moments were used to calculate the forces. All the forces that were determined in this analysis are stored in Table 3.1.

Table 3.1. Vertical forces at the tyres of the articulated vehicle

	Unloaded	Loaded
$F_{z,fr}$	5151 N	5211 N
$F_{z,fl}$	5151 N	5211 N
$F_{z,lr}$	5403 N	5207 N
$F_{z,rr}$	5403 N	5207 N
$F_{z,t}$	4564 N	15008 N
$F_{z,H}$	1027 N	755 N

3.4 Land Rover Model and Parameters

The towing vehicle parameters are defined in this section as they are necessary for the mathematical models that shall be used in the development of the controller. The Land Rover used in this study has already been modified to include a controllable suspension and a brief discussion on this system is included to give the reader some more understanding surrounding the SUV model. The Land Rover has been used many times over the years in the Vehicle Dynamics Group (VDG) by many researchers at the University of Pretoria. All the vehicle parameters are, therefore known and are defined in Table 3.2 [Uys et al., 2006]. These parameters are also confirmed in the ADAMS model.

Table 3.2. Vehicle Parameters

Parameter	Description	**Value**
l_1	Length from front axle to rear axle	2.8 m
a_1	Length from front axle to CG	1.3 m
b_1	Length from CG to rear axle	1.5 m
c_1	Length from CG to hitch point	2.754 m
e_1	length from rear axle to hitch point	1.254 m
h_1	Length from CG to roll axis	0.14 m
m_1	Vehicle mass	2047 kg
m_{s1}	Vehicle sprung mass	1576 kg
I_{z1}	Yaw moment of inertia	2057 kgm^2
I_{xs1}	Roll moment of inertia	839 kgm^2

3.4.1 Land Rover Suspension

The suspension and damping of the SUV is more complicated due to the fact that a controllable suspension has been implemented on it. This suspension is known as the 4 State Semi-active Suspension System ($4S_4$) [Els, 2006]. This system enables switching between low and high damping as well as between soft and stiff springs for optimal ride comfort and handling. The strut is connected to two accumulators via the control valves and the hydraulic damper valves. The spring stiffness is created using hydro-pneumatic springs [Els, 2006]. The system has two accumulators, one with a large volume and one with a smaller volume. The damping is controlled with the use of bypass valves, where the oil can be passed through a low resistance channel during the low damping setting but otherwise it can be forced through an orifice when the valve is closed for the high damping setting. The basic diagram of the system can be seen in Figure 3.2.

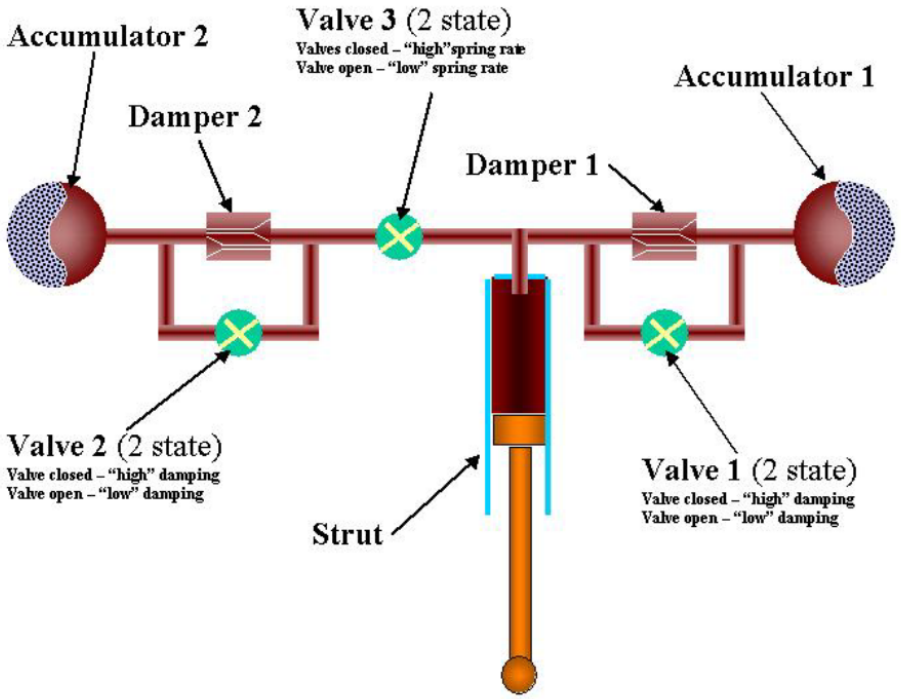

Figure 3.2. $4S_4$ Circuit diagram [Els, 2006]

If we close valve 3, the oil can only pass to accumulator 1, with a small volume, and therefore acts like a stiff spring. When valve 3 is open, the oil is able to pass to both accumulators which then has a large total gas volume and hence acts as a soft spring. Valves 1 and 2 function as the low resistance bypass valves, which, when closed, forces the oil to pass through the high flow resistance dampers 1 and 2 to achieve high damping. When valves 1 and 2 are open the oil will bypass these damper packs and have a low flow resistance and hence low damping [Els, 2006]. The hydro-pneumatic spring is modelled by making use of an ideal gas model and adiabatic compression assumption.

3.5 Trailer Parameters

The trailer parameters have been previously measured by van de Merwe, (2018). He measured the inertia's for each loading condition as well as the centre of gravity, providing the required distances needed. There were unfortunately some discrepancies with the yaw inertia. A simple CAD model was generated in SOLIDWORKS to find the yaw inertia's. These yaw inertias were finalized during the model validation. All the parameters that are known about the trailer and are needed for the modelling of the trailer are recorded in Table 3.3.

Table 3.3. Trailer Parameters

		Loading Condition	
Trailer Parameters	**Description**	**Unloaded**	**Fully-loaded**
m_2 $[kg]$	Trailer Mass	633	1610
m_{s2} $[kg]$	Trailer Sprung Mass	404	1381
I_{z2} $\left[kgm^2\right]$	Yaw moment of inertia	911	1790
I_{xs2} $\left[kgm^2\right]$	Roll moment of inertia	66.36	476.95
l_2 $[m]$	Length from hitch to axle	4.48	4.48
b_2 $[m]$	Length from CG to axle	0.823	0.223
a_2 $[m]$	Length from hitch to CG	3.657	4.257
h_2 $[m]$	Length fom CG to roll axis	0.503	0.503

The parameters that were defined in this section are essential in order to solve the mathematical models that are used in the development of the controller.

3.6 Experimental validation of the ADAMS model

Since a control system is implemented in this research study, it is imperative that there is confidence in the simulation model. Ultimately, the simulation model must be deemed as realistic or as close to the real vehicle as possible. It is therefore necessary to run experimental tests with the real vehicle and compare the results to the simulation results. In this section, validation is performed using a loaded trailer using two manoeuvres. The manoeuvres used include a Double Lane Change(DLC) as well as a constant radius turn.

3.6.1 Vehicle Instrumentation

In this study, a MicoAutoBox II (MABX) [dSPACE, 2020] is used as well as a two VBox 3i differential GPS that has been integrated with an inertial measurement unit [VBOX automotive, 2020]. The MABX is used to process signals as well as record the data of the vehicle states. The two Vboxes are used to record the vehicle and trailers roll, pitch and yaw rates, the lateral, longitudinal and vertical accelerations as well as the GPS location, vehicle speed and heading. The Vbox also contains an integrated Kalman Filter that is used to find the yaw and roll angles of both the vehicle and the trailer. The Vbox 3i data is sampled through a CAN bus interface and other sensor measured data is measured using analogue channels. The other data that is measured includes the steering angle, hitch angle and

trailer CG accelerations. Table 3.4 and Table 3.5 summarises the vehicle and trailer measured states respectively along with the corresponding measurement device. For the loaded trailer validation tests, two outriggers were added to the setup at the front of the Land Rover and the rear of the trailer. The outriggers were added as a safety concern and are depicted in Figure 3.3.

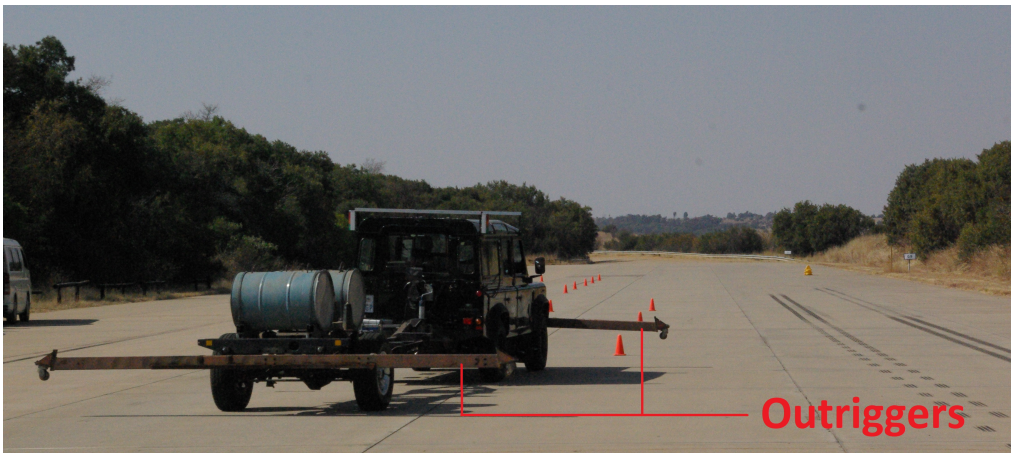

Figure 3.3. Articulated vehicle setup showing outriggers

Table 3.4. State and corresponding measurement device for the tow vehicle

State	Sensor/Actuator
Vehicle Position	Vbox 3i
Vehicle Speed	
Longitudinal, Lateral, Vertical Acceleration	
Yaw angle, Rate	
Roll angle, Rate	
Steering Angle	Celesco Potentiometer
Suspension Displacements	String Potentiometer x4
Brake Pressure	Pressure Transducers

Table 3.5. State and corresponding measurement device for the trailer

State	Sensor/Actuator
Trailer Position	Vbox 3i
Trailer Speed	
Longitudinal, Lateral, Vertical Acceleration	
Yaw angle, Rate	
Roll angle, Rate	
Hitch Angle	String Potentiometer
X,Y, Z accelerations at the CG	MEMSIC Accelerometer

3.6.2 Handling Manoeuvres

Different handling manoeuvres and how they are applied are a key part of this study as these manoeuvres shall be used to validate the model as well as to test how the articulated vehicle is controlled. Two handling manoeuvres shall be used for the duration of this study, a Double Lane Change (DLC) and a constant radius turn.

3.6.2.1 Double Lane Change

A DLC is a standardised manoeuvre that has been prescribed by the ISO3888-1 standard. A double lane change is most commonly used to evaluate the handling characteristic and vehicle dynamics of a particular vehicle.

A DLC or severe lane change is executed by driving the vehicle out of its driving lane to a lane that is parallel and next to the original driving lane, this is the first part of the manoeuvre. The second part is completed when that vehicle swerves back into the original driving lane from the current driving lane, hence the name 'double' lane change. A pre-determined speed must remain constant throughout the duration of the manoeuvre. A situation in which a driver would execute this manoeuvre on the road is when an obstacle in the road forces the driver to swerve into another lane such as oncoming traffic for a brief period before having to swerve back into the original lane. According to the standard, successful completion of the double lane occurs when the vehicle can execute the manoeuvre at a constant speed while remaining within the set bounds and without knocking any of the cones or boundary markers over. Vehicle performance is rated on the maximum speed a vehicle can successfully complete the

double lane change [International Standard of Organisation, 1999]. The main disadvantage of this manoeuvre is that the test is highly based on driver input and therefore, the maximum speed of the vehicle is directly related to the driving skills of the driver. This effect can be minimised by using the same driver for every test as well as running the test a couple of times to get a well-averaged result. The DLC is set up using cones placed on the outer edge of the boundary lines. Five equidistant cones are placed on either side of the boundary lines that are denoted as E where three equidistant cones are placed on either side of the lanes that have been denoted as A and C. The layout of the DLC is depicted in Figure 3.4.

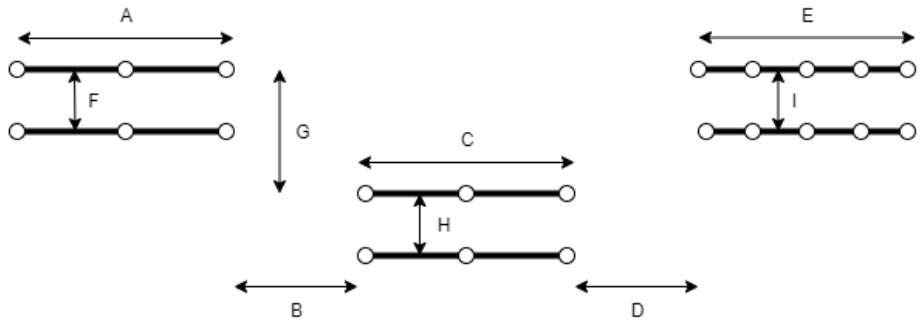

Figure 3.4. Schematic of a DLC [International Standard of Organisation, 1999]

The cones that are used to set up the path must be of standard size and dimensions. This is done to ensure that the test is as standardised as possible. The variables defined as A-I in Figure 3.4 are based on set distances as well as distances based on vehicle width. This parameters are recorded in Table 3.6.

Table 3.6. Double lane change dimensions [International Standard of Organisation, 1999]

Parameter	Dimension [m]
A	15
B	30
C	25
D	25
E	30
F	1.1 x vehicle width
G	1.2 x vehicle width
H	1.3 x vehicle width
I	1.3 x vehicle width

3.6.2.2 Constant Radius Turn

The second manoeuvre that shall be used to analyse the handling of an articulated vehicle is a constant radius turn. The procedure of this manoeuvre is to drive around a circle at a low speed, when the lateral acceleration is negligible, and note the steering angle needed to maintain the turn [Gillespie, 1992]. The speed of the vehicle is then increased in steps in order to produce lateral acceleration at certain increments and noting the steering angle at each increment [Gillespie, 1992]. Figure 3.5 depicts a schematic of a constant radius turn.

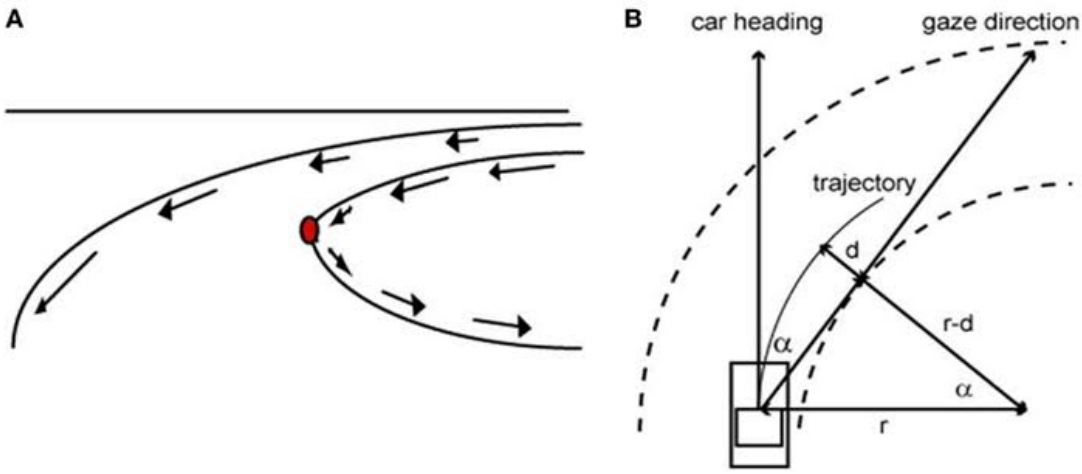

Figure 3.5. Schematic of a constant radius turn handling manoeuvre [Rybarczyk and Mestre, 2012]

3.6.3 Articulated vehicle model validation for a loaded trailer

The lateral dynamics of the simulation model with a loaded trailer were validated by performing experimental tests at the Gerotek Testing Facility [defenceWeb, 2019]. Lateral Validation of the model is completed by comparing the experimental results of a DLC at 40 km/h, 50 km/h and 55 km/h and a clockwise and counter-clockwise constant radius turn using, both the soft and hard suspension. The yaw rate, lateral acceleration and roll angle of both the Land rover and trailer as well as the hitch angle and the lateral acceleration of the trailer measured by the accelerometer are used for validation. The steering angle and speed of the vehicle that was measured during the experimental tests are filtered to remove high frequency noise and are then used as inputs into the simulation model in order to simulate the experimental tests as accurate as possible. The results for a DLC at 55 km/h and the clockwise constant radius turn shall be discussed in this section.

Figure 3.6 and 3.9 portrays the steering angle and speed inputs to the model for a soft and hard suspension for a DLC at 55 km/h respectively. Figure 3.7 depicts the results for the soft suspension during a DLC at 55 km/h whereas Figure 3.10 presents the results for a hard suspension.

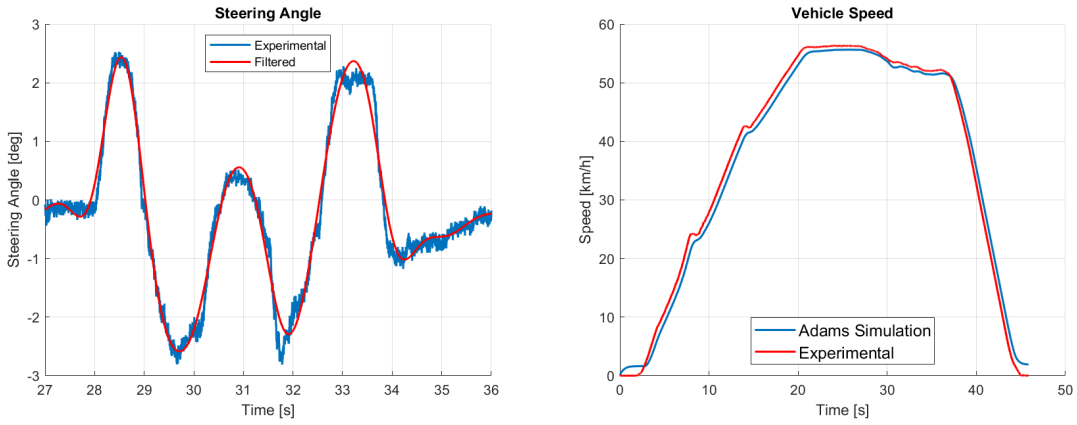

(a) Steering Angle **(b)** Vehicle Speed

Figure 3.6. Speed and steering angle through a DLC at 55 km/h with a soft suspension

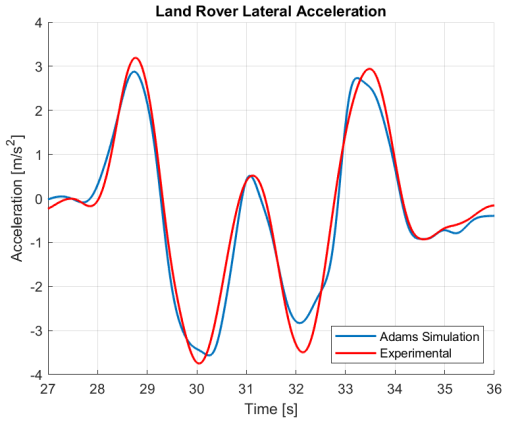

(a) Land Rover Lateral Acceleration

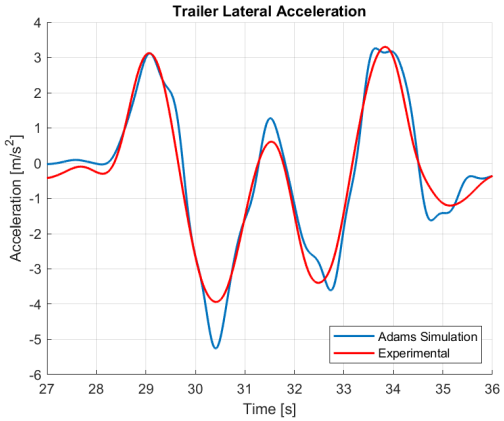

(b) Trailer Lateral Acceleration

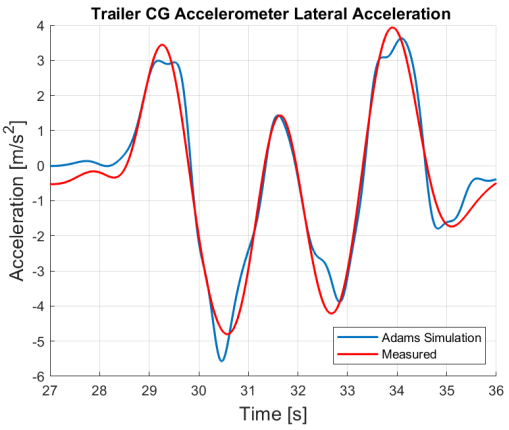

(c) Trailer CG Lateral Acceleration

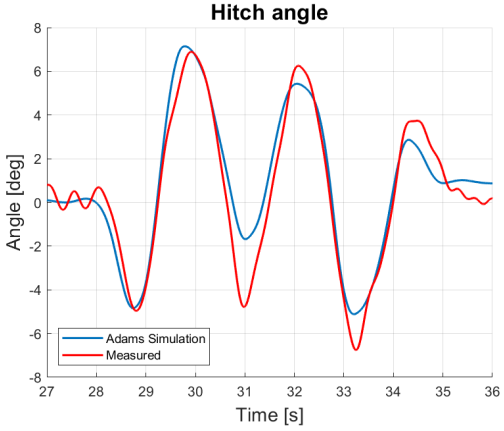

(d) Hitch Angle

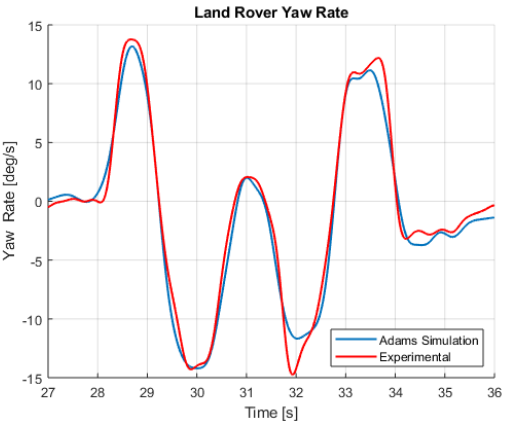

(e) Land Rover Yaw Rate

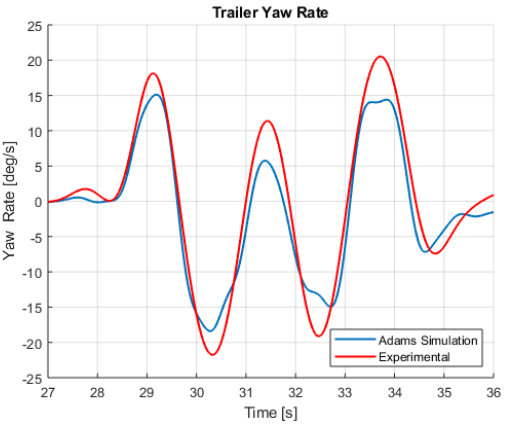

(f) Trailer Yaw Rate

Figure 3.7. 55 km/h loaded DLC soft suspension validation

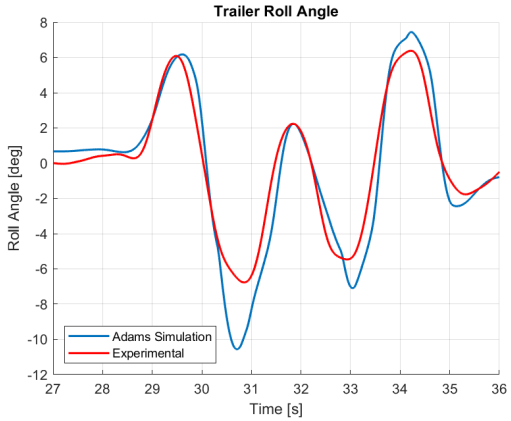

(g) Trailer Roll Angle

Figure 3.7. 55 km/h loaded DLC soft suspension validation (Cont.)

From Figure 3.7, it can be seen that an overall good correlation with the soft suspension is achieved. There are some discrepancies in certain measurements, these include the trailer lateral acceleration, hitch angle, trailer yaw rate and the trailer roll angle. There is a 33.5% difference between the simulated and experimental second peak in the trailer lateral acceleration. When analysing the middle peak of the hitch angle in Figure 3.7(d), there is a 64.44% difference between simulation and experimental results. There is also a 29.71% difference between the fifth peak when investigating the validation results of the trailer yaw rate, Figure 3.7(f). Finally we see a 55.29% difference in the second peak of the trailer roll angle. All the error percentages for each set of results is recorded in Table 3.7 below. These percentage differences could be due to overly smooth steering which suggests the steering angle should have been filtered less. The discrepancies could also be due to differences in inertial parameters and terrain friction as well as differences in the tyre models. Another reason for these discrepancies could be because a completely flat road was used in the simulations and the experimental surface might not be as flat as the simulated road. It is also believed that the soft suspension setting could possibly be affecting the trailer dynamics. There were issues during the gas filling process which means that the exact gas volumes and suspension friction may contribute to the suspension affects which are coupled to other states. It was noticed when analysing the SUV roll angle results that they were not correlating as expected. It is for this reason that the suspension displacements were investigated to give better certainty. They are depicted in Figure 3.11 below.

Table 3.7. Percentage errors in the experimental and simulation results at the main peaks

	Peaks				
Parameters	**One**	**Two**	**Three**	**Four**	**Five**
Land Rover Lateral Acceleration	9.72	5.07	1.92	18.91	7.14
Trailer Lateral Acceleration	0.32	33.50	52.76	5.88	1.23
Trailer CG Lateral Acceleration	13.37	16.04	0.00	7.84	7.87
Hitch Angle	2.42	3.63	64.44	13.12	24.15
Land Rover Yaw Rate	4.36	0.56	2.91	20.79	8.77
Trailer Yaw Rate	16.67	15.39	49.47	22.00	29.71
Trailer Roll Angle	1.48	55.29	0.00	29.80	16.61

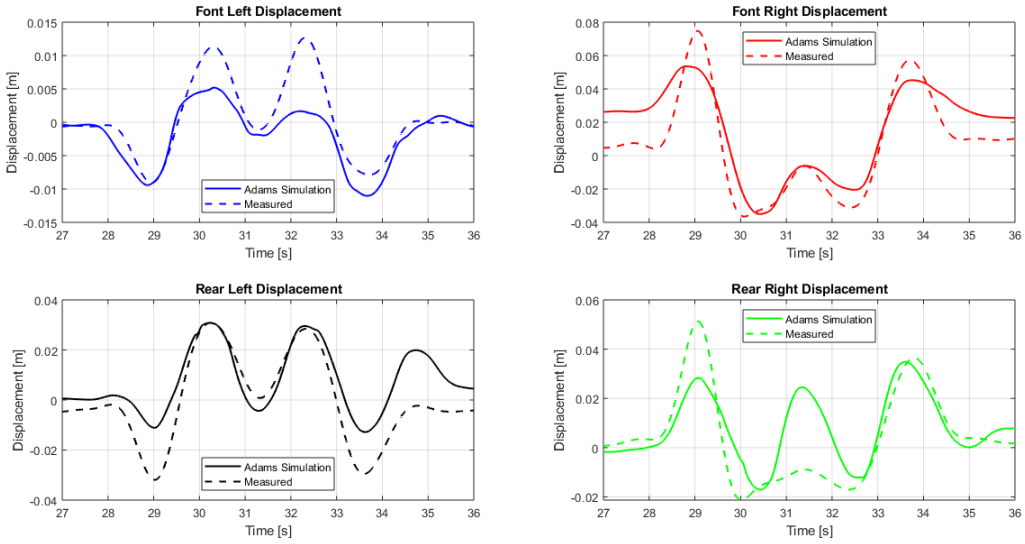

Figure 3.8. Land Rover soft suspension Displacements through a DLC at 55 km/h

From Figure 3.11, discrepancies with the Land Rover suspension displacements are seen. The discrepancy is mainly due to the gas volume uncertainty and suspension friction. There was difficulty in setting up and charging the gas in the Land Rover during experimental tests. To further investigate as to why these discrepancies occurred, further testing should be done to discover what is at fault. A longer amount of time should be used to ensure the gas volumes are properly loaded, leaks that were encountered during tests should be fixed and perhaps the Vbox should be setup for roll mode. The suspension model on the Land Rover should also be re-validated to account for any differences that have occurred over its years of service. These discrepancies could possibly be caused by the current suspension system, friction in the struts as well as overall wear and tear.

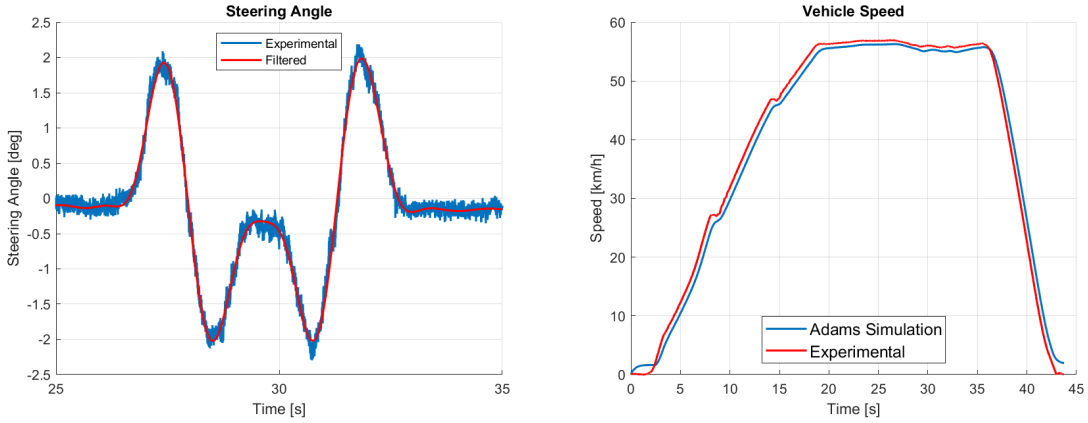

(a) Steering Angle **(b)** Vehicle Speed

Figure 3.9. Speed and steering angle through a DLC at 55 km/h with a hard suspension

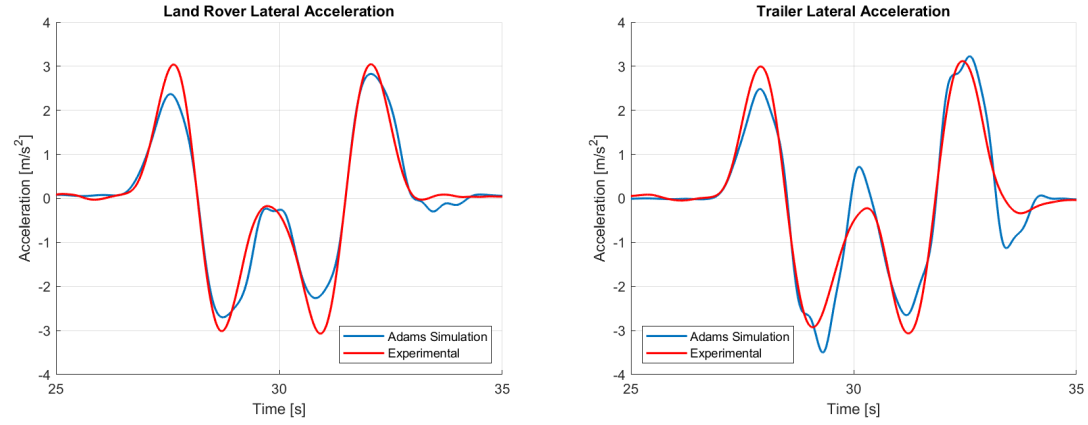

(a) Land Rover Lateral Acceleration **(b)** Trailer Lateral Acceleration

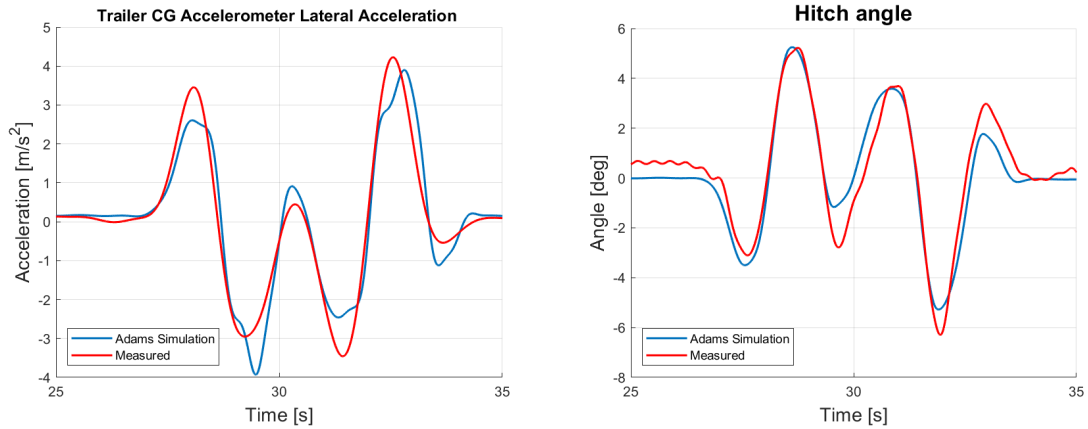

(c) Trailer CG Lateral Acceleration **(d)** Hitch Angle

Figure 3.10. 55 km/h loaded DLC hard suspension validation

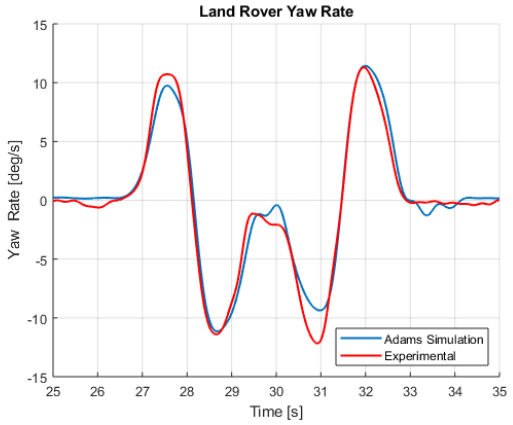

(e) Land Rover Yaw Rate

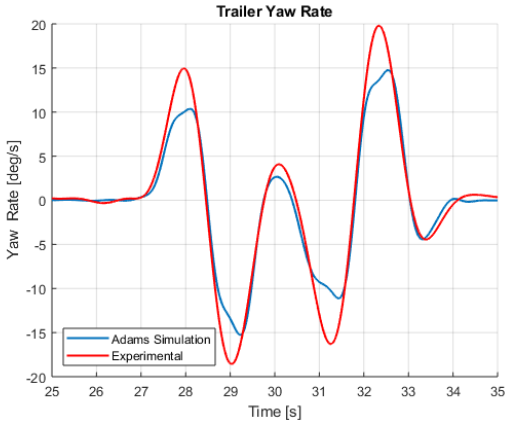

(f) Trailer Yaw Rate

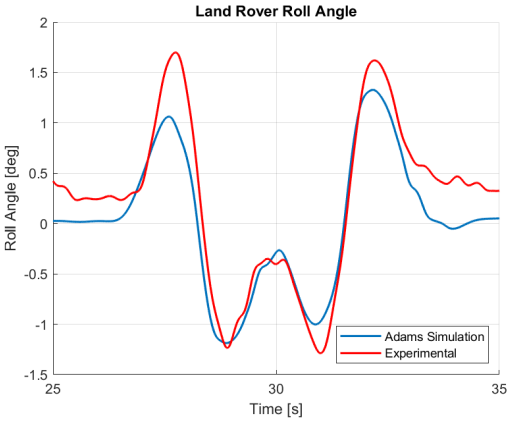

(g) Land Rover Roll Angle

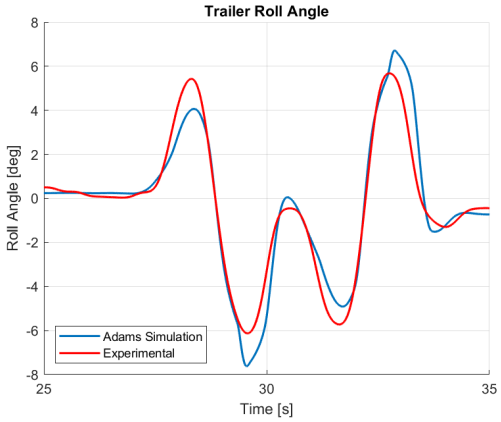

(h) Trailer Roll Angle

Figure 3.10. 55 km/h loaded DLC hard suspension validation (Cont.)

The hard suspension results seen in Figure 3.10 correlate quite well. This statement is reinforced by looking at the error percentages seen in Table 3.8. Majority of the errors between the peaks are below 30% with a few outliers. The largest difference is seen at the middle peak of the hitch angle but overall the differences are quite small. This reinforces that there is not anything really wrong with the model and the discrepancies within the soft suspension model are just a result of differences in the suspension strut.

Table 3.8. Percentage errors in the experimental and simulation results at the main peaks

	Peaks				
Parameters	**One**	**Two**	**Three**	**Four**	**Five**
Land Rover Lateral Acceleration	22.04	10.60	0.59	26.38	6.91
Trailer Lateral Acceleration	17.33	19.45	9.62	13.40	3.53
Trailer CG Lateral Acceleration	24.35	33.22	4.40	28.99	7.80
Hitch Angle	12.90	0.38	57.91	2.72	16.19
Land Rover Yaw Rate	8.96	2.15	1.74	23.03	1.15
Trailer Yaw Rate	30.64	17.77	35.26	32.05	25.59
Land Rover Roll Angle	37.65	4.84	25.00	23.08	17.90
Trailer Roll Angle	25.28	24.14	3.83	14.49	18.34

The steering angle and speed for the clockwise constant radius turn can be seen in Figure 3.11 for a soft suspension and Figure 3.13 for a hard suspension. The validation results are depicted in Figures 3.12 and 3.14.

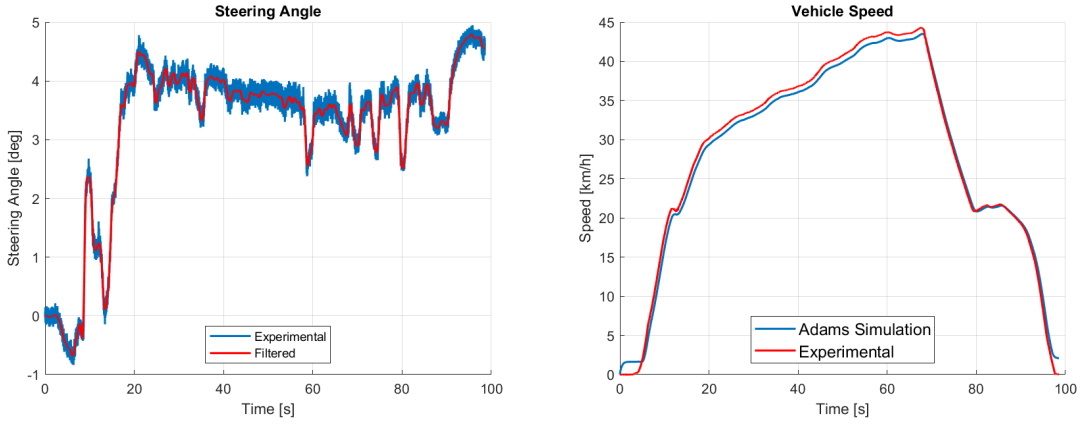

(a) Steering Angle **(b)** Vehicle Speed

Figure 3.11. Speed and steering angle through clockwise constant radius turn with a soft suspension

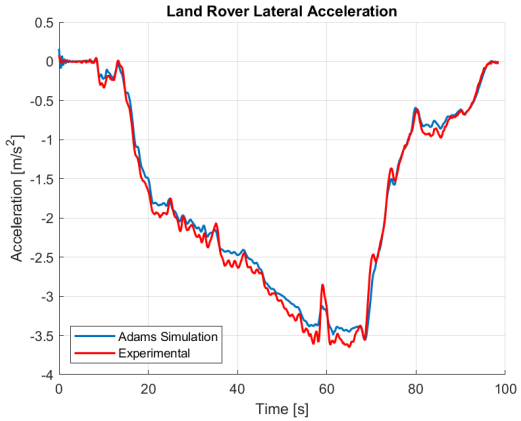

(a) Land Rover Lateral Acceleration

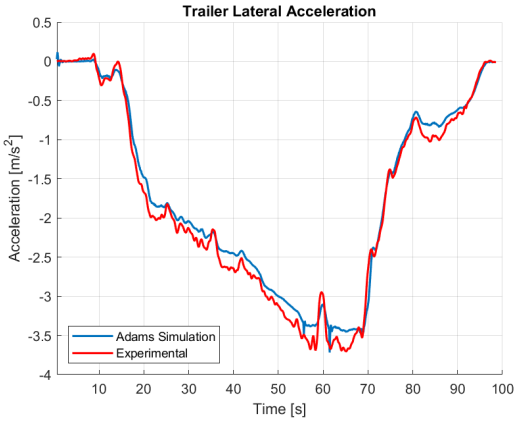

(b) Trailer Lateral Acceleration

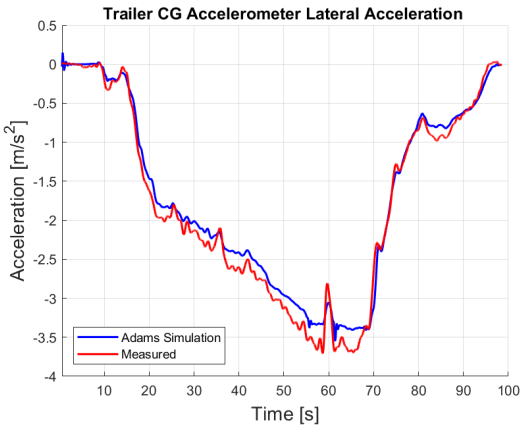

(c) Trailer CG Lateral Acceleration

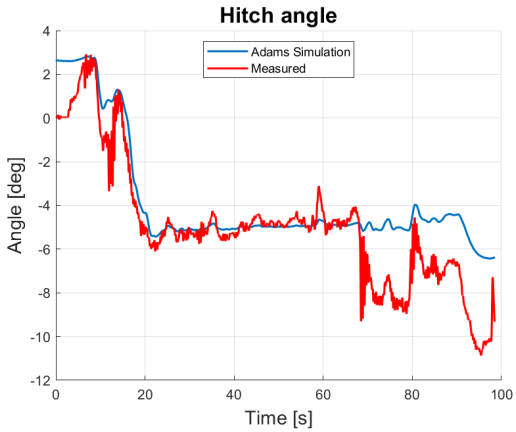

(d) Hitch Angle

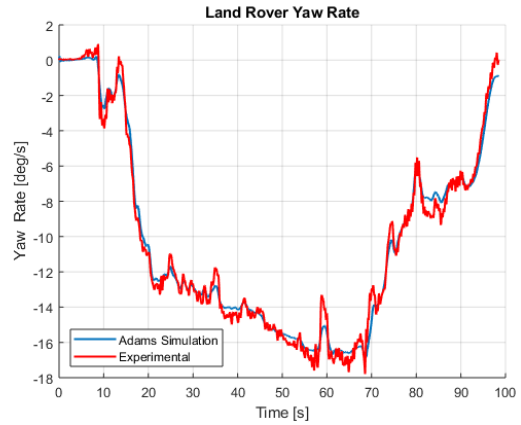

(e) Land Rover Yaw Rate

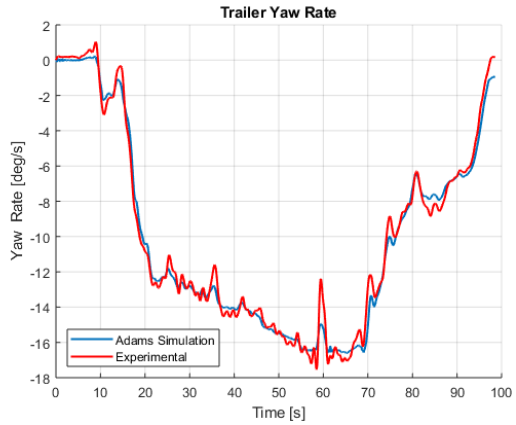

(f) Trailer Yaw Rate

Figure 3.12. Clockwise constant radius turn soft suspension validation

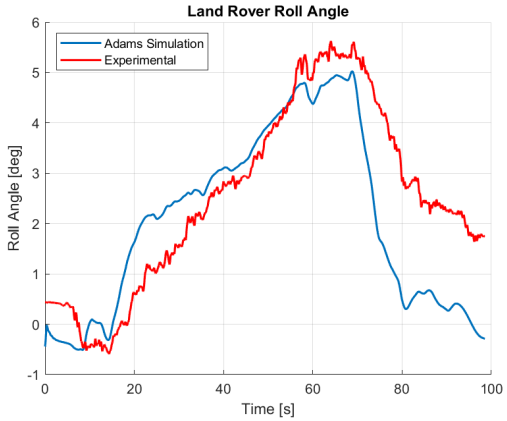

(g) Land Rover Roll Angle

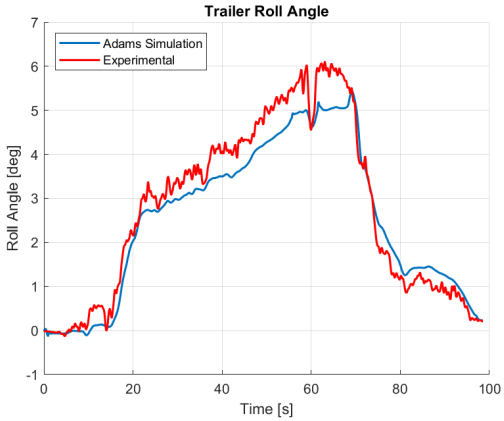

(h) Trailer Roll Angle

Figure 3.12. Clockwise constant radius turn soft suspension validation (Cont.)

From Figure 3.12, it can be seen that majority of the parameters correlate really well. The only discrepancies we see is in the Land Rover roll angle and the hitch angle. The roll angle deviation is mostly due to the suspension differences that were mentioned above in the DLC results. In Figure 3.12(d), it is noticed that there is some oscillation in the experimental hitch angle. This indicates that either the steering was not perfect or the surface changed slightly, meaning the friction coefficient changed during the manoeuvre.

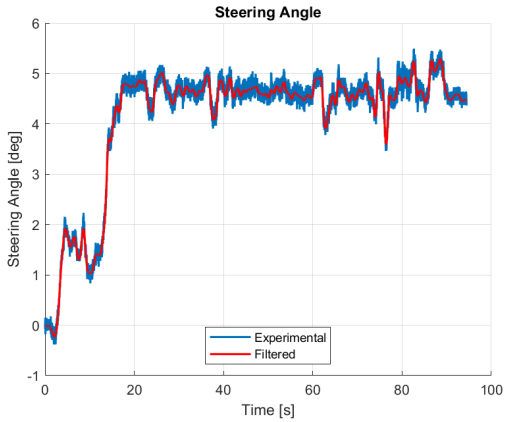

(a) Steering Angle

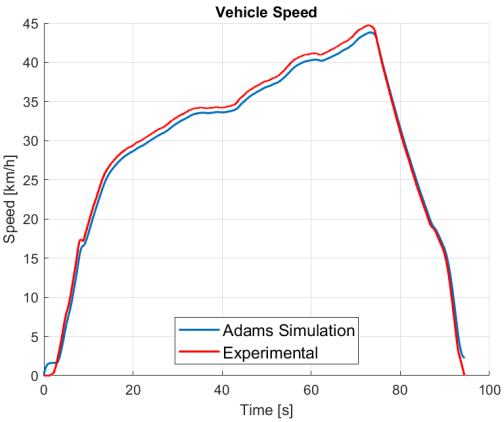

(b) Vehicle Speed

Figure 3.13. Speed and steering angle through clockwise constant radius turn with a hard suspension

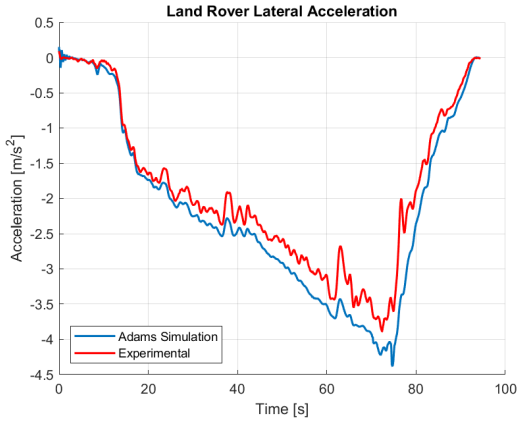

(a) Land Rover Lateral Acceleration

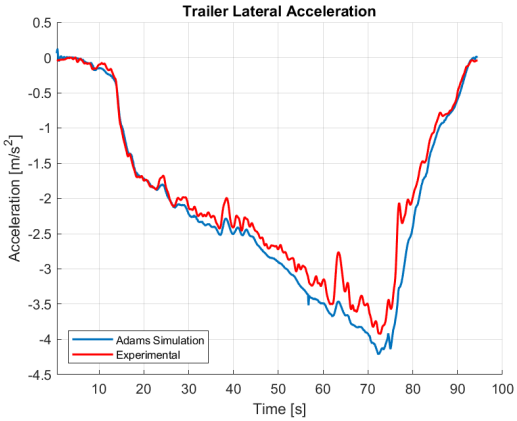

(b) Trailer Lateral Acceleration

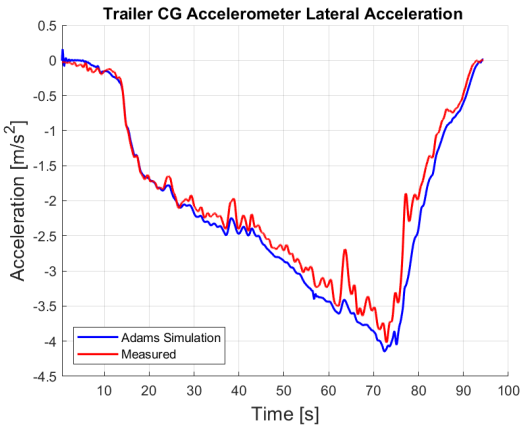

(c) Trailer CG Lateral Acceleration

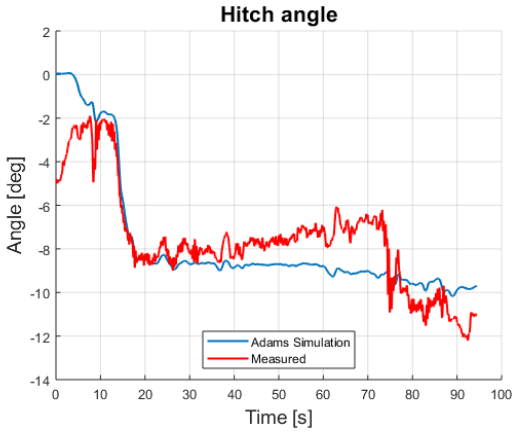

(d) Hitch Angle

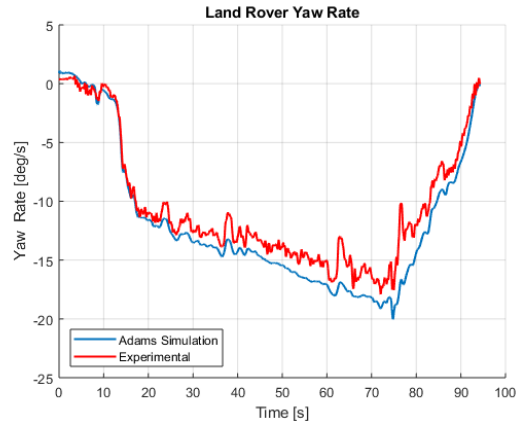

(e) Land Rover Yaw Rate

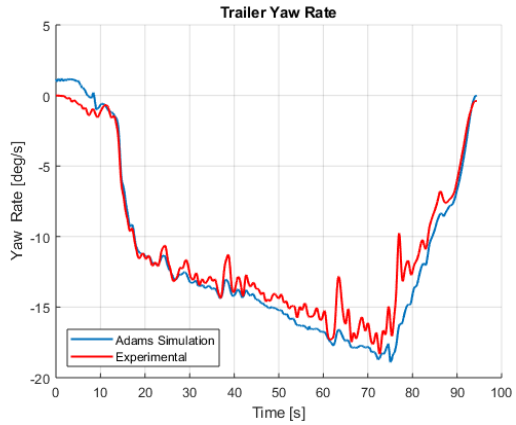

(f) Trailer Yaw Rate

Figure 3.14. Clockwise constant radius turn hard suspension validation

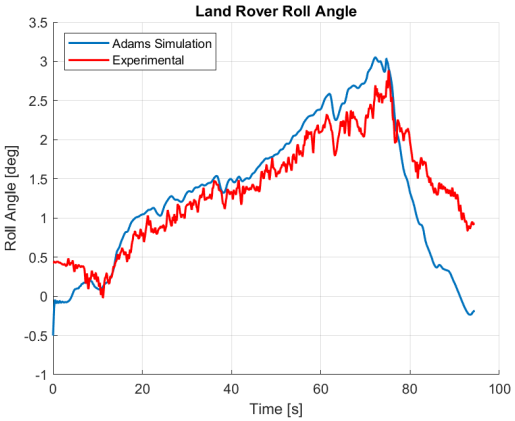

(g) Land Rover Roll Angle

(h) Trailer Roll Angle

Figure 3.14. Clockwise constant radius turn hard suspension validation (Cont.)

It can be seen from Figure 3.14, that the same trend from the soft suspension can be seen here. All the results correlate relatively well with some discrepancies seen in the hitch angle and roll angles. The hitch angle discrepancies are once again due to a change in friction coefficient or imperfect steering. Since the experiments were performed by a human driver, there is also a possibility for human error. The roll angle is once again due to the suspension differences and could also be due to the fact that there were some difficulties encountered with the suspension setup on the day of experimental tests. Ultimately the correlation seen here is very good and proves that the simulation model is quite accurate in replicating a constant radius turn.

3.6.4 Conclusion

In this section, the validation of the simulation model was performed for a loaded trailer. A double lane change as well as a constant radius turn were used as the handling manoeuvres to perform experimental tests using the Land Rover and testing trailer. The results of these experimental tests were then compared to the simulation model results. From the loaded trailer validation results, it can be seen that the model correlates quite well with the simulation model despite small differences, due to errors in the suspension. From the results it can be concluded that the model adequately captures the dynamics of the vehicle for the purpose of developing the controller.

3.7 Conclusion

This chapter placed the focus on the MSC ADAMS model and parameters of an articulated vehicle, how it was constructed and its validation. The highlight of this chapter is the model validation in which the simulation model is validated against experimental tests in order to ensure that it is an accurate representation of real life situations. Two handling manoeuvres, a DLC and constant radius were used to validate the lateral dynamics of the model as well as its roll aspects for both types of the Land Rover suspension settings.

From the validation results we can see that the lateral dynamics of the articulated vehicle model are well captured. Although there are some difference that can be visually seen in the results, this is attributed to the friction within the suspension system as well as the uncertainty of the gas volumes. Overall, the trend of the lateral dynamics in both the experimental and simulation correlate relatively well. It can therefore be stated that the simulation model is properly validated for the purpose of developing a control system.

4. Development of the control system

4.1 Introduction

This chapter shall discuss the Nonlinear Model Predictive Controller (NMPC), an NMPC is developed since a nonlinear prediction model is used. This controller focuses on yaw rate control using differential braking or torque vectoring of the trailer. The NMPC is developed here, with the help of the ACADO toolkit, as it has the ability to handle nonlinear models as well as a variety of constraints that can be solved in real time. This chapter also discuses two mathematical models, a Single Track Model (STM) that is used as the vehicle reference model as well as an Extended Single Track Model (ESTM) that is used to predict the future states of the vehicle for the NMPC. Finally a brief description of a proportional controller on the yaw moment of the trailer is described. This controller is used to create a comparative between the NMPC and what is a more generic and simple controller.

4.2 Model Predictive Control

This section places its focus on the development of the NMPC. The derivation of the controller and its constraints as well as the two mathematical models it needs to function is performed. This NMPC optimises the left and right trailer brake forces based on the future state predictions. The torque vectoring algorithm that is used to convert the output control forces into torques is also defined. Finally, the Simulink implementation of the controller is also described to show how the controller interlinks with the validated nonlinear ADAMS model.

4.2.1 Controller Design

The NMPC was developed and implemented with the help of the ACADO toolkit. ACADO toolkit is a software environment as well as an algorithm collection that has been written in C++ specifically for automatic control and dynamic optimisation [Ariens et al., 2011]. It is an Open-source software and is free to download and install. It provides a variety of algorithms that can be used for direct optimal control and is hence very well developed for model predictive control. More, specifically, the ACADO toolkit that was used for this controller is called ACADO for Matlab. ACADO for Matlab is just a Matlab interface for the ACADO toolkit and hence brings all the ACADO algorithms and integrators for direct optimal control to Matlab [Ariens et al., 2011]. ACADO can also be used in conjunction with Simulink as it can be used to automatically generate an S-function interface or it generates the C code that can be used to call from your own S-function. The ACADO toolkit has great functionality

and capabilities for the control that is performed here and it makes implementing model predictive control a lot simpler and it is for this reason that it was selected for this study. ACADO is used to define the problem, this includes: the predictive model, the online data, the cost function, the optimisation as well as the constraints, and then exports the problem to be used by the S-function in Simulink to run simulations.

The first step in the formulation of the optimisation problem is to select the cost function or objective function. The NMPC finds the optimal control inputs which minimises a cost function. The cost function is chosen to be of the form:

$$J_0(x_0,U) \triangleq \min_{U_0} \sum_{k=0}^{N-1} \left[y_k^{'} Q y_k + uk^{'} R u_k \right] + y_N^{'} P y_N \tag{4.1}$$

subject to:

$$y = x_{ref} - x_{actual}$$

$$\mathbf{x} = \begin{bmatrix} \dot{\psi}_1 & \dot{\psi}_2 & \theta \end{bmatrix}$$

$$\dot{\mathbf{x}} = f(\mathbf{x}, \delta)$$

$$x_0 = x(0)$$

with:

- N as the horizon length
- $x_0, ..., x_N$ and $u_0, ..., u_{N-1}$ as the states and input optimisation variables
- $U \triangleq [u_0, ..., u_{N-1}]$ as the vector of inputs that minimises the cost function
- The input weight **R** being positive definite and symmetric
- The state weight **Q** being positive semi-definite and symmetric
- The terminal weight **P** being positive semi-definite and symmetric

The states and inputs that occur in the cost function are minimised using least squares minimisation. The least squares minimisation minimises the error between the current states and the desired states.

These states do not need to include all the vehicle states to ease computation. The yaw rates of both the vehicle and trailer and the hitch angle are selected because they deliver the most information regarding whether an articulated vehicle is stable or not. The output of the controller $\boldsymbol{U}$. is a brake force vector that includes the left and right braking force on the trailer, that should be able to recover the vehicle in a finite horizon. The integrator that is used is, 4th order Runge-kutta and the quadratic programming solver is QPOASES. There are two types of constraints that are used in the controller. They include a brake force constraint as well as rollover prevention constraints. Constraints are placed on the trailer braking forces. These constraints are applied to ensure that the amount of braking applied to the vehicle is realistic and not too excessive for the vehicle to handle. The constraints are defined in Equation 4.2 and Equation 4.3 respectively. The maximum amount of deceleration this braking force will cause is 0.95 m/s^2. This deceleration is not too excessive and thus does not cause an unrealistic disturbance to the system.

$$0\,N \leq F_{xl} \leq 3500\,N \tag{4.2}$$

$$0\,N \leq F_{xr} \leq 3500\,N \tag{4.3}$$

The rollover prevention constraints are derived using the measure for rollover propensity, which is the inverse of the rollover threshold, as well as the yaw rates of the trailer and tow vehicle. The rollover threshold is the maximum lateral acceleration that a vehicle driving in steady-state is able to resist in order to prevent rollover from occurring [Dahlberg and Stensson, 2006b]. The derivation for the rollover prevention constraints are defined in Equations 4.4 to 4.7. The definition of the rollover propensity is defined in Equation 4.4.

$$\frac{g}{a_y} = \frac{2h_{CG}}{t} \tag{4.4}$$

where g = gravitational acceleration, a_y = lateral acceleration, h_{CG} = the CG height and t = track width.

The yaw rate is brought into the equation using the lateral acceleration as well as the longitudinal velocity as defined in Equation 4.5 below.

$$a_y = \dot{\psi} v_x \tag{4.5}$$

By substituting Equation 4.5 into Equation 4.4, the resulting equation can be rearranged into the constraints defined in Equations 4.6 and 4.7.

$$-g \leqslant \frac{2h_{CG} v_x \dot{\psi}_1}{t} \leqslant g \tag{4.6}$$

$$-g \leqslant \frac{2h_{CG} v_x \dot{\psi}_2}{t} \leqslant g \tag{4.7}$$

The weights of the controller are used as tuning parameters and were determined using an iterative process to get the best results. The process began by normalising these weights to values that we expect to get during a handling manoeuvre and then proceed to increase these values until the controller is working at its optimum. The input weight, state weight and terminal weight have been recorded in Table 4.1. These weights can be increased or decreased depending on the amount of interventions that is desired by the controller. The time step and preview horizon selected for this controller can also be seen in Table 4.1.

Table 4.1. Weights used for the NMPC

State Weight	
Vehicle Yaw Rate	$\left(\frac{1}{0.6°/s}\right)^2 = \left(\frac{1}{0.01rad/s}\right)^2$
Trailer Yaw Rate	$\left(\frac{1}{1.7°/s}\right)^2 = \left(\frac{1}{0.03rad/s}\right)^2$
Hitch angle	$\left(\frac{1}{0.6°/s}\right)^2 = \left(\frac{1}{0.01rad/s}\right)^2$
Terminal Weight	
Vehicle Yaw Rate	$\left(\frac{1}{0.4°/s}\right)^2 = \left(\frac{1}{0.007rad/s}\right)^2$
Trailer Yaw Rate	$\left(\frac{1}{1.15°/s}\right)^2 = \left(\frac{1}{0.02rad/s}\right)^2$
Hitch angle	$\left(\frac{1}{0.4°/s}\right)^2 = \left(\frac{1}{0.007rad/s}\right)^2$
Input Weight	
Left Brake Force	$\left(\frac{1}{60N}\right)^2$
Right Brake Force	$\left(\frac{1}{60N}\right)^2$
Preview Horizon	
25	
Time Step	
0.005	

As mentioned, this NMPC works by minimising the error between the actual and the desired states. In order for this to occur, the actual and desired states need to be defined. This is done through the generation of two mathematical models. The desired vehicle states or reference states are determined using a vehicle reference model in the form of a linear Single Track Model(STM). The actual states are predicted by the NMPC using a more complex model in the form of a non-linear Extended Single Track Model(ESTM). Both models shall be defined in the following sections.

4.2.2 Vehicle Reference Model

The purpose of a mathematical model involves modelling the dynamics of a system theoretically, and is a great way to highlight the dynamics of the system. Another reason why having a mathematical model is useful is because in most controllers, a stable or idealised reference model is required and the mathematical model can be used as this reference model. Over the years, several analytical or mathematical models have been developed. The majority of research makes use of a linear single

track model that has 3-DOFs: yaw, side-slip angle of the vehicle and lateral acceleration of the towing vehicle with a constant velocity in the longitudinal direction. These types of model has been used by various past researchers [Anderson and Kurtz, 2019, Zhang et al., 2017, He et al., 2005]. Anderson and Kurtz (2019) went on to extend this model to a 4-DOF and 6-DOF model. The 6-DOF model also takes the dynamics of roll into account. A more complex analytical model that was generated using Lagrange equations, that has 24-DOFs, includes roll, yaw and pitch motions, was also built [Darling et al., 2009].

The vehicle reference model is an important requirement for both controllers as it defines the desired response that the vehicle must follow. The mathematical model defined here is a conventional linear 3DOF bicycle model that shall only take the steering angle and velocity of the towing vehicle as an input [Hac et al., 2008]. The following model was proposed by Hac et al (2008) for the main aim being to study the yaw plane dynamics of an articulated vehicle.A linear model is chosen as it solves faster and eases computation. This model has also been used in copious journal articles providing evidence that this model is a simple yet accurate representation of a car-trailer combination. The schematic of an articulated vehicle in the yaw-plane is portrayed in Figure 4.1, showing both the free body diagram and kinetic diagram. The assumptions made to generate this model are highlighted below. The nomenclature seen in Figure 4.1 are defined in the nomenclature table at the beginning of this document.

Assumptions:

- Assume the effects of aerodynamics are negligible.
- Assume the effects of longitudinal deceleration on the lateral dynamics are negligible.
- Assume small angles for the steering angle, therefore $\sin\delta \approx \delta$ and $\cos\delta \approx 1$.
- Assume constant longitudinal velocity therefore, $v_{x1} = v_{x2} = v_x$

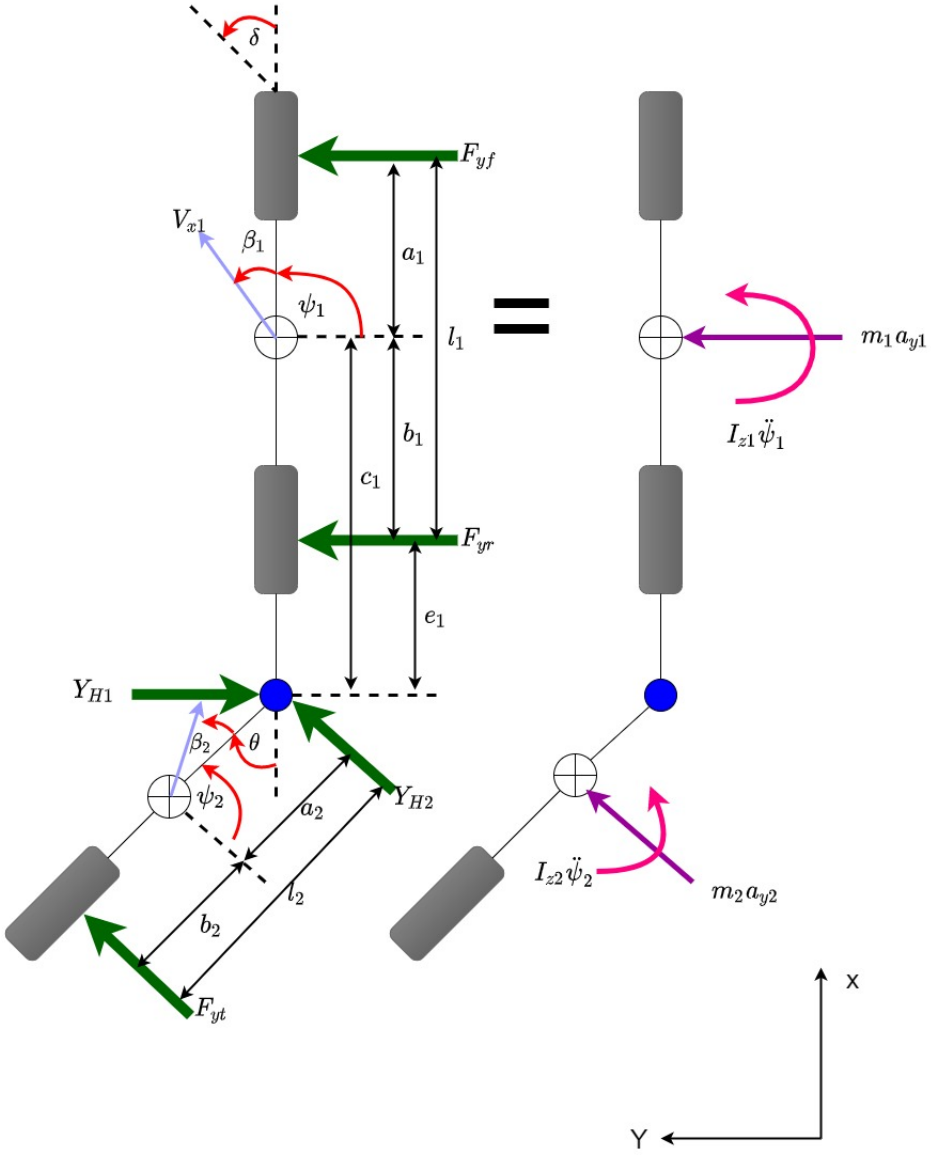

Figure 4.1. Linear single-track model for a single axle trailer for an articulated vehicle

4.2.2.1 Yaw Equations of motion

The equations defining the yaw motions for the towing vehicle and trailer are represented in Equations 4.8 and 4.9 respectively.

$$I_{z1}\ddot{\psi}_1 = F_{yf}a_1 - F_{yr}b_1 + Y_{H1}c_1 \tag{4.8}$$

$$I_{z2}\ddot{\psi}_2 = Y_{H2}a_2 - F_{yt}b_2 \tag{4.9}$$

4.2.2.2 Lateral Equations of motion

The lateral equations of motion for the towing vehicle and trailer are defined in Equations 4.10 and 4.11.

$$m_1 a_{y1} = F_{yf} + F_{yr} - Y_{H1} \tag{4.10}$$

$$m_2 a_{y2} = F_{yt} + Y_{H2} \tag{4.11}$$

4.2.2.3 Kinematic Relationships

With the combination of the towing vehicle and the single axle trailer it was found that certain kinematic relationships hold. These relationships are defined in Equations 4.12, 4.13 and 4.14.

$$\dot{\psi}_2 = \dot{\psi}_1 + \dot{\theta} \tag{4.12}$$

$$a_{y1} = \dot{v_{y1}} + v_x \dot{\psi}_1 \tag{4.13}$$

$$a_{y2} = \dot{v_{y1}} + v_x \dot{\psi}_1 - c_1 \ddot{\psi}_1 - a_2 \left(\ddot{\psi}_1 + \ddot{\theta}\right) \tag{4.14}$$

4.2.2.4 Lateral Tyre Forces

The tyre forces for the front and rear tyres of the towing vehicle as well as the tyre force for the trailer tyres are defined in Equations 4.15, 4.16 and 4.17.

$$F_{yf} = -C_{yf}\alpha_f = -C_{yf}\left(\frac{v_{y1} + a_1\dot{\psi}_1}{v_x} - \delta\right) \tag{4.15}$$

$$F_{yr} = -C_{yr}\alpha_r = -C_{yr}\left(\frac{v_{y1} - b_1\dot{\psi}_1}{v_x}\right) \tag{4.16}$$

$$F_{yt} = -C_{yt}\alpha_t = -C_{yt}\left(\frac{v_{y1} - (c_1 + l_2)\dot{\psi}_1 - l_2\dot{\theta}}{v_x} - \theta\right) \tag{4.17}$$

4.2.2.5 Linear Model

Equations 4.8 to 4.16 were then combined to form a linear set of equations represented by Equation 4.18. The equations were combined using the assumption that the hitch force at the vehicle is equal to the hitch force at the trailer, hence $Y_{H1} = Y_{H2} = Y_H$.

$$\mathbf{M}\dot{\mathbf{x}} = \mathbf{D}\mathbf{x} + \mathbf{E}\delta \tag{4.18}$$

Equation 4.18 can be written in the alternative form defined in Equation 4.19 where $\mathbf{A} = \mathbf{M}^{-1}\mathbf{D}$ and $\mathbf{B} = \mathbf{M}^{-1}\mathbf{E}$.

$$\dot{\mathbf{x}} = \mathbf{A}\mathbf{x} + \mathbf{B}\delta \tag{4.19}$$

The state vector $\mathbf{x}$ contains the lateral velocity of the towing vehicle, the yaw rate of the towing vehicle, the hitch rate and the hitch angle as defined in Equation 4.20.

$$\mathbf{x} = \begin{bmatrix} v_{y1} & \dot{\psi}_1 & \dot{\theta} & \theta \end{bmatrix}^T \tag{4.20}$$

Finally the matrices $\mathbf{M}$, $\mathbf{D}$ and $\mathbf{E}$ in Equation 4.19 are defined in Equations 4.21 - 4.23.

$$\mathbf{M} = \begin{bmatrix} m_1 + m_2 & -m_2(c_1 + a_2) & -m_2 a_2 & 0 \\ m_1 c_1 & I_{z1} & 0 & 0 \\ -m_2 a_2 & I_{z2} + m_2 a_2 (c_1 + a_2) & I_{z2} + m_2 a_2^2 & 0 \\ 0 & 0 & 0 & 1 \end{bmatrix} \tag{4.21}$$

$$\mathbf{D} = \begin{bmatrix} -\frac{C_{yf}+C_{yr}+C_{yt}}{v_x} & -\frac{C_{yf}a_1+C_{yr}b_1+C_{yt}(c_1+l_2)-(m_1+m_2)v_x^2}{v_x} & \frac{C_{yt}l_2}{v_x} & C_{yt} \\ -\frac{C_{yf}(a_1+c_1)+C_{yr}e_1}{v_x} & -\frac{C_{yf}(a_1+c_1)+C_{yr}b_1e_1-m_1c_1v_x^2}{v_x} & 0 & 0 \\ \frac{C_{yt}l_2}{v_x} & -\frac{C_{yt}l_2(c_1+l_2)+m_2a_2v_x^2}{v_x} & -\frac{C_{yt}l_2^2}{v_x} & -C_{yt}l_2 \\ 0 & 0 & 1 & 0 \end{bmatrix} \tag{4.22}$$

$$\mathbf{E} = \begin{bmatrix} C_{yf} \\ C_{yf}(a_1+c_1) \\ 0 \\ 0 \end{bmatrix} \tag{4.23}$$

This model has now been completely derived and is able to model the coupled dynamics of the vehicle and trailer successfully. This model is setup for an unloaded trailer due to the fact that for control purposes we want the laden articulated vehicle to behave as if it was an unladen vehicle. In other words, it is known that an unloaded trailer remains stable constantly and hence we want to use this to ensure that the loaded trailer remains stable as well. The initial conditions for this model are received by the validated nonlinear ADAMS model. The reference trajectories are then solved using Eulers method with a step size of 0.005 and the current states of the vehicle as the initial conditions. These initial conditions are updated for every solution period.

All the required parameters are known and were defined in Chapter 3 except for the cornering stiffnesses. The cornering stiffness of the front and rear tyres on the SUV as well as the trailer tyres were calculated using the Pacejka tyre model. The reason for calculating the cornering stiffness is because the reference model is linear and the cornering stiffness are defined as a constant value. The Pacejka tyre model or the Magic Formula tyre model is a set of formulae that describes how the forces and moments between the road and tyre can be calculated using longitudinal, lateral and camber slip conditions. The aim of the Magic Tyre model is to create an accurate description of steady-state tyre conditions between the tyre and the road. The Magic Formula is defined by Equations 4.24 to 4.26 [Pacejka and Bakker, 2004].

$$y(x) = D\sin[Ctan^{-1}(Bx - E(Bx - \tan^{-1}(Bx)))] \tag{4.24}$$

where

$$Y(X) = y(x) + S_v \tag{4.25}$$

$$x = X + S_h \tag{4.26}$$

With $Y(X)$ standing for side force, brake force or self-aligning torque and (X) denotes either the slip angle (α) or longitudinal slip. The equations that relate the coefficients to the parameters are defined in Equations 4.27 to 4.32. They are used to predict the tyre characteristics by solving for the coefficients that are then applied to the Magic Formula.

$$D = (a_1 F_z + a_2)(1 - a_{15}\gamma)F_z \tag{4.27}$$

$$BCD = a_3 sin\left(2arctan\left(\frac{F_z}{a_4}\right)\right)(1 - a_5\gamma) \tag{4.28}$$

$$C = a_0 \tag{4.29}$$

$$E = (a_6 F_z + a_7) \tag{4.30}$$

$$S_h = a_8 F_z + a_9 + a_{10}\gamma \tag{4.31}$$

$$S_v = a_{11} F_z + a_{12} + (a_{13} F_z^2 + a_{14} F_z)\gamma \tag{4.32}$$

The Magic Formula Tyre Model has been proved to be quite accurate in its predictions even though the vertical force on the tyre is represented as a point load. The mathematical model that is to be generated shall use the magic formula. The coefficients of the tyres currently on the Land Rover and trailer are known and are recorded in Appendix A.

The vertical force at the tyres are needed as an input to the magic formula tyre model. The vertical force for the front and rear tyres have been calculated in the force analysis in Chapter 3. The lateral force as a function of slip angle for the towing vehicle is depicted in Figure 4.2 using the Pacejka model. A bicycle model is used, therefore the vertical force at each tyre for the front and for the rear are multiplied by two.

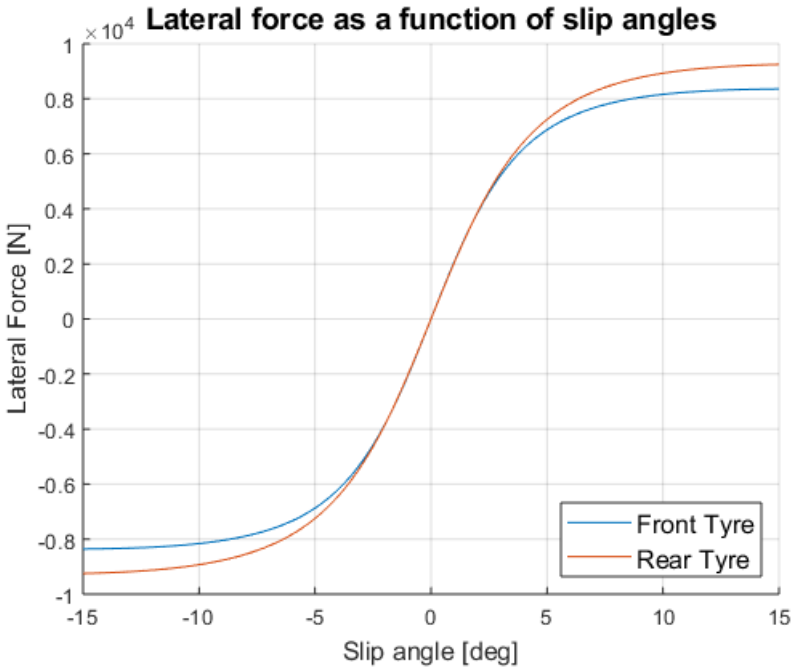

Figure 4.2. Lateral force vs slip angle for the towing vehicle

Figure 4.2 was then used to calculate the cornering stiffness for the front and rear tyres by finding the gradient of the function as close to the origin as possible. A similar process is followed to determine the cornering stiffness of the trailer. The tyres on the trailer are the same tyres that are on the vehicle and therefore the same coefficients, seen in Table A.1 were used. The determined cornering stiffnesses for the SUV and trailer are recorded in Table 4.2.

Table 4.2

Parameter	Value
C_{yf} [N/rad]	1.216 x 10^5
C_{yr} [N/rad]	1.196 x 10^5
C_t [N/rad]	9.885 x 10^4

4.2.3 Extended Single Track Model derivation

This model is more complex than that of the reference model which is why it is used for predictions. It is more complex but it is also limited as to ensure the controller is not too computationally expensive. An extended version of the STM (ESTM) described above was developed by Zhang et al (2017) for the main purpose of analysing the dynamic stability of CTC's with non-linear suspension damper properties. The roll dynamics of the articulated vehicle is taken into account with the yaw dynamics to produce a mathematical model that describes both types of dynamics of the vehicle [Zhang et al., 2017]. The ESTM was used as a baseline to adapt it for a single axle trailer. All symbols with a subscript of 1 indicate the towing vehicle and a subscript of 2 represents the trailer. The model has 5-DOFs where the masses of the vehicle and trailer are denoted as m_1 and m_2. The sprung and unsprung masses of the vehicle and trailer are denoted as $m_{s,1}$, $m_{us,1}$, $m_{s,2}$ and $m_{us,2}$. The yaw moments of inertia are defined as I_{z1} and I_{z2} and the roll moments of inertia are $I_{xs,1}$ and $I_{xs,2}$. The products of inertia for the towing vehicle are $I_{xz,1}$ and $I_{zx,1}$. The suspension spring stiffness coefficients are denoted as c_1 and c_2 while the damping forces are $F_{d,1}$ and $F_{d,2}$. The front steering angle is given as δ_w. The front and rear axle slip angles for the vehicle and the trailer are defined as $\alpha_{f,1}$, $\alpha_{r,1}$, $\alpha_{f,2}$ and $\alpha_{r,2}$ respectively where $C_{\alpha f,1}$, $C_{\alpha r,1}$, $C_{\alpha f,2}$ and $C_{\alpha r,2}$ are the cornering stiffness's for the vehicle and trailer. The lateral forces are defined as $F_{yf,1}$, $F_{yr,1}$, $F_{yf,2}$ and $F_{yr,2}$. The yaw angle and yaw rate are represented as ψ and $\dot{\psi}$. Figure 4.1 can be referred to for most of these symbols. The roll and roll rate is denoted as ϕ and $\dot{\phi}$. v_y and a_y denotes lateral velocity and acceleration and h_1 and h_2 defines the distance from the CG to the roll axis of the vehicle and trailer respectively. The parameters for the yaw dynamics that are seen in Figure 4.1 are the same in this model and the roll dynamic's can be seen in Figure 4.3.

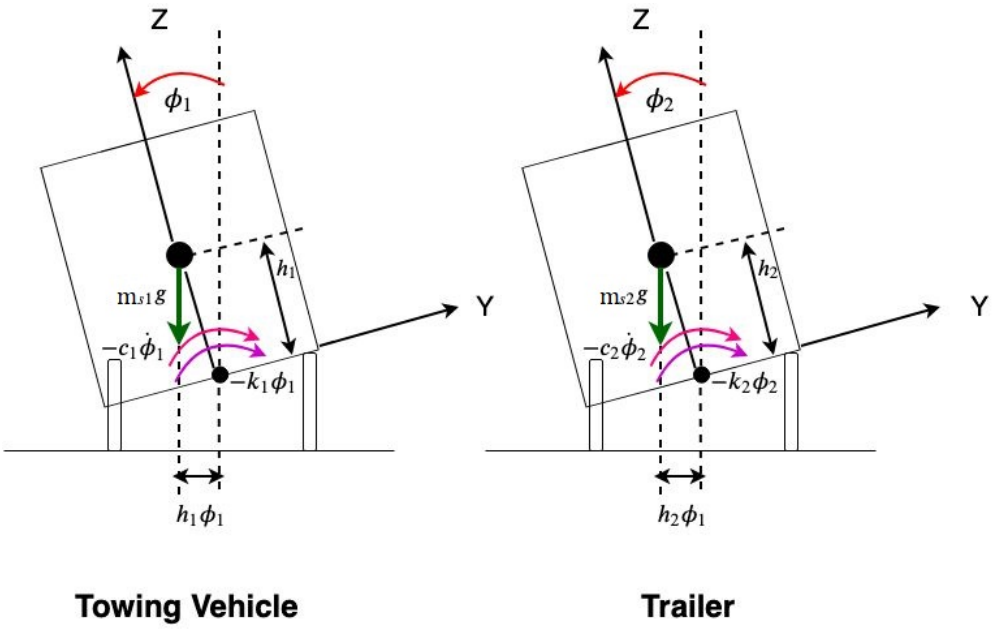

Figure 4.3. Roll dynamics of an articulated vehicle

4.2.3.1 Equations of motion for the SUV

The equations of motion defining the yaw and roll dynamics of the towing vehicle can be found in Equations 4.33 to 4.35. The roll equations do not take the load transfer into account which would alter the vertical forces in the yaw model, thus the roll and yaw are not perfectly coupled. This was done to limit the amount of complexities in the model.

$$m_1 a_{y1} + m_{s1} h_1 \ddot{\phi}_1 = F_{yf} + F_{yr} - Y_H \tag{4.33}$$

$$I_{z1} \ddot{\psi}_1 = F_{yf} a_1 - F_{yr} b_1 + Y_H c_1 \tag{4.34}$$

$$I_{xs1} \ddot{\phi}_1 + m_{s1} h_1 a_{y1} = -C_{\phi 1} \dot{\phi}_1 + (-K_{\phi 1} + m_{s1} g h_1) \phi_1 \tag{4.35}$$

where $Y_H = Y_{H1} + Y_{H2}$

4.2.3.2 Equations of motion for the Trailer

The equations of motion defining the yaw and roll dynamics of the trailer can be found in Equations 4.36 to 4.38. Equation 4.37 includes the control braking forces of the trailer, defined as F_{xr} for the right braking force and F_{xl} as the left braking force. This braking forces are necessary to include as these forces are solved for by the NMPC. They are the control outputs and they are used to introduce the trailer braking to the system.

$$m_2 a_{y2} + m_{s2} h_2 \ddot{\phi}_2 = F_{yt} + Y_H \tag{4.36}$$

$$I_{z2} \ddot{\psi}_2 = -F_{yt} b_2 + Y_H a_2 + \left(-F_{xl} \left(\frac{t}{2} \right) + F_{xr} \left(\frac{t}{2} \right) \right) \tag{4.37}$$

$$I_{xs2} \ddot{\phi}_2 + m_{s2} h_2 a_{y2} = -C_{\phi 2} \dot{\phi}_2 + (-K_{\phi 2} + m_{s2} g h_2) \phi_2 \tag{4.38}$$

4.2.3.3 Kinematic Relationships

The same kinematic relationships that were defined in Equations 4.12, 4.13 and 4.14 are applied to the ESTM.

4.2.3.4 Lateral Tyre Forces

The tyre forces are obtained from the nonlinear Magic Formula tyre model. The Magic Formula tyre model is used to determine the required lateral forces. As mentioned before, the Pacejka tyre model is a function of the tyre slip angle and current vertical force. The slip angles for the front and rear of the SUV as well as the trailer are defined in Equations 4.39, 4.40 and 4.41 respectively. The Pacejka tyre model is represented in Equation 4.42 and is multiplied by 2 since this is a single track model and hence combines the two individual tyres into a single one. The slip angles are converted from radians to degrees because the Pacejka tyre model takes the slip angle input in degrees.

$$\alpha_f = \left(\frac{v_{y1} + a_1 \dot{\psi}_1}{v_x} \right) \frac{180}{\pi} - \delta \tag{4.39}$$

$$\alpha_r = \left(\frac{v_{y1} - b_1 \dot{\psi}_1}{v_x} \right) \frac{180}{\pi} \tag{4.40}$$

$$\alpha_t = \left(\frac{v_{y1} - (c_1 + l_2)\,\dot{\psi}_1 - l_2 \dot{\theta}}{v_x} - \theta \right) \frac{180}{\pi} \tag{4.41}$$

$$F_{yi} = 2f(\alpha_i, F_{zi}) \tag{4.42}$$

where $i = f$ for the front tyre, r for the rear tyre and t for the trailer tyre.

4.2.3.5 Nonlinear System of Equations

Equations 4.33 to 4.42 were then combined using the assumption that the hitch force at the vehicle is equal to the hitch force at the trailer, hence $Y_{H1} = Y_{H2} = Y_H$. Combining these equations led to Equations 4.43 - 4.47 below. The longitudinal deceleration is also taken into account for this model since the stability of an articulated vehicle is closely related to a decrease in speed. The longitudinal deceleration is defined in Equation 4.48.

$$(m_1 + m_2)\dot{v}_{y1} - m_2(c_1 + a_2)\ddot{\psi}_1 - m_2 a_2 \ddot{\theta} + M_{s1} h_1 \ddot{\phi}_1 + M_{s2} h_2 \ddot{\phi}_2 = F_{yt} + F_{yf} + F_{yr} - (m_1 + m_2) v_x \dot{\psi}_1 \tag{4.43}$$

$$-m_2 c_1 \dot{v}_{y1} + (I_{z1} + m_2 c_1 (a_2 + c_1))\ddot{\psi}_1 + m_2 c_1 a_2 \ddot{\theta} - M_{s2} h_2 \ddot{\phi}_2 = F_{yf} a_1 - F_{yr} b_1 - F_{yt} c_1 + m_2 c_1 v_x \dot{\psi}_1 \tag{4.44}$$

$$-m_2 a_2 \dot{v}_{y1} + (I_{z2} + m_2 a_2 (c_1 + a_2))\ddot{\psi}_1 + (I_{z2} + m_2 a_2^2)\ddot{\theta} = m_2 a_2 v_x \dot{\psi}_1 - F_{yt} L_2 + \left(-F_{xl} \frac{t}{2} + F_{xr} \frac{t}{2} \right) \tag{4.45}$$

$$m_{s1} h_1 \dot{v}_{y1} + I_{xs1} \ddot{\phi}_1 = -C_{\phi 1} \dot{\phi}_1 + (-K_{\phi 1} + m_{s1} g h_1)\phi_1 - m_{s1} h_1 v_x \dot{\psi}_1 \tag{4.46}$$

$$m_{s2}h_2\dot{v}_{y1} - m_{s2}h_2(c_1+a_2)\ddot{\psi}_1 - m_{s2}h_2a_2\ddot{\theta} + I_{xs2}\ddot{\phi}_2 = -C_{\phi 2}\dot{\phi}_2 + (-K_{\phi 2} + m_{s2}gh_2)\phi_2 - m_{s2}h_2v_x\dot{\psi}_1 \tag{4.47}$$

$$\dot{v}_x = \frac{(-F_{xl} - F_{xr})\cos\theta}{m_1 + m_2} \tag{4.48}$$

Equations 4.43 to 4.48 are written such that the derivatives of the state vector is the subject of the equation using Matlab, seen in Equation 4.49.

$$\dot{\mathbf{x}} = f(\mathbf{x}, \delta) \tag{4.49}$$

The state vector **x** is defined in Equation 4.50.

$$\mathbf{x} = \begin{bmatrix} x_{y1} & \psi_1 & \theta & \phi_1 & \phi_2 & v_{y1} & \dot{\psi}_1 & \dot{\theta} & \dot{\phi}_1 & \dot{\phi}_2 \end{bmatrix}^T \tag{4.50}$$

The model defined here shall be used by the NMPC to make future predictions of the states described in Equation 4.50. The control braking forces are determined based on an optimisation problem that is solved by the NMPC. Like the reference model, the initial conditions for this model come from the validated nonlinear ADAMS model and they are updated for every solution period. The NMPC trajectories are solved within the controller using 4th order Runge-kutta. All the parameters required for this model are known and were discussed in Chapter 3 except for the roll stiffness and damping of both the SUV and the trailer.

4.2.3.6 Roll stiffness and damping of the SUV

As mentioned in Chapter 3, the SUV has a suspension system known as the $4S_4$. The spring stiffness of the SUV is determined by making the assumption that the process is adiabatic and that the ideal gas law is applicable. This assumption is made due to the hydro-pneumatic springs of the $4S_4$ suspension system. Assuming adiabatic system, the modelling of the spring stiffness begins with Equation 4.51.

$$P_2V_2 = P_1V_1^n \tag{4.51}$$

where n = 1.3 for Nitrogen, P denotes pressure and V denotes volume.

Equation 4.51 is re-arranged in such a way to determine the required pressure using the known volumes. This pressure is needed to determine the spring force, which is defined in Equation 4.52.

$$F = P_1A_{strut} \tag{4.52}$$

The final step is to find the spring stiffness which can be done by deriving the force in terms of $\triangle z_{strut}$ using the forward difference method. The only unknown that is left is $\triangle z_{strut}$, this is determined using the roll dynamics of the SUV, more specifically the roll angle ϕ_1. A relation between the roll moment and the suspension displacements is made based on small angles and is defined in Equations 4.53 to 4.56. s_f and s_r represent this distance between the suspension struts on the front and rear axles respectively. This process does neglect all vertical motion of the vehicle sprung mass.

$$\triangle z_{lf} = \phi_1 \frac{s_f}{2} \tag{4.53}$$
$$\triangle z_{fr} = -\triangle z_{fl} \tag{4.54}$$
$$\triangle z_{lr} = \phi_1 \frac{s_r}{2} \tag{4.55}$$
$$\triangle z_{rr} = -\triangle z_{lr} \tag{4.56}$$

The same relation can be made for the damping of the system using the roll rate $\dot{\phi}_1$. These equations are defined in Equation 4.57 to 4.60.

$$\triangle \dot{z}_{lf} = \dot{\phi}_1 \frac{s_f}{2} \tag{4.57}$$
$$\triangle \dot{z}_{fr} = -\triangle \dot{z}_{fl} \tag{4.58}$$
$$\triangle \dot{z}_{lr} = \dot{\phi}_1 \frac{s_r}{2} \tag{4.59}$$
$$\triangle \dot{z}_{rr} = -\triangle \dot{z}_{lr} \tag{4.60}$$

The damping force of the SUV was modelled using an already existing and validated damper model which produces the damping force as an output. The forward different method is used again to find the damping coefficient by deriving the damping force in terms of the strut velocity. The spring stiffness and damping that have now been determined are then used to calculate the roll stiffness and roll damping using Equations 4.61 and 4.62 respectively. The stiffness and damping coefficients of automobiles are usually presented by assuming that they are collinear.

$$K_{\phi 1} = \frac{s_f^2}{4} K_f + \frac{s_r^2}{4} K_r \tag{4.61}$$

$$C_{\phi 1} = \frac{s_f^2}{4} C_f + \frac{s_r^2}{4} C_r \tag{4.62}$$

Since the stiffness and damping of the SUV is constantly changing, it becomes computationally expensive to continue updating the roll stiffness and damping with every iteration. The decision was hence made to linearize the roll stiffness and damping to provide faster solve times. The linearization was performed by plotting the suspension forces against displacement and the damping forces against velocity to view how linear the change is using a severe double lane change manoeuvre. The DLC was implemented in the simulation. The gradient of these plots are then found to calculate the final value of the roll stiffness and damping that shall be used in the mathematical model. These values are recorded in Table 3.2. The spring force vs displacement is depicted in Figure 4.4(a) and the damping force vs velocity is depicted in Figure 4.4(b).

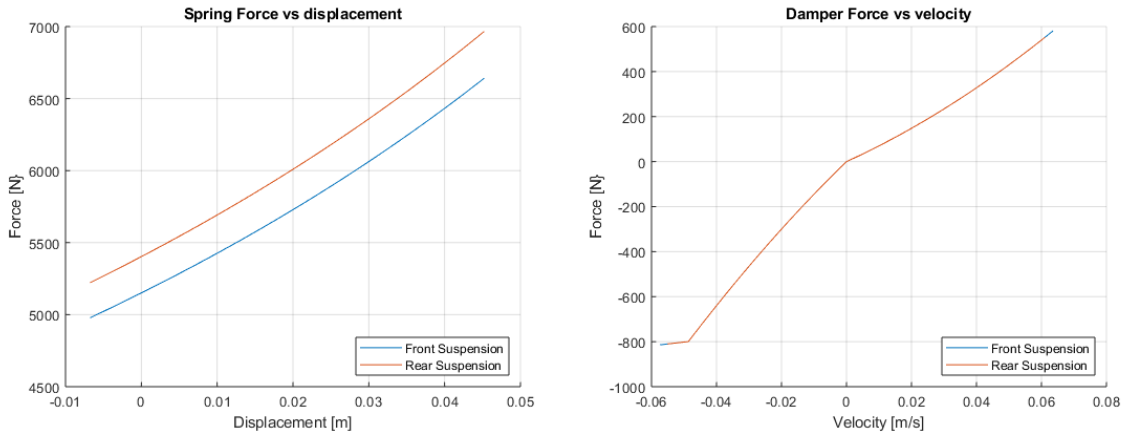

(a) SUV Spring Force vs Displacement

(b) SUV Damper Force vs Velocity

Figure 4.4. Spring and damper plots for the SUV for linearization for a soft suspension for small displacements and velocities

From Figure 4.4(a), it can be seen that the spring of the SUV is fairly linear and the same can be said for Figure 4.4(b). The gradient of these plots was therefore used to calculate roll stiffness and roll damping coefficient's for the SUV, these values can be found in Table 4.3.

4.2.3.7 Roll stiffness and damping of the trailer

The suspension system of the trailer is a lot simpler than that of the SUV and it can therefore be linearized quite easily. Like the damper model of the SUV, a spring and damper model has already been developed and validated for the testing trailer. The same simulation that was used to find the SUV spring stiffness and damping was used to plot the spring and damper force and these plots are depicted in Figure 4.5.

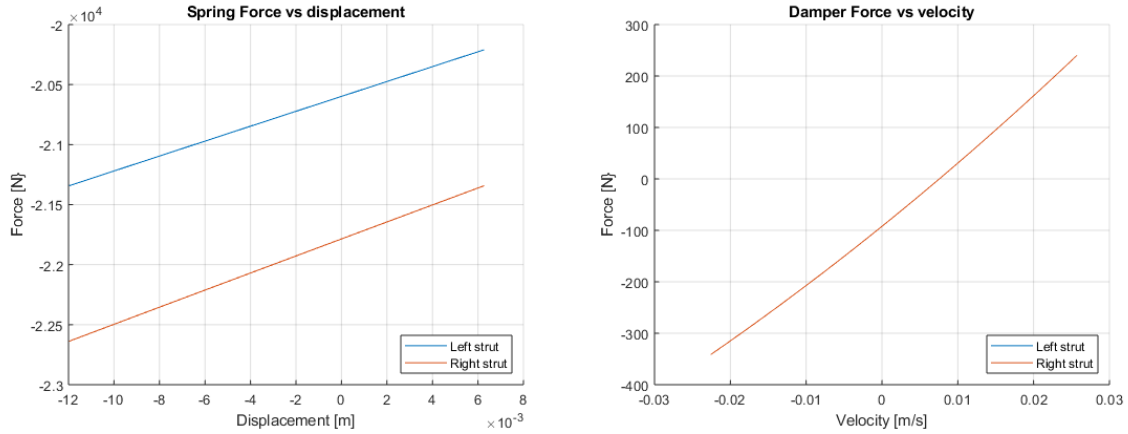

(a) Trailer Spring Force vs Displacement

(b) Trailer Damper Force vs Velocity

Figure 4.5. Spring and damper plots for the trailer for linearization for small displacements and velocities

From Figure 4.5, it can clearly be seen that the spring force is definitely linear and that the damper force is relatively linear. The coefficients that were found using the plots above were used as a baseline to manually tune the values until the optimum fit was found. The final values used are recorded in Table 4.3.

Table 4.3. Roll stiffness and damping of the SUV and trailer

Parameter	Value
$K_{\phi 1}$ $[N/m]$	1.5 x 10^5
$K_{\phi 2}$ $[N/m]$	1.2 x 10^5
$C_{\phi 1}$ $[Ns/m]$	5 x 10^3
$C_{\phi 2}$ $[Ns/m]$	4.5 x 10^3

All the required parameters for this model have now all been defined. This model can therefore be solved and the relevant states can be used in the NMPC.

4.2.4 Force Distribution Model

The optimal trailer yaw moment is generated by the controller via the brakes. A yaw enhancing moment that is in the direction of the yaw rate will act on the tyre that is closest to the radius of the

turn, whereas a yaw opposing moment that is opposite to the yaw rate will act on the opposite wheel. The NMPC has been designed such that it determines the optimal brake forces of the left and right trailer tyres. These optimal brake forces are converted to individual wheel brake torques before being sent back to the simulation model by means of a force distribution algorithm.

A friction circle is determined for each wheel based on its vertical loading and estimated tyre side-slip angle. The lateral tyre force is calculated using the Pacejka tyre model of the Michelin LTX^2 tyres that occur on the trailer. As mentioned before, the Pacejka tyre model relates the tyre lateral force with the side-slip angle which affects the vehicles handling and steering response. The Pacejka tyre model was chosen due to is real time implementation as well as the fact that is has low computation requirements. The Pacejka tyre model is used where the terms are solely dependent on the vertical tyre load as well as the camber and slip angle. The SUV and trailer that form the articulated vehicle in this study both have solid axles. These solid axles ensure that the tyres remain relatively vertical and hence the influence of the camber is neglected. The tyre is able to experience camber due to tyre deflection, but the assumption is made that this is small and therefore negligible.

Each tyres maximum longitudinal brake force is determined based on the friction circle and the road surface friction coefficient. The equations used to define the maximum brake force is defined in Equation 4.63.

$$F_{x,max} = \sqrt{\mu F_z^2 - F_y^2} \tag{4.63}$$

where μ is the road friction coefficient, F_x is the vertical load of the tyre and F_y is the lateral tyre force as determined by the Pacejka tyre model.

The reason the maximum brake force is calculated is to prevent the over saturation of the tyre. If the optimal brake force from the NMPC is greater than the maximum force then the maximum brake force is used instead. However, due to the constraints placed on the forces in the controller, the articulated vehicle should never run into this limitation. Finally, the desired brake torque is calculated as a function of the optimal brake force and the tyres rolling radius, defined in Equation 4.64.

$$T_i = F_{x,i}R \tag{4.64}$$

where R = 0.38 m is the rolling radius and i is l for the left tyre and r for the right tyre.

4.2.5 Simulink Implementation

All simulation work that is completed for this study is performed using a co-simulation between the multibody dynamics software MSC Adams [MSC Software, 2020] and Matlab and Simulink. The validated fully non-linear model of the articulated vehicle is simulated through this process and the controller is implemented through the use of S-function and Matlab function blocks in Simulink. The simulation process of the controller is portrayed in Figure 4.6.

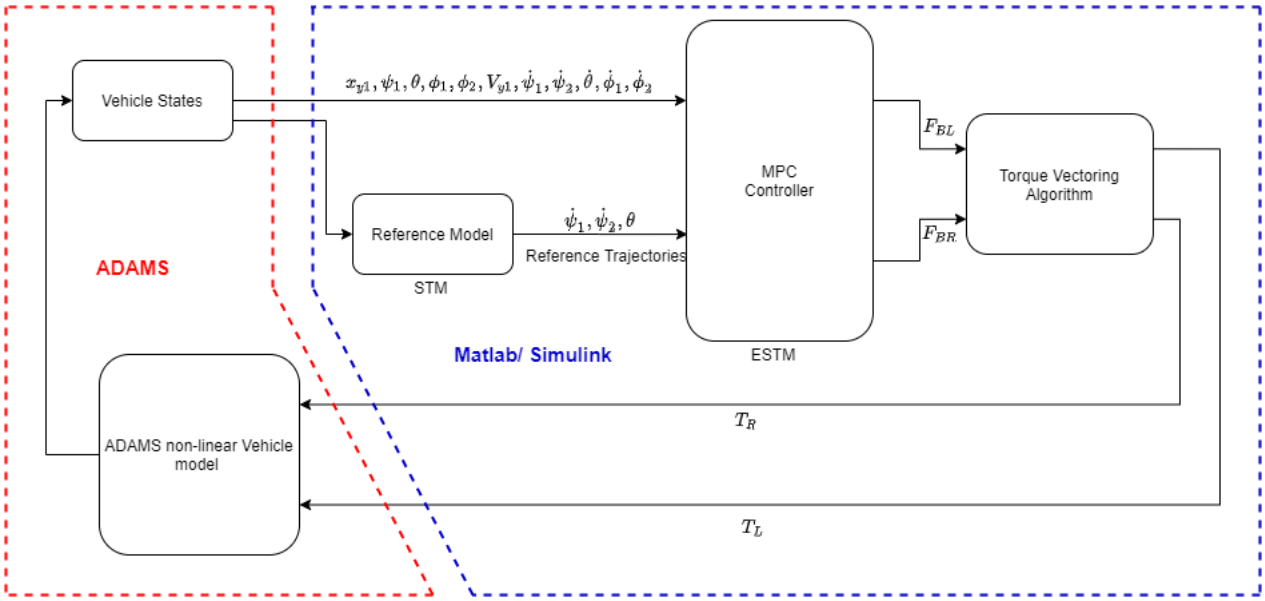

Figure 4.6. Simulation process schematic

Figure 4.6 depicts how the non-linear vehicle provides all the required vehicle states that are needed by the reference model and the controller. The reference model is implemented in Simulink by the use of a Matlab function block. These reference trajectories are then sent to the NMPC controller block. The NMPC controller block is an S-function block that is exported with the use of the ACADO toolkit and contains the predictive model and constraints as well as the optimisation problem that is solved. The weightings are also sent from Matlab to the controller block. The output of the controller is the two optimal brake forces for the left and right tyre of the trailer. A delay is implemented on the control signal. This delay is added to realistically simulate the transient response of the actual brake system. Simulink has the ability to instantly apply the control outputs to the simulation model whereas

in real life there is an actuation, system and process delay. These delayed forces are then passed to the torque vectoring algorithm, implemented using a Matlab function block. The final step is sending these optimised braking torques back to the simulation model where they act on the trailer tyres therefore stabilising the articulated vehicle.

4.3 Proportional Controller Design

A proportional controller is the simplest controller in the PID control family. It is a type of linear feedback control that is based on a response in proportion to the difference between what is set as a desired process variable or reference and the current value of the variable. A proportional controller is created for this study to generate a comparative between the NMPC and a simple controller. The controller developed here is a yaw rate controller that uses the same vehicle reference model as in the NMPC model and works by using the trailer yaw rate as the process variable by reading the current yaw rate on the trailer from the ADAMS simulation model and taking the desired trailer yaw rate from the reference model to determine the error between the two, seen in Equation 4.65. This error is then multiplied by some gain K to produce the control output defined by Equation 4.66. This control output is then sent back to the ADAMS model as a reverse control torque that acts at the trailer CG, this is therefore, a representation of a braking situation. This control torque is what is applied to the trailer in order to counteract the instability of the system, thus stabilising the vehicle. The controller schematic is depicted in Figure 4.7.

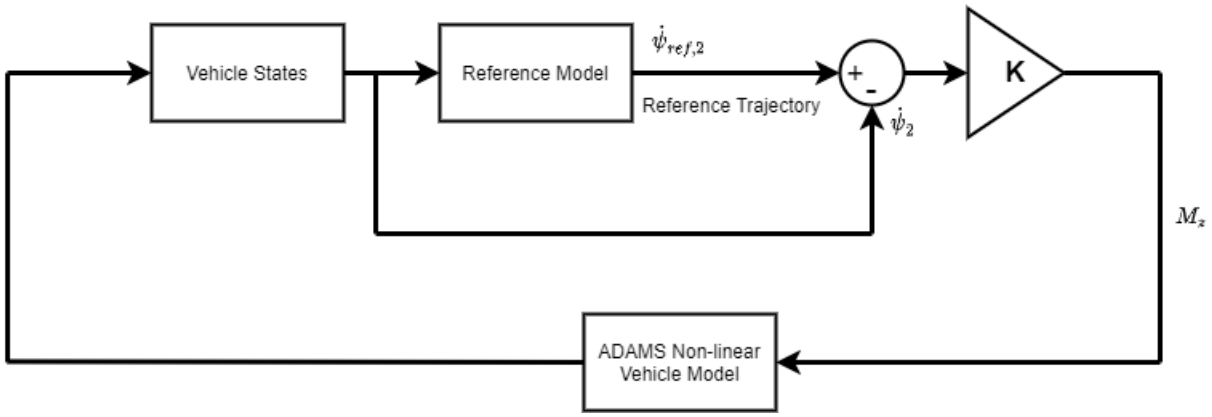

Figure 4.7. Schematic of the proportional controller

$$e(t) = \dot{\psi}_{ref,2} - \dot{\psi}_2 \tag{4.65}$$

$$u(t) = Ke(t) \tag{4.66}$$

The gain K, seen in Equation 4.66, was selected using a manual tuning process. The value was chosen based on a compromise between effectiveness and realistic results. A final value of 1000 was selected. A constraint is also applied to the controller and this constraint is in place to limit the moment within reasonable ranges. The constraint is split into left and right and is defined in Equation 4.67 and 4.68. This is done due to the fact that a negative moment is applied due to the braking of the left trailer tyre and a positive moment is applied when the right trailer tyre is braked.

$$0\,Nm \leq M_{z,r} \leq 2600\,Nm \tag{4.67}$$

$$-2600\,Nm \leq M_{z,l} \leq 0\,Nm \tag{4.68}$$

Equation 4.67 and 4.68 defines that the moment applied at the CG of the trailer shall never be less than -2600 Nm or greater then 2600 Nm. This is the same as applying a maximum braking force of 3500 N at either the left or right wheels of the trailer. This constraint is therefore the same for the NMPC and the proportional controller.

As mentioned before, this controller was developed to generate a comparison between the proportional controller and the NMPC to highlight the differences between such a simple controller and the more complex and elegant control of the NMPC.

4.4 Conclusion

This chapter gave insight into how the control system was developed for this study. A linearised time-invariant state-space equation for a Single Track Model was defined to solve for the desired vehicle response. A more complex non-linear model represented by differential equations was also developed to be used by the NMPC, to predict the future states of the vehicle and produce optimal trailer braking forces that shall minimise the error between the current vehicle states and the desired response. The constraints as well as the weightings implemented on the controller were described. The torque vectoring algorithm that is used to convert the optimal brake forces into torques for the simulation model, is described in detail and finally, the simulation process used to test the controllers capabilities is highlighted. The next step of this study shall be to verify the controller in simulation to ensure it is performing to its best ability.

5. Controller evaluation in simulation

5.1 Introduction

The performance of the controllers is investigated through simulations. This chapter shall show how the controllers react to different steering inputs and different conditions. Three scenarios are investigated, they include two articulated vehicle instabilities: snaking and jack-knifing as well as the articulated vehicle driving through a severe stable manoeuvre. The two instabilities are used to test the controllers ability to prevent or at least reduce the instabilities. The severe stable manoeuvre is used to show that the controller is not intrusive when remaining stable. All simulations made use of the Ftire tyre model except for the jack-knifing simulations. The Pacejka tyre model was used for jack-knifing due to the fact that the Ftire model did not instigate the instability.

5.2 Snaking

Snaking occurs when the tyres of the trailer saturate which causes the trailer to move from side to side divergently. The position of the trailer CG plays a very important role in the stability of the articulated vehicle which is why it is imperative to load a trailer properly. If the CG of a trailer lies towards the rear of the trailer, it makes the trailer vulnerable to snaking [Abroshan et al., 2020]. Snaking causes the oscillation of the hitch angle to increase progressively until the articulated vehicle can no longer be recovered [Zanchetta et al., 2019]. Snaking is instigated using the simulation model as is but reducing the road friction coefficient to 0.7 through a DLC at 55 km/h. The road friction coefficient is reduced to make the road slippery which helps to instigate snaking. It must also be noted that the torque vectoring capabilities of the controller were investigated independent of speed by running these simulations at a constant velocity. This is done as the vehicle slows down due to the braking and the dynamics of the vehicle become more stable at lower speeds. The vehicle speed is kept constant by applying a driving force on the vehicle. The steering angle input used is portrayed in Figure 5.1. This is an open loop simulation due to the fact that we want to test the capabilities of the braking controller and not that of the steering controller. The reference trajectories were generated using the same initial conditions at the start of the simulation and supplying the vehicle speed and steering angle. However, in the controllers, the reference trajectory is generated using current vehicle states as the initial conditions. Thus, as soon as the vehicle states change slightly the reference trajectory for each controller and at each control point will change. Thus, the reference trajectory is only shown as a guidance to the

optimal trajectory. The reference model is on an unloaded trailer and the NMPC model is of a loaded trailer but with the loads in their normal position. The road friction coefficient of the NMPC model is the same as the simulation model so 0.7.

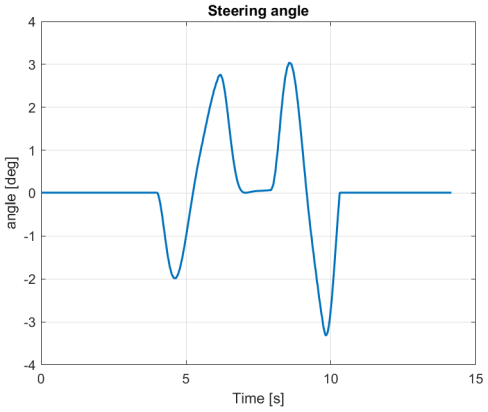

Figure 5.1. Steering angle used to instigate snaking

5.2.1 Hard Suspension

The results in this section shall depict both controllers capabilities of removing the snaking instability. The 4S4 is set to a hard suspension for handling. The dynamics of the articulated vehicle with and without control can be seen in Figure 5.2. The results are used to test whether the gain controller and NMPC are capable of removing the instability and also to create a comparison between what is known as a very simple controller and that of a more complex controller.

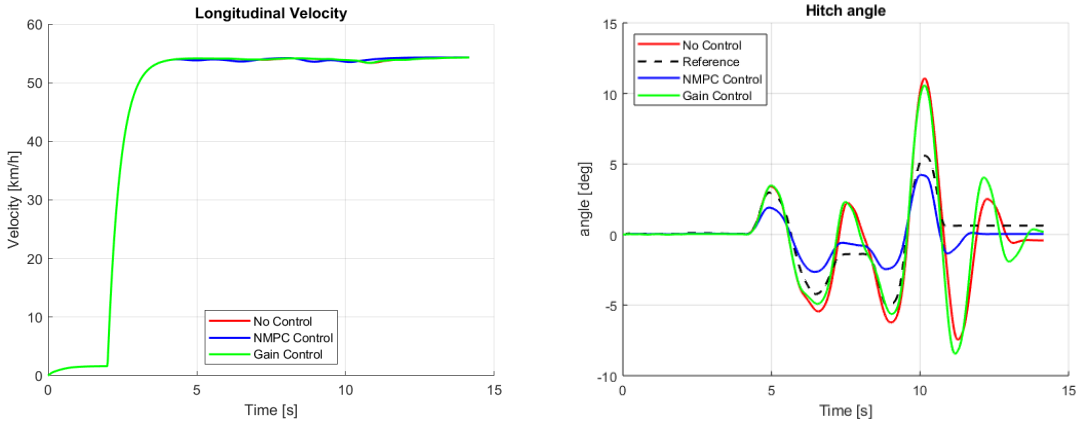

(a) Vehicle Speed **(b)** Hitch Angle

Figure 5.2. Controller capabilities through snaking with a hard suspension

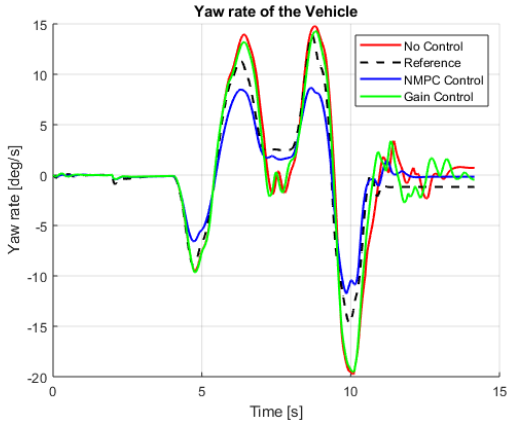

(c) Land Rover Yaw Rate

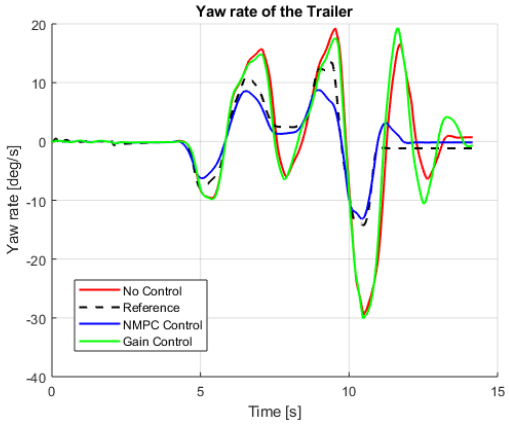

(d) Trailer Yaw Rate

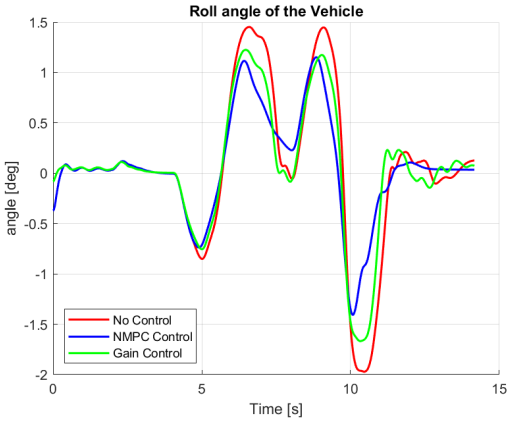

(e) Land Rover Roll Angle

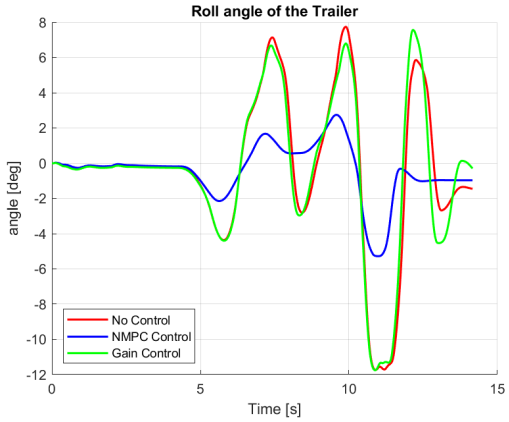

(f) Trailer Roll Angle

Figure 5.2. Controller capabilities through snaking with a hard suspension (Cont.)

The snaking of the trailer can be clearly seen when looking at the oscillatory behaviour of the hitch angle, Figure 5.2(b), and the trailer yaw rate, Figure 5.2(d). The NMPC is highly successful in not only preventing the snaking from occurring but also in reducing the peaks through the manoeuvre. This can be seen when reviewing the percentage difference between the results without control and the NMPC control, seen in Table 5.1. The largest differences are seen in the trailer parameters and hitch angle, which is expected. These objective measurements were made only with the NMPC results as is can be seen visually that the gain controller was unable to prevent instability. The reference model or desired vehicle response is set to that of an unladen trailer. The NMPC results are similar to the reference trajectories. The discrepancies could be due to the fact that the reference model used by the NMPC is linear where as the trajectory seen in the plots was generated using the nonlinear simulation model. Another reason as to why the reference is not the same as the NMPC can be because since the

states change every iteration in the NMPC and this affects the results. It can be stated that due to the NMPC, the articulated vehicle is behaving as if the trailer was unloaded. It is also important to note that even though snaking is a yaw instability, the roll angle also increases significantly which can result in roll over. It can be seen in the roll angles of both the SUV and the trailer that the NMPC is capable of reducing the roll angle significantly hence preventing the rollover of the vehicle. When analysing the gain or proportional controller, it can be clearly seen that it is unable to prevent or even improve the articulated vehicles response. With reference to the hitch angle, Figure 5.2(b), it can be seen that the gain controller attempts to reduce the hitch angle at the beginning of the DLC but ultimately ends up making the situation worse by increasing the amount of oscillations. A further comparison between the two controllers can be made when comparing the brake forces that are applied to the trailer. These brake forces are depicted in Figure 5.3.

Table 5.1. Percentage difference between no control and NMPC control during snaking

Peaks	One	Two	Three	Four	Five
Hitch Angle	81.12	106.44	69.82	156.79	166.02
Land Rover Yaw Rate	44.75	65.09	76.97	71.00	67.86
Trailer Yaw Rate	49.92	66.07	78.33	78.30	122.56
Land Rover Roll Angle	13.33	18.46	61.11	23.93	18.07
Trailer Roll Angle	101.39	77.34	120.59	189.73	120.60

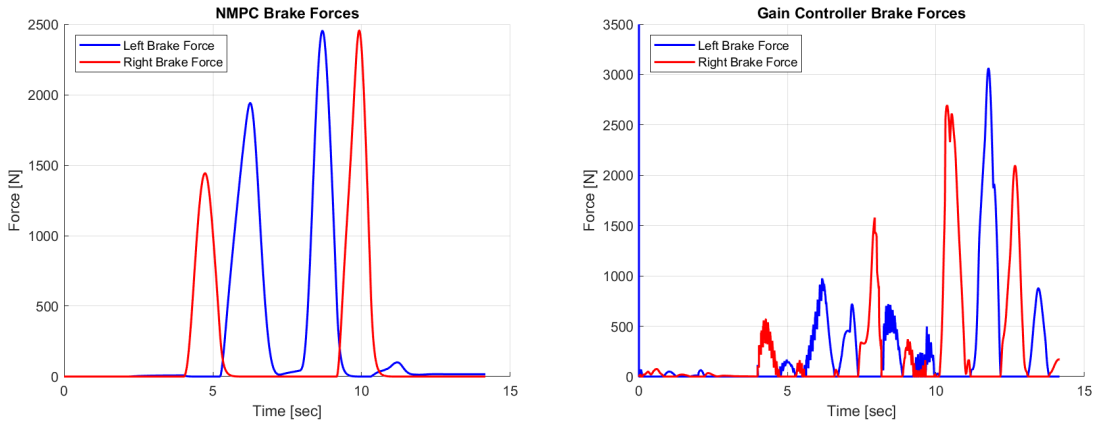

(a) NMPC brake forces

(b) Gain controller brake forces

Figure 5.3. Brake forces applied by the two controllers during snaking for a hard suspension

From Figure 5.3, it can be seen that there is a significant difference in the braking forces between the NMPC and gain controller. The NMPC brake forces are a lot smoother and never saturate at the maximum braking force of 3500 N. This shows that the braking is not too intrusive but is still able to remove instability. When looking at the forces that are applied by the gain controller, it can be seen that not much braking is applied in the beginning of the manoeuvre but then more severe braking is applied towards the end. The reference model takes the vehicle states from ADAMS as its initial states and since not much effect is occurring due to braking in the beginning of the DLC it allows the vehicle to become unstable. The controller attempts to counteract this with higher braking forces towards the end of the DLC. Unfortunately this has an adverse effect and ends up making the instability worse. A possible way to counteract this is to increase the gain that is used which will hence increase the amount of braking applied. Ultimately these results clearly show that the NMPC is a far more elegant and successful and that the increased complexity is worth it.

5.2.2 Soft Suspension

The same trends that were seen in the hard suspension results were seen in the soft suspension results. It is for this reason that it was decided to place the soft suspension results in Appendix B.

5.3 Jack-knifing

jack-knifing is a type of instability that occurs when the tyres of the towing vehicle saturate or in other words, when the towing vehicle reaches the friction limit but the trailer does not [Abroshan et al., 2020, Zanchetta et al., 2019]. The momentum generated by the trailer pushes the towing vehicle, causing it to spin. The articulated vehicle ultimately ends up in a "folded" position [Zanchetta et al., 2019]. jack-knifing is more likely to occur when the payload is situated close to the hitch point. The jack-knifing instability is generated using a step steer manoeuvre at 55 km/h.The mass of each weight is increased to 800 kg and is moved closer to the hitch by 3m with weight one being 1m from the hitch point. The road friction coefficient is set at 0.7. The reference model is on an unloaded trailer and the NMPC model is of a loaded trailer but with the loads in their normal positions. The step steer steering angle input is depicted in Figure 5.4. Open loop steering with a constant velocity is used once again and the reference trajectories were generated using the same manner as in snaking. It should be noted that the NMPC model was not updated to compensate for the change in model. Thus, the friction and the loading conditions are still of a normally fully loaded trailer. This will also test the robustness of the controller to a change in parameters which are not compensated for.

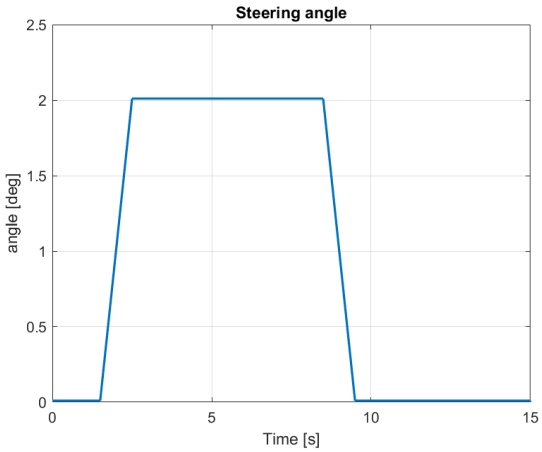

Figure 5.4. Steering angle through a jack-knife

5.3.1 Hard Suspension

This particular manoeuvre did not create a jack-knife while the Land Rover 4S4 suspension was set on hard. It is for this reason that the soft suspension results are rather shown in this chapter. However, the hard suspension results still show how the controllers are able to reduce the yaw and roll dynamics of the articulated vehicle during this handling manoeuvre. It is for this reason that they can be found in Appendix B.

5.3.2 Soft Suspension

As mentioned above, a jack-knife is when the towing vehicle reaches the friction limit and hence the SUV yaw rate was used as an indication for jack-knifing. The soft suspension setting was used for these simulations and the results can be seen in Figure 5.5. The brake forces that were applied by each individual controller are portrayed in Figure 5.6.

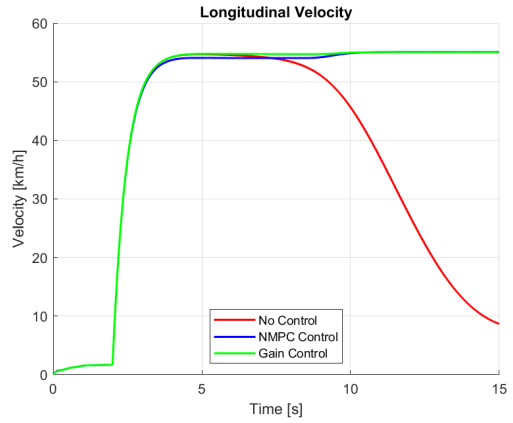

(a) Vehicle Speed

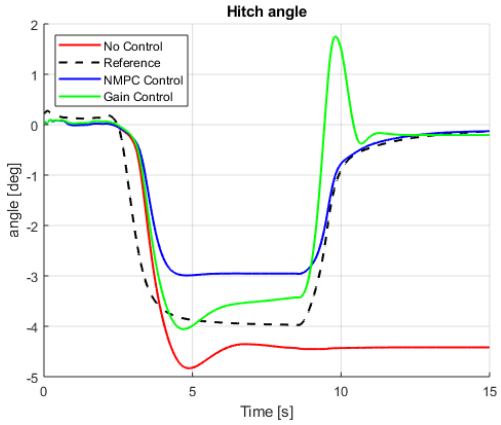

(b) Hitch Angle

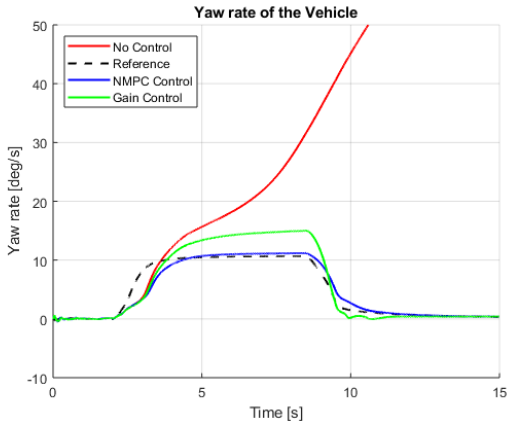

(c) Land Rover Yaw Rate

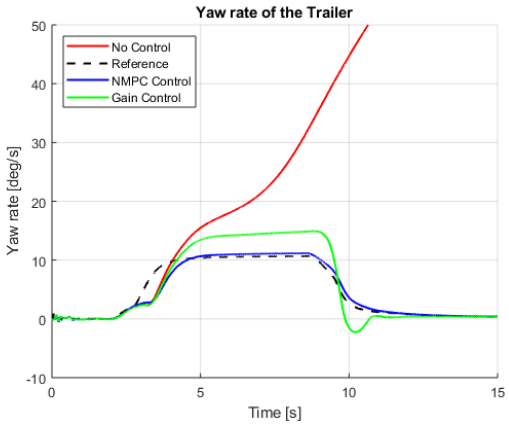

(d) Trailer Yaw Rate

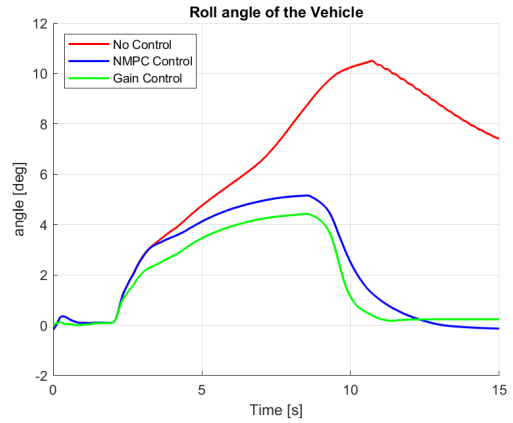

(e) Land Rover Roll Angle

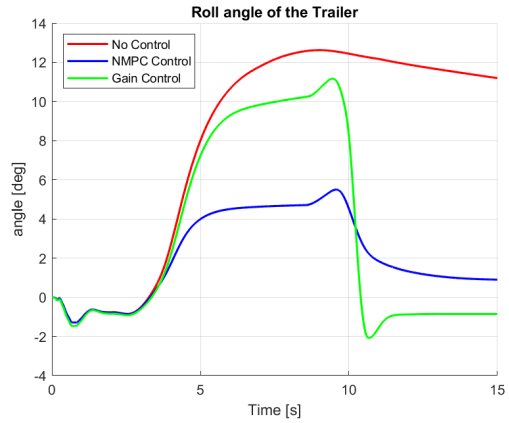

(f) Trailer Roll Angle

Figure 5.5. Controller capabilities through jack-knifing with a soft suspension

The actual jackknife can be seen through looking at the SUV and trailer yaw rates, Figures 5.5(c) and 5.5(d) which indicates that the articulated vehicle spins out. In contrast to the snaking instability, it is clearly seen from Figure 5.5 that the gain controller is also capable of preventing this particular instability. It is now possible to more closely analyse the differences and similarities between the two controllers. The NMPC performs more efficiently and produces a better result. This can be seen by looking at the percentage difference between the reference trajectory and the controller results in Table 5.2. The yaw rates of the NMPC closely match that of the reference and reduces the hitch angle significantly. The difference between the reference and the controllers are used objectively as the results without control were too unstable to select a good measuring point. These results shows that trailer braking using the hitch angle, SUV yaw rate and trailer yaw rate as design variables is more capable of preventing instability than that of the gain controller that only uses the trailer yaw rate. This is also proved by the fact that the NMPC is able to prevent both snaking and jack-knifing but the gain controller is only capable of preventing one. This particular manoeuvre also shows the robustness of the NMPC. The robustness is seen through the fact that a different tyre model was used here in comparison to the snaking model which shows the robustness to changing tyre parameters. The robustness of the controller can also be analysed due to the fact that the trailer weights have been moved towards the hitch point and have increased in mass. These changes were made to the ADAMS non-linear vehicle model but no changes were made to the NMPC predictive model or the reference model, this is an asset as it shows the controllers lack of sensitivity to inertial changes. It can therefore be stated that the controller shall perform well without the need for any major changes. The yaw rate reference trajectories closely match the NMPC results. The discrepancies in the hitch angle could once again be due to the linear nature of the reference model. The brake forces that were applied to achieve the results in Figure 5.5 are depicted in Figure 5.6 below.

Table 5.2. Percentage difference between the controller results and the reference trajectory during jack-knifing

	NMPC Control	**Gain Control**
Hitch Angle	25.06	8.35
Land Rover Yaw Rate	4.47	34.67
Trailer Yaw Rate	3.99	34.89

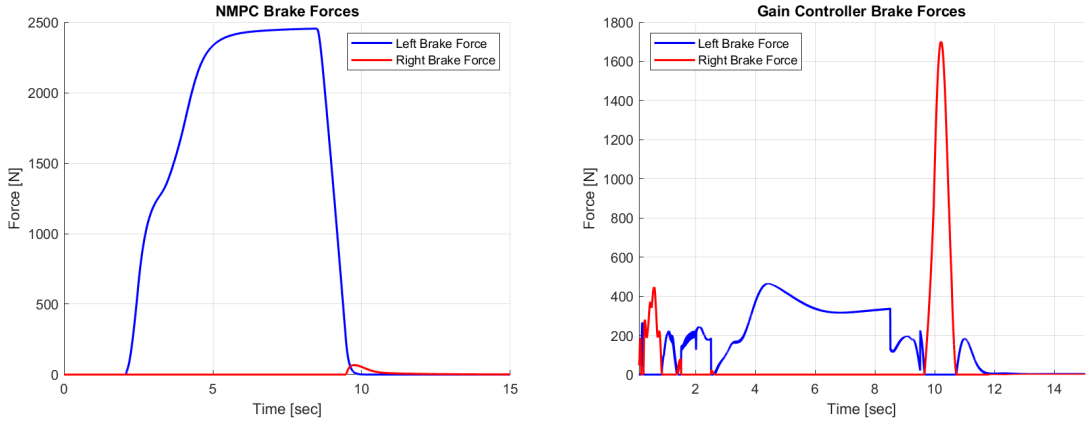

(a) NMPC brake forces

(b) Gain controller brake forces

Figure 5.6. Brake forces applied by the two controllers during jack-knifing for a soft suspension

The same trends in the controller forces that were seen during snaking are seen in Figure 5.7. Ultimately the optimal left and right trailer braking forces generated by the NMPC are a lot smoother and the transition is far more efficient. This is due to the fact that a delay has been added to the NMPC brake forces in order to simulate real life where there shall be an actuation, system and process delay whereas the gain controller applies the moment immediately which is not realistic. The high right brake force seen in Figure 5.6(b) occurs because it is possible that the trailer snaps back and overshoots hence the larger control action of the right wheel. Since the NMPC controller has now proved its worth against an unstable articulated vehicle as well as a simple proportional controller, it is necessary to investigate how this controller shall behave under stable driving conditions.

5.4 Severe Stable Manoeuvre

As mentioned above, the purpose of this section is to show that the controller shall not be too intrusive to the vehicle while the articulated vehicle is stable. Speed reduction was also investigated in this section as it also gives an indication of intrusion. This was simulated by turning the drive force off after the vehicle reached 55 km/h. In a realistic situation turning the drive force off would represent the driver taking his foot off the accelerator during the manoeuvre. The reference model or desired vehicle response is set to that of an unladen trailer which means that it is expected that the controller shall interfere to ensure the loaded trailed is behaving like an unloaded trailer. For these results, the steering angle that was measured during experimental loaded validation test for a DLC at 55 km/h is used as a steering input to the simulation model, seen in Figure 5.7.

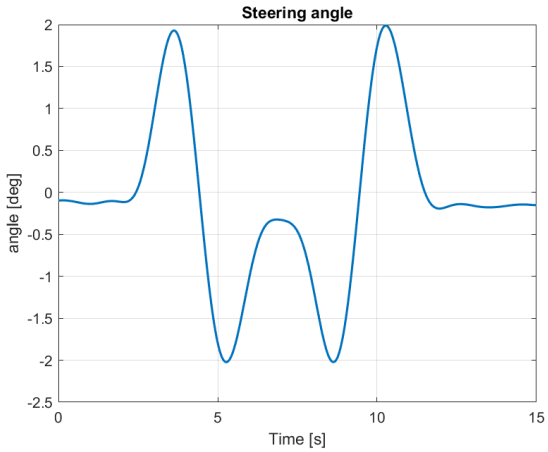

Figure 5.7. Steering angle during a severe stable manoeuvre

5.4.1 Hard Suspension

The simulation results for an articulated vehicle driving through a severe stable manoeuvre with the SUV set on a hard suspension setting shall be discussed in this section. The dynamics of the vehicle system is depicted in Figure 5.8 and the control braking forces that were applied for each individual controller is portrayed in Figure 5.9.

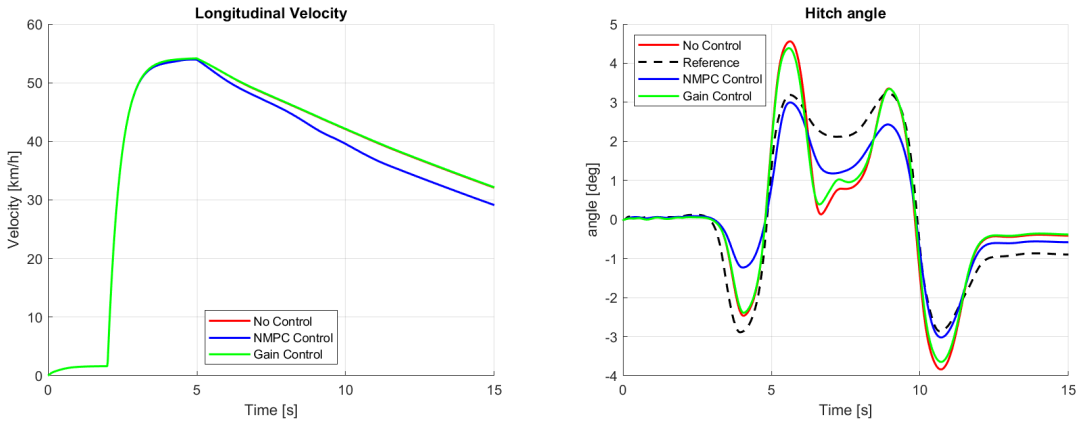

(a) Vehicle Speed **(b)** Hitch Angle

Figure 5.8. Controller capabilities during a severe stable manoeuvre with a hard suspension

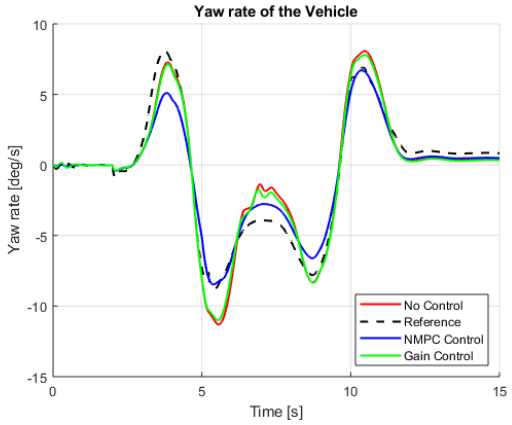

(c) Land Rover Yaw Rate

(d) Trailer Yaw Rate

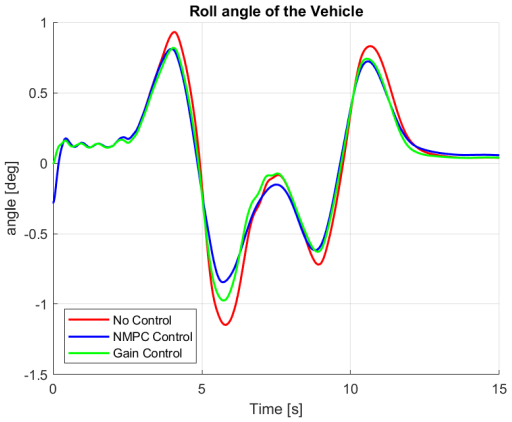

(e) Land Rover Roll Angle

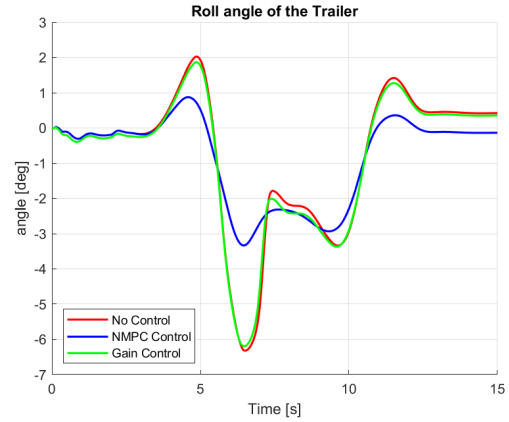

(f) Trailer Roll Angle

Figure 5.8. Controller capabilities during a severe stable manoeuvre with a hard suspension (Cont.)

As expected, it can be seen from Figure 5.8, that the NMPC does alter the dynamics of the articulated vehicle due to the fact that the NMPC ensures the vehicle is performing as if the trailer was unloaded. The affect of speed reduction can clearly be seen in Figure 5.8(a). There is a clear decrease in the speed. It must be noted that the reduction in speed is due to tyre scrubbing. There is only a 3 km/h difference between the NMPC and the speed without control. This clearly shows that the braking due to the NMPC is not too intrusive. There is relatively no difference between the gain controller and the articulated vehicle without control. This is due to the fact that a relatively low amount of braking is applied, which can be seen in the brake force plots seen below in Figure 5.9.

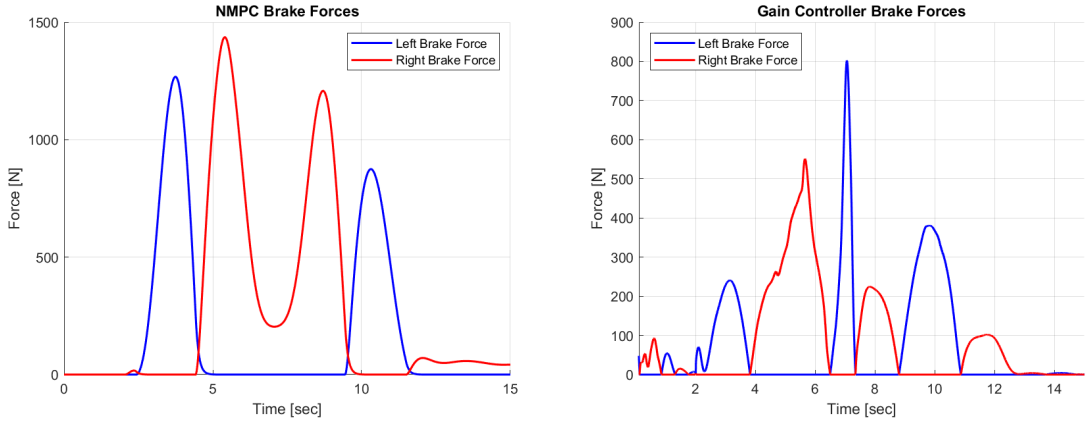

(a) NMPC brake forces

(b) Gain controller brake forces

Figure 5.9. Brake forces applied by the two controllers during a severe stable manoeuvre for a hard suspension

The main purpose of analysing these results is to show that the controller shall not be intrusive towards the vehicle in a stable environment. It can be seen from Figure 5.9(b) that the gain controller applies almost no braking with the maximum being around 600 N. Once again, this is based purely on the gain. If the gain is increased, the amount of braking will also increase. The NMPC brake forces, seen in Figure 5.9(a), are significantly higher than that of the gain controller hence the difference seen in the dynamics above. The reason they are higher is because the NMPC solves for the optimal brake forces required to minimise the difference between the actual and desired vehicle response whereas the gain controller forces are simply a gain multiplied by the error between the actual and desired trailer yaw rate. Even though the NMPC applies more braking than the gain controller, it is still relatively low with a maximum of 1500 N. It can therefore be confidently stated that the NMPC controller shall not affect the driving environment significantly while the articulated vehicle is stable. The controller can also be made less intrusive by changing the weights or by having variable weights also known as weight scheduling.

5.4.2 Soft Suspension

The simulations for an articulated vehicle under a sever stable manoeuvre for a soft suspension can be found in Appendix B.

5.5 Conclusion

From the simulations, we can conclude that the NMPC works very well in not only removing the instabilities but also reducing the yaw and roll dynamics to behave like that of an unloaded trailer. It was also found that the controllers are not too intrusive by analysing the controllers during a severe stable manoeuvre with speed reduction. By comparing the NMPC to a simple proportional controller, it shows how valuable the complexities of a more advanced system such as the NMPC can be. The NMPC performed significantly better than that of the proportional controller. The NMPC uses three design variables, the hitch angle and towing vehicle and trailer yaw rates, whereas the gain controller is limited to one, the trailer yaw rate. This is a downside of PID control and it is worth noting that the gain controller could possibly be improved by changing this design variable. The NMPC is far more valuable as it determines the optimum braking that is required based on a future prediction of the states of the articulated vehicle which is clearly seen in the results of this chapter.

6. Conclusion and Recommendations

This research study aimed to design and implement a control system for an articulated vehicle that is capable of preventing instability. This aim was achieved through the development of a nonlinear model predictive controller. In order to develop this controller, a MSC ADAMS non-linear articulated vehicle model was constructed for a Land Rover Defender TDI towing a testing trailer that was built from a standard Land Rover chassis. Once built, the model was validated through experimental testing for a loaded trailer. This validation is done to ensure that the simulation model that was constructed is a realistic representation of the test vehicle. Two handling manoeuvres were used, these included a double lane change as well as a constant radius turn. The validation results show that the lateral dynamics of the articulated vehicle model are well captured, while there are some discrepancies it is still a realistic representation and therefore the simulation model is properly validated for the purpose of developing a control system. Two controller methods were developed, the first which is the main contribution to this research area, is a nonlinear model predictive controller. The second controller method is a simple proportional controller used to create a comparison between the two. Both controllers placed focus on yaw rate control by implementing torque vectoring on the trailer. The controllers were analysed using the snaking and jack-knifing instabilities as well as normal driving conditions. The results proved that the gain controller based solely on trailer yaw rate was unable to prevent the instability of an articulated vehicle. On the other hand, the NMPC performed very well and is very successful in altering the dynamics of the articulated vehicle to prevent instability from occurring. The results also show that the NMPC is not too intrusive while the vehicle remains stable. Ultimately the work provided in this study shows the NMPC is able to prevent instability within articulated vehicles and therefore the main objective of this study was achieved. The success of this work has opened many doors for the future research into the instability of articulated vehicles.

6.1 Recommendations

There is definite potential for further and future work in this particular research area. The articulated vehicle simulation model constructed in this study is the first of its kind at VDG and it therefore opens many doors into the world of articulated vehicles. There are vast areas into which articulated vehicles can be used for research and this validated model allows for further investigation of these areas.

The main recommendation for the future of this study would be to experimentally test the capabilities of the controller. This would include implementing the controller on the test vehicle and trailer and determine if the controller is as efficient during real time experimental tests as it is in simulations.

It would also be beneficial to investigate the possibilities of the model and the controller on off-road terrains. This study placed the focus on flat roads only so it would be interesting to test the performance of the controller on a rougher profile.

On that note, rougher terrains would cause a decrease in the ride comfort of the vehicle. Therefore, it would be interesting to alter the controller to take ride comfort into account as well. This will be during manoeuvres that cause instability as safety is always more important than comfort.

The more finer details of the controller can also be improved on. These include upgrading both the reference model and the predictive model from a single track model to a full vehicle model and adding complexities to the model such as load transfer. The controller could also be upgraded to a switching NMPC in which a combination of towing vehicle and trailer braking could be analysed.

It would be beneficial when performing experimental tests to eradicate the driver from the system by using a steering robot and speed controller. This will help with model validation as well as determine the controller effects without the uncertainty of driver error.

If the system is applied to an articulated vehicle more permanently then it would be necessary to estimate brake temperature. This is due to the fact that when brake temperature increases it causes the brake power to decrease which should be monitored.

References

[Abroshan et al., 2020] Abroshan, M., Hajiloo, R., Hashemi, E., and Khajepour, A. (2020). Model predictive-based tractor-trailer stabilisation using differential braking with experimental verification. *Vehicle System Dynamics*, 0(0):1–24.

[Anderson and Kurtz, 2019] Anderson, R. and Kurtz, E. F. (2019). Handling-Characteristics Simula of Car-Trailer System. 89(1980):2097–2113.

[Anwar, 2005] Anwar, S. (2005). Generalized predictive control of yaw dynamics of a hybrid brake-by- wire equipped vehicle. *Mechatronics*, 15(9).

[Ariens et al., 2011] Ariens, D., Houska, B., and Ferreau, H. (2010–2011). Acado for matlab user's manual. http://www.acadotoolkit.org.

[Azad, 2006] Azad, N. L. (2006). Dynamic Modelling and Stability Controller Development for Articulated Steer Vehicles. *Analysis*.

[Blet et al., 2002] Blet, N., Megías, D., Serrano, J., and Prada, C. D. (2002). Nonlinear mpc versus mpc using on-line linearisation — a comparative study. *IFAC Proceedings Volumes*, 35(1):147–152.

[Cronje, 2008] Cronje, P. H. (2008). Improving off road vehicle handling an active anti roll bar.

[Dahlberg, 2000] Dahlberg, E. (2000). A method determining the dynamic rollover threshold of commercial vehicles. *SAE Technical Paper Series*.

[Dahlberg and Stensson, 2006a] Dahlberg, E. and Stensson, A. (2006a). The dynamic rollover threshold - a heavy truck sensitivity study. *International Journal of Vehicle Design*, 40(1/2/3):228.

[Dahlberg and Stensson, 2006b] Dahlberg, E. and Stensson, A. (2006b). The dynamic rollover threshold - a heavy truck sensitivity study. *International Journal of Vehicle Design - INT J VEH DES*, 40.

[Darling et al., 2009] Darling, J., Tilley, D., and Gao, B. (2009). An experimental investigation of car-trailer high-speed stability. *Proceedings of the Institution of Mechanical Engineers, Part D: Journal of Automobile Engineering*, 223(4):471–484.

[de Saxe et al., 2018] de Saxe, C., Nordengen, P., and Berman, R. (2018). *Piloting PBS in South Africa*.

[defenceWeb, 2019] defenceWeb (2019). Gerotek is a world class vehicle testing facility.

[dSPACE, 2020] dSPACE (n.d (accessed June 17, 2020)). *MicroAutoBox II*.

[Edwards and Spurgeon, 1998] Edwards, C. and Spurgeon, S. (1998). Sliding mode control.

[El-Gindy, 1995] El-Gindy, M. (1995). An overview of performance measures for heavy commercial vehicles in north america. *International Journal of Vehicle Design*, 16(4).

[Els, 2006] Els, P. S. (2006). *The ride comfort vs. handling compromise for off-road vehicles*. PhD thesis.

[Falcone et al., 2008] Falcone, P., Tseng, E., Asgari, J., and Hrovat, D. (2008). Mpc-based yaw and lateral stabilisation via active front steering and braking. *Vehicle System Dynamics*, 46(1).

[Farr and Neilson, 2012] Farr, B. and Neilson, I. (2012). A survey into the accident rates of articulated and rigid commercial vehicles.

[Fu and Cebon, 2002] Fu, T.-T. and Cebon, D. (2002). Analysis of a truck suspension database. *International Journal of Heavy Vehicle Systems*, 9(4):281.

[Gillespie, 1992] Gillespie, T. D. (1992). *Fundamentals of Vehicle Dynamics*. SAE International.

[Gipser, 2004] Gipser, M. (2004). The ftire tire model family.

[Grīslis, 2011] Grīslis, A. (2011). Longer combination vehicles and road safety.

[Hac et al., 2008] Hac, A., Fulk, D., and Chen, H. (2008). Stability and Control Considerations of Vehicle-Trailer Combination. *SAE International Journal of Passenger Cars - Mechanical Systems*, 1(1):925–937.

[He et al., 2005] He, Y., Elmaraghy, H., and Elmaraghy, W. (2005). A design analysis approach for improving the stability of dynamic systems with application to the design of car-trailer systems. *Journal of Vibration and Control*, 11(12):1487–1509.

[Ibraheem et al., 2000] Ibraheem, A., Bahgat, A., and Motelb, M. A. (2000). Fuzzy logic sliding mode controller for dc drive. *Current Advances in Mechanical Design and Production VII*, page 75–83.

[International Standard of Organisation, 1999] International Standard of Organisation (1999). Passenger cars - test track for a severe lane-change manoeuvre - part 1: Double-lane change.

[International Standard of Organisation, 2002] International Standard of Organisation (2002). General conditions for heavy vehicles and buses. *Vehicle dynamic test methods – Part2*.

[Koenigsberg, 2008] Koenigsberg, S. (2008). Trailer Accident Statistics. 8995.

[Kurtz and Anderson, 1977] Kurtz, E. F. and Anderson, R. J. (1977). Handling characteristics of car-trailer systems; a state-of-the-art survey. *Vehicle System Dynamics*, 6(4):217–243.

[Lee and Yoo, 2009] Lee, J.-H. and Yoo, W.-S. (2009). An improved model-based predictive control of vehicle trajectory by using nonlinear function. *Journal of Mechanical Science and Technology*, 23(4):918–922.

[Li et al., 2016] Li, X., Li, J., Su, L., and Cao, Y. (2016). Control methods for roll instability of articulated steering vehicles.

[Macnabb et al., 2002] Macnabb, M. J., Brewer, E., Baerg, R., and Billing, J. R. (2002). Static and dynamic roll stability of various commercial vehicles. *SAE Technical Paper Series*.

[Martinez and Cao, 2019] Martinez, C. M. and Cao, D. (2019). *IHorizon-enabled energy management for electrified vehicles*. Butterworth-Heinemann is an imprint of Elsevier.

[Milani et al., 2019] Milani, S., Ünlüsoy, Y. S., Marzbani, H., and Jazar, R. N. (2019). Semitrailer steering control for improved articulated vehicle manoeuvrability and stability. *Nonlinear Engineering*, 8(1):568–581.

[Miyahara et al., 2019] Miyahara, K., Fujimoto, H., Hori, Y., and Ivanov, V. (2019). Performance benchmark of yaw rate controllers by active front steering: Comparative analysis of model predictive control, linear quadratic integral control and yaw moment observer. *IECON 2019 - 45th Annual Conference of the IEEE Industrial Electronics Society*.

[Mokhiamar, 2015] Mokhiamar, O. (2015). Stabilization of car-caravan combination using independent steer and drive/or brake forces distribution. *Alexandria Engineering Journal*, 54(3):315–324.

[MSC Software, 2020] MSC Software (n.d (accessed July 8, 2020)). *Adams The Multibody Dynamics Simulation Solution*.

[Nayl, 2013] Nayl, T. (2013). *Modeling, control and path planning for an articulated vehicle*. PhD thesis.

[O'Neal Arant, 2013] O'Neal Arant, M. (2013). Stability Control of Triple Trailer Vehicles.

[Pacejka and Bakker, 2004] Pacejka, H. B. and Bakker, E. (2004). The magic formula tyre model. *Vehicle System Dynamics*, 21:1–18.

[Pacejka et al., 1989] Pacejka, H. B., Bakker, E., and Lidner, L. (1989). A new tire model with an application in vehicle dynamics studies. In *SAE Technical Paper*. SAE International.

[Prem, 2014] Prem, A. (2014). Articulated vehicle systems.

[Road Traffic Management Corporation, 2018] Road Traffic Management Corporation (2018). Quarter 4 Road Traffic Report.

[Rybarczyk and Mestre, 2012] Rybarczyk, Y. P. and Mestre, D. (2012). Effect of temporal organization of the visuo-locomotor coupling on the predictive steering.

[Shamim et al., 2011] Shamim, R., Islam, M. M., and He, Y. (2011). A Comparative Study of Active Control Strategies for Improving Lateral Stability of Car-Trailer Systems. In *SAE Technical Paper*.

[Thoresson, 2007] Thoresson, M. J. (2007). Efficient gradient-based optimisation of suspension characteristics for an off-road vehicle.

[Uys et al., 2006] Uys, P., Els, P., and Thoresson, M. (2006). Suspension settings for optimal ride comfort of off-road vehicles travelling on roads with different roughness and speeds.

[van der Merwe, 2018] van der Merwe, N. A. (2018). ABS braking on rough terrain.

[Vandoren, 2012] Vandoren, V. (2012). Feedback controllers do their best.

[VBOX automotive, 2020] VBOX automotive (n.d (accessed June 17, 2020)). *Data Loggers*.

[Williams and Mohn, 2004] Williams, J. M. and Mohn, F.-W. (2004). Trailer stabilization through active braking of the towing vehicle.

[Wrinkler and Ervin, 1995] Wrinkler, C. and Ervin, R. (1995). Rollover of heavy commercial vehicles. *University of Michigan: University of Michigan Transportation Research Institute.*, (UMTRI-99- 19).

[Young et al., 2008] Young, D., Grzebieta, R., Rechnitzer, G., Bambach, M., and Richardson, S. (2008). (pdf) rollover crash safety: Characteristics and issues.

[Zanchetta et al., 2019] Zanchetta, M., Tavernini, D., Sorniotti, A., Gruber, P., Lenzo, B., Ferrara, A., Sannen, K., Smet, J. D., and Nijs, W. D. (2019). Trailer control through vehicle yaw moment control: Theoretical analysis and experimental assessment. *Mechatronics*, 64:102–282.

[Zhang, 2015] Zhang, N. (2015). Stability Investigation of Car-trailer Combinations based on Time-Frequency Analysis.

[Zhang et al., 2017] Zhang, N., Yin, G. D., Mi, T., Li, X. G., and Chen, N. (2017). Analysis of Dynamic Stability of Car-trailer Combinations with Nonlinear Damper Properties. *Procedia IUTAM*, 22:251–258.

A. Additional Parameters

A.1 Pacjeka Tyre Model Coefficients

The values in Table A.1 are the Pacjeka tyre model coefficients that were used to determine the cornering coefficients needed for the controller reference model.

Table A.1. Magic Formula Coefficients

Parameters	
a_0	1.45
a_1	-24.48
a_2	1125
a_3	2125.2
a_4	8.896
a_5	0.00501
a_6	-0.02103
a_7	0.77394
a_8	0.0001
a_9	0.0001
a_{10}	0.0001
a_{11}	0.0001
a_{12}	0.0001
a_{13}	0.0001

B. Controller Results

B.1 Snaking

B.1.1 Soft Suspension

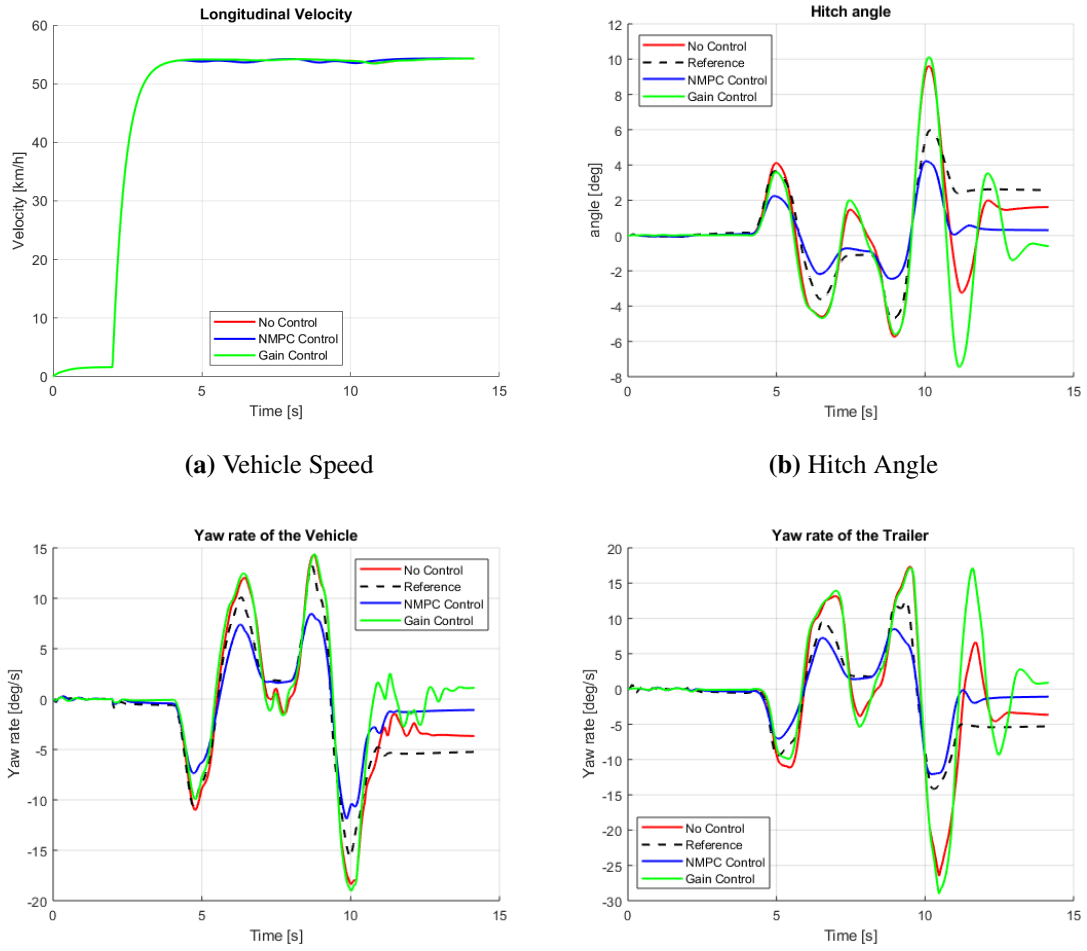

(a) Vehicle Speed

(b) Hitch Angle

(c) Land Rover Yaw Rate

(d) Trailer Yaw Rate

Figure B.1. Controller capabilities through snaking with a soft suspension

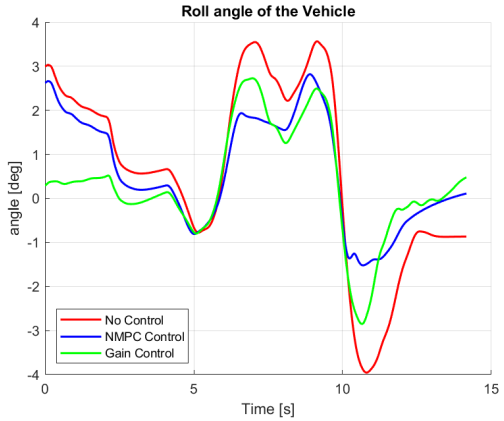

(e) Land Rover Roll Angle

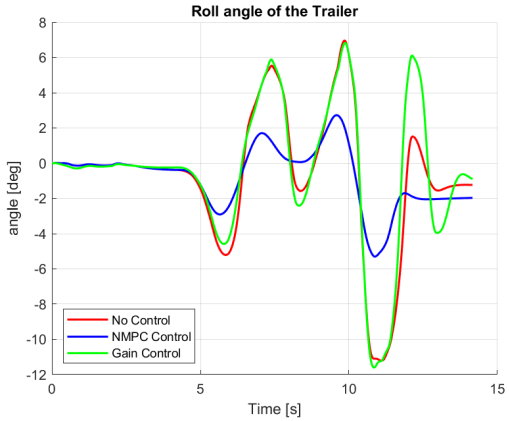

(f) Trailer Roll Angle

Figure B.1. Controller capabilities through snaking with a soft suspension (Cont.)

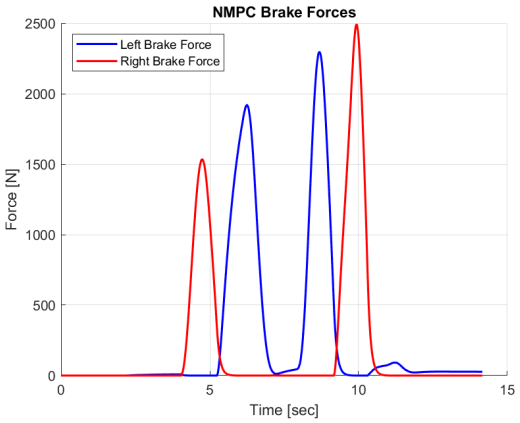

(a) NMPC brake forces

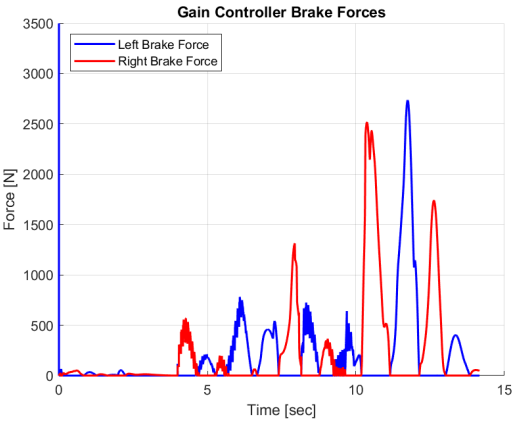

(b) Gain controller brake forces

Figure B.2. Brake forces applied by the two controllers during snaking for a soft suspension

B.2 Jack-knifing

B.2.1 Hard Suspension

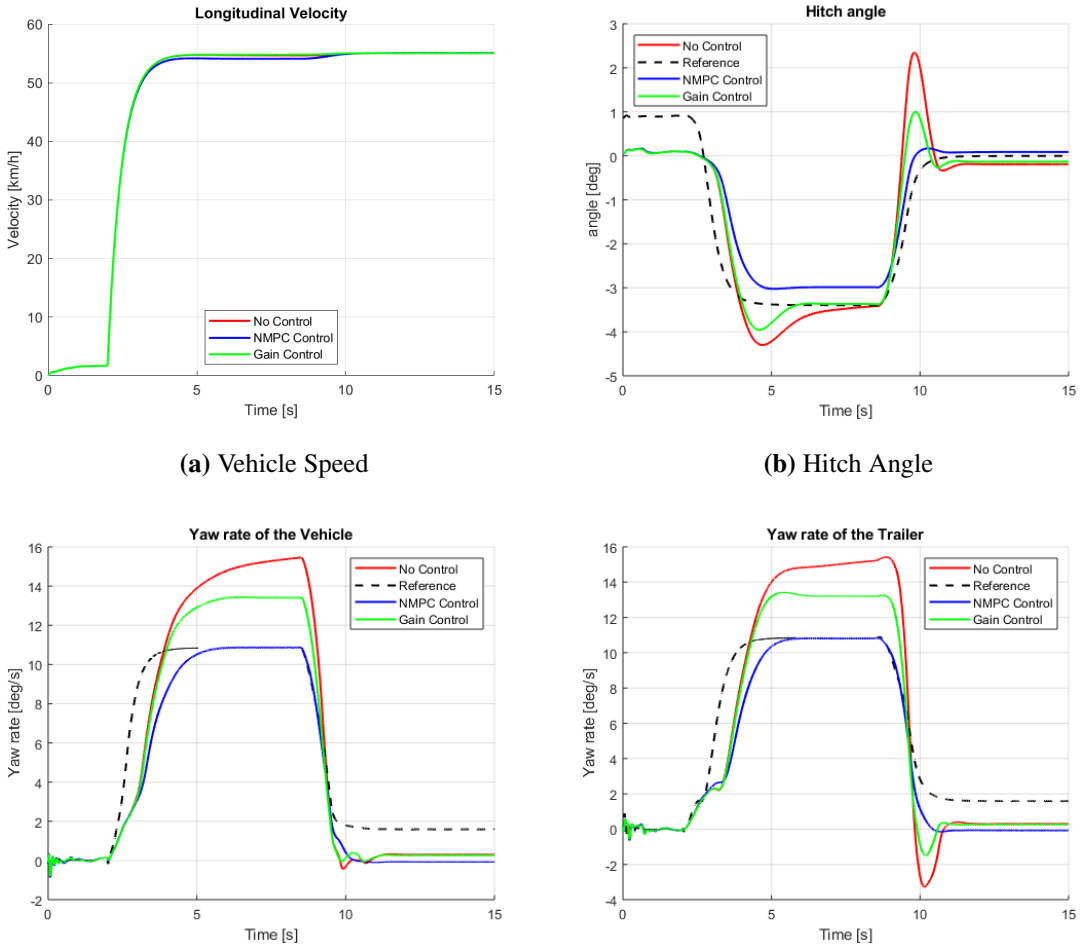

(a) Vehicle Speed

(b) Hitch Angle

(c) Land Rover Yaw Rate

(d) Trailer Yaw Rate

Figure B.3. Controller capabilities through jack-knifing with a hard suspension

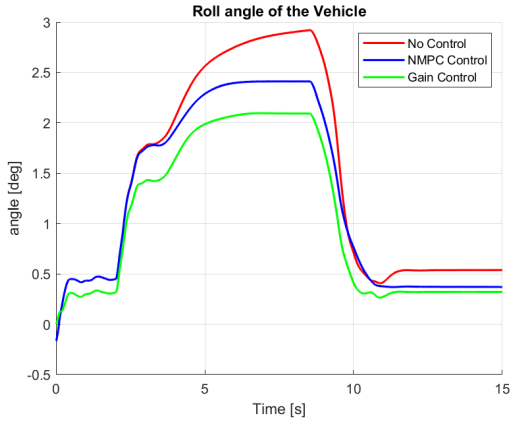

(e) Land Rover Roll Angle

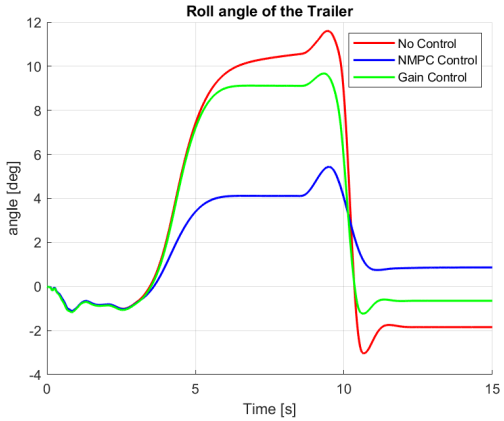

(f) Trailer Roll Angle

Figure B.3. Controller capabilities through jackknifing with a hard suspension (cont.)

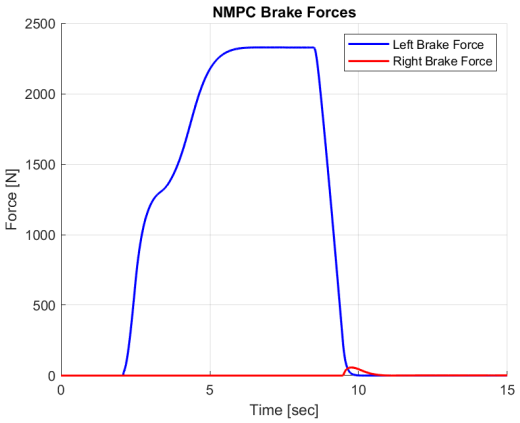

(a) NMPC brake forces

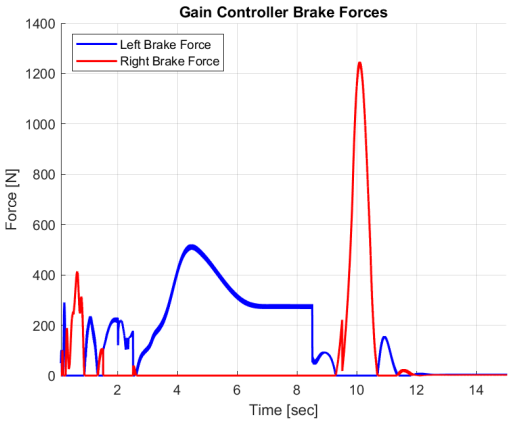

(b) Gain controller brake forces

Figure B.4. Brake forces applied by the two controllers during jack-knifing for a hard suspension

B.3 Severe stable manoeuvre

B.3.1 Soft Suspension

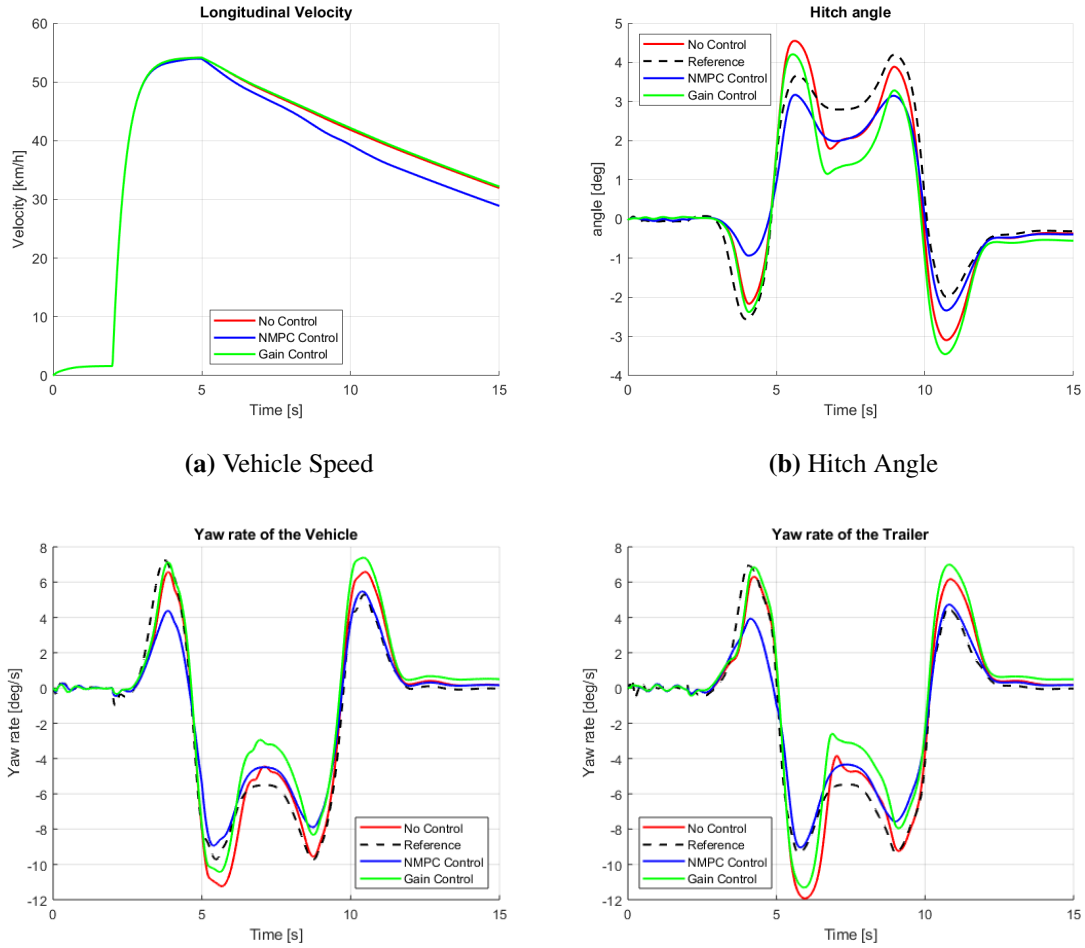

(a) Vehicle Speed

(b) Hitch Angle

(c) Land Rover Yaw Rate

(d) Trailer Yaw Rate

Figure B.5. Controller capabilities during a severe stable manoeuvre with a soft suspension

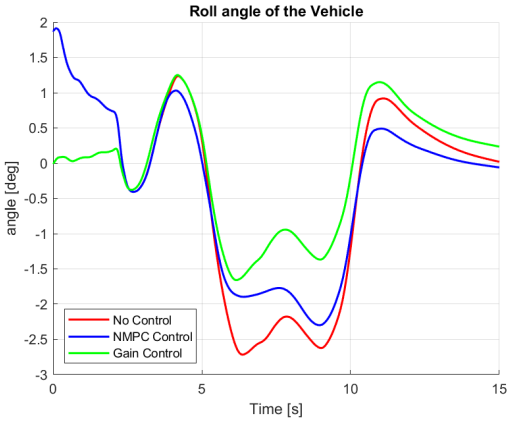

(e) Land Rover Roll Angle

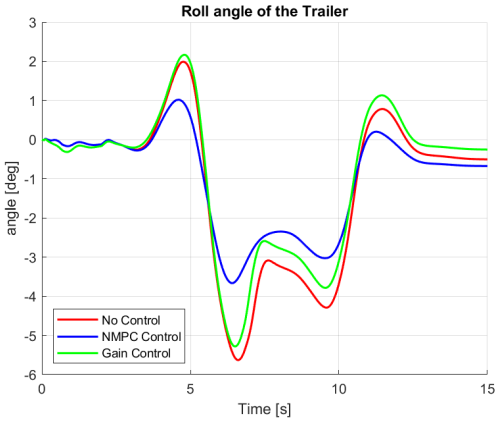

(f) Trailer Roll Angle

Figure B.5. Controller capabilities during a severe stable manoeuvre with a soft suspension (Cont.)

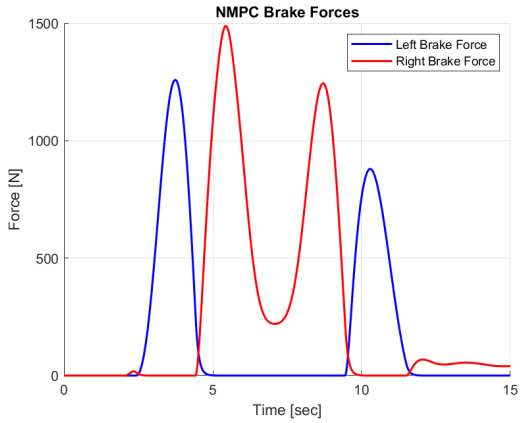

(a) NMPC brake forces

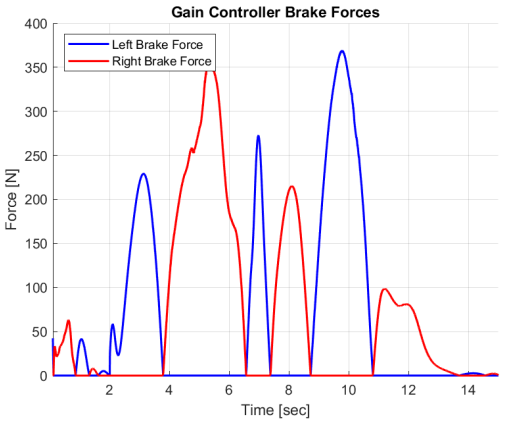

(b) Gain controller brake forces

Figure B.6. Brake forces applied by the two controllers during a severe stable manoeuvre for a soft suspension